Comparative study of different methods for superstructure-foundation interactions

by

Prakriti Sharma

B.Eng., Pokhara University, 2015

A Thesis Submitted in Partial Fulfillment

of the Requirements for the Degree of

MASTER OF APPLIED SCIENCE

in the Department of Civil Engineering

Comparative study of different methods for superstructure-foundation interactions

by

Prakriti Sharma

B.Eng., Pokhara University, 2015

Supervisory Committee

Dr. Cheng Lin, Co-Supervisor Department of Civil Engineering

Dr. Min Sun, Co-Supervisor Department of Civil Engineering

Abstract

Bridge failures in the past decade due to structural deficiencies demonstrated the clear need for a review of the current bridge analysis approaches. This study focuses on pile-supported bridges under predominantly static loading. A critical review of the current analysis approaches was performed. It was concluded that in the absence of an onerous iteration process, the current approaches often produce inaccurate and, in many cases, unsafe results since the interactions between superstructure and foundation are not fully considered. To address the inherent limitations of the current approaches, a computer program [Soil Spring Module (SSM) 2.0] was developed as a part of the study. SSM 2.0 can be used in conjunction with a frame analysis program to capture nonlinear load transfer from foundation elements to soil in different directions simultaneously. STAAD.Pro was selected for demonstration in this study. Using SSM 2.0 and STAAD.Pro, this study proposes a new analysis approach using the Integrated Analysis Process (IAP). The same methodology can be applied in other frame analysis programs. Kansas Bridge 45 was selected as a case study. Using the IAP approach, a series of integrated analyses including all superstructure elements (e.g., deck, girders and piers) and all foundation elements (e.g., pile caps and piles) were performed on Kansas Bridge 45 for different soil types and properties. Different from the conventional approaches, the full interactions between superstructure and foundation were considered simultaneously in a single analysis using the IAP approach. The analysis results from the IAP approach and the conventional approaches were examined. The advantages of the IAP approach were identified. Comparing to the conventional approaches in current practice, the proposed IAP approach does not involve crude assumptions or intensive iterations. Using the IAP approach, design engineers can complete structural and foundation analysis of pile-supported

bridges with good accuracy in a timely manner. The same methodology can potentially be applied to other structure types.

Table of Contents

List of Tables

List of Figures

List of Symbols

α	dimensionless shaft friction factor for cohesive soil
A_s	a constant for y_{50}
b	pile diameter
β	dimensionless shaft friction factor for cohesionless soil
c_u	undrained shear strength
e_{50}	principal strain @ 50 %
EI	flexural stiffness
f	unit shaft friction
ϕ	effective friction angle
γ'	average effective unit weight of the soil
k	subgrade modulus
N_q	dimensionless bearing capacity factor
N_{60}	mean uncorrected standard penetration test (SPT) blow count at the point of when 60 % of the hammer energy is transferred to the drill string
p	lateral soil resistance
p_{ult}	ultimate soil resistance
q	the unit end bearing
σ_v	effective vertical stress
y	lateral displacement
y_{50}	lateral displacement at one half the p_{ult}
z	depth from ground surface
SBC	simplified boundary condition
SSM	soil spring module
EPL	equivalent pile length
IAP	integrated analysis process
MAD	maximum allowable displacement
k_{qz}	elastic soil spring of q-z
k_{tz}	elastic soil spring of t-z curve
$k_{ij,py}$	slope of p-y at point of calculation zi and lateral displacement yj
$k_{ij,qz}$	slope of q-z curve at a point of calculation zi and displacement yj
$k_{ij,tz}$	slope of t-z curve at a point of calculation zi and displacement yj
L_i	length of element at a point of calculation zi
A_{ci}	surface area of the pile segment at point of calculation zi
$K_{ij,\ py}$	Multilinear soil spring of p-y curve at a point of calculation z_i and lateral displacement y_j

$K_{ij,\ tz}$	Multilinear soil spring of t-z curve at a point of calculation z_i and axial displacement z_j
$K_{ij,\ qz}$	Multilinear soil spring of q-z curve at a point of calculation z_i and axial displacement z_j
K_{FX}	superstructure stiffness along translational X
K_{FY}	superstructure stiffness along translational Y
K_{FZ}	superstructure stiffness along translational Z
K_{MX}	superstructure stiffness along rotational X
K_{MY}	superstructure stiffness along rotational Y
K_{MZ}	superstructure stiffness along rotational Z

Acknowledgement

First of all, I would like to thank my supervisors Dr. Cheng Lin and Dr. Min Sun for providing me the opportunity to work on this project and pursue my MASc program at the University of Victoria. I cannot emphasize enough, how their patience, invaluable guidance, kindness and constant motivation throughout this degree has helped me complete the research work as well as this thesis. Despite their busy schedule, they were always available to help me with any issue. In addition, their diligence and enthusiasm have been inspiring factors for me to pursue further even during tough times.

Moreover, I take this opportunity to thank the staffs of the Department of Civil Engineering for their constant efforts and prompt services that helped me a lot with my administrative and technical queries.

I am also grateful towards my lab mates in CARSA and E-hut for proving me with a great company, and making my time at the university fun and memorable.

I would also like to extend my sincere gratitude towards my friends Mahesh Khatiwada and Karan Tongay for their generous support during different stages of my research.

Finally, I am very grateful to my friends and family for continuously supporting me throughout my MASc journey and the life in general. The life during the pandemic has not been so easy for many of us and it is the immense support and love of these wonderful people in my life that acted as a constant source of motivation.

1 Introduction

Bridge failures in the past decade due to structural deficiencies [1] demonstrated the clear need for a review of the current bridge analysis approaches. This study focuses on pile-supported bridges. In current practice, frame analysis programs (e.g., STAAD.Pro, SAP2000, and RISA) are often used to model bridge superstructure (deck, girders and piers). For complete modelling of bridge superstructure, foundation loads and pier base boundary conditions (often in the form of nonlinear springs) must be defined first. Since the existing frame analysis programs are in general not capable of capturing nonlinear load transfer from foundation to soil in different directions simultaneously [2] [3], design engineers often pair them with special-purpose foundation analysis programs (e.g., LPILE and FB-MultiPier). The foundation analysis programs are often used to compute internal forces, deflection, and soil response over the length of pile. The results can then be used to compute and define, in the frame analysis programs, the foundation loads and spring stiffnesses at the bottom of bridge superstructure (i.e., pier bases). However, as a result of the causality dilemma, often the above approach cannot adequately consider the interaction among soil, pile foundation and bridge superstructure [2] [3]. In practice, a foundation analysis is usually performed prior to a complete bridge superstructure analysis. For a complete foundation analysis, loading and support conditions at pile head need to be defined in the special-purpose programs. However, such pile head loading and boundary conditions cannot be determined accurately until the superstructure analysis is completed which requires the input from the foundation analysis. Therefore, in the absence of a very intensive iteration process, when using the above approach, crude assumptions are often made by the design engineers throughout the analysis. The details of the conventional approaches are discussed in Chapter 2.

In this study, a computer program [Soil Spring Module (SSM) 2.0] is developed (Chapter 3). SSM 2.0 can be used in conjunction with a frame analysis program to capture nonlinear load transfer from foundation to soil in different directions simultaneously. STAAD.Pro [4] is selected for demonstration in this study. The same methodology can be applied in other general frame analysis programs. By entering the required parameters in the user interface of SSM 2.0, the computer program can be used to:

(a) generate and mesh pile foundations in STAAD.Pro;
(b) add nonlinear springs over the length of pile in different directions based on state-of-the-art literature and procedures; and
(c) launch an integrated analysis in STAAD.Pro including all superstructure elements (e.g., deck, girders and piers) and all substructure elements (e.g., pile caps and piles).

Using the integrated approach, design engineers can complete structural and foundation analysis of pile-supported bridges with good accuracy in a timely manner. Comparing to the conventional approaches in current practice, the integrated approach does not involve crude assumptions or intensive iteration since all computation is performed at the same time in the frame analysis program. In Chapter 4, Kansas Bridge 45 is selected as a case study. The bridge analysis results from different approaches are evaluated and compared in Chapter 5. The case study covers a wide range of soil types and properties. Chapter 6 includes conclusions and design recommendations.

2 Current approaches

In a frame analysis program, the definition of boundary conditions is critical in the assemble of stiffness matrices. The underlying assumptions (e.g., pinned, semi-rigid, or rigid supports) affects the static and dynamic responses of the structure model. This study focuses on pile-supported bridges under predominantly static loading. The same methodology can potentially be applied to other bridge types and loading conditions.

According to the PEER bridge analysis guidelines [5], for "Ordinary Standard bridge structures" with "normal soil conditions", the underlying soil can be assumed rigid, where the soil-structure interaction can be safely ignored. For "Ordinary Standard bridge structures" with "non-conventional soil conditions", [5] suggests the use of semi-rigid connections at the pier bases in the bridge superstructure model. For "Nonstandard and Important bridge structures", soil-structure interaction should always be considered in the analysis. Therefore, depending on the type of bridge structure and soil condition, the interaction between pile shaft and soil often has a significant effect on the response of bridge model. In particular, the soil-pile interaction introduces flexibility to pier bases, which can be different from the simple assumption of pinned or rigid supports. In general, the pier-base boundary conditions defined in the frame analysis programs are verified with the geotechnical report. However, as discussed in Chapter 1, due to the causality dilemma (special-purpose foundation analysis program versus general frame analysis program), especially in the initial design stage, it can be challenging to perform an integrated analysis in the absence of an intensive integration process. Therefore, simplified approaches based on crude assumptions are often used in the initial design stage. Several of the commonly used simplified approaches are shown in Fig 2.1, including Simplified Boundary Condition (SBC) method, Maximum Allowable

Displacement (MAD) method and Equivalent Pile Length (EPL) method. The background, detailed procedures and limitations of the simplified approaches are discussed in Section 2.1-Section 2.3.

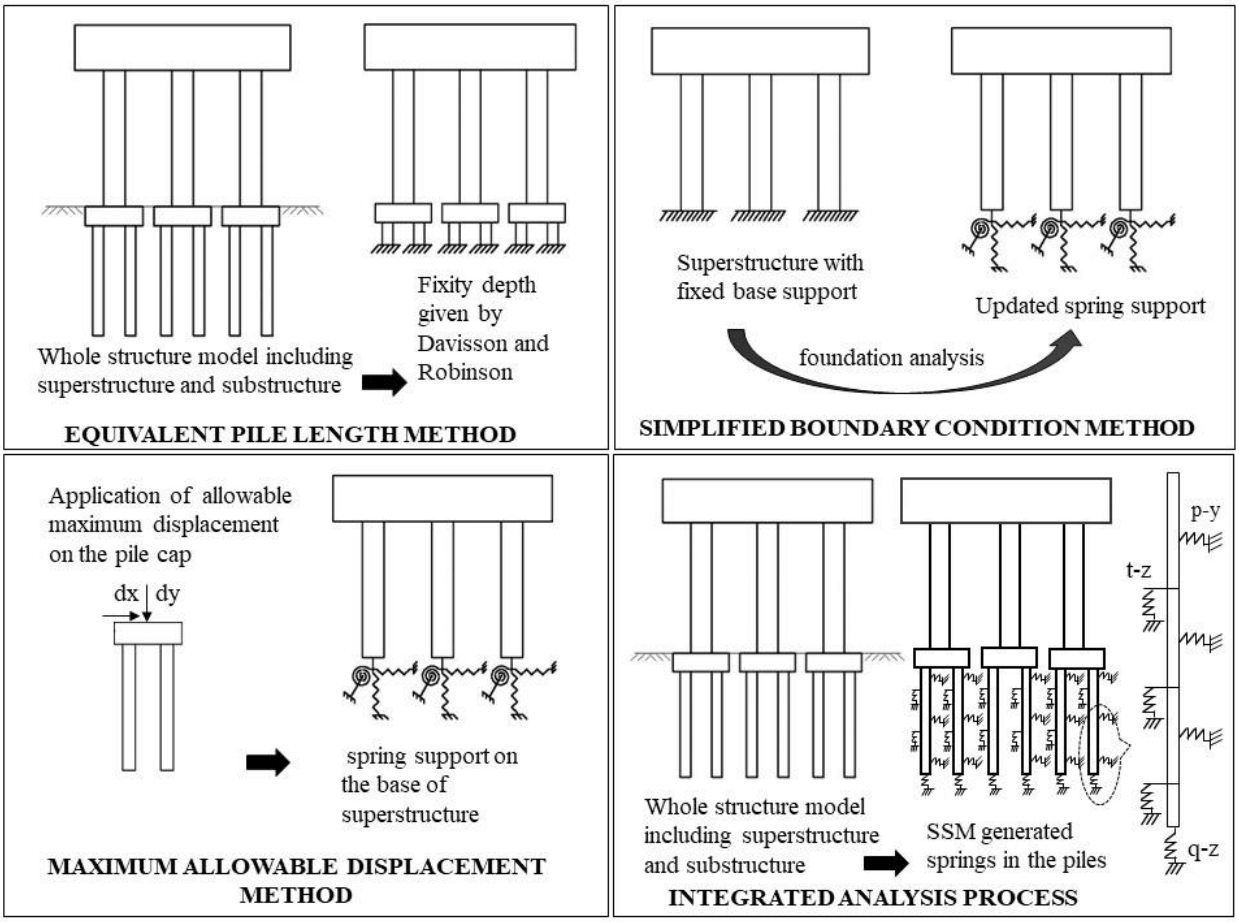

Fig 2.1: Different analysis approaches

This research aims to propose an Integrated Analysis Process (IAP) using SSM 2.0 in conjunction with a general frame analysis program. IAP is developed based on state-of-the-art literature and procedures. Different from the simplified approaches, design engineers can use IAP to perform accurate bridge analysis even in the initial design stage without an intensive interaction process. In other words, design engineers can use IAP to achieve accurate analysis in a timely

manner at a much earlier design stage, comparing to the conventional approaches. The basic procedures of IAP are shown in Fig 2.1, with the details discussed in Chapter 3.

2.1 Simplified Boundary Condition (SBC) approach

The Simplified Boundary Condition (SBC) method is commonly used in the initial design stage [2][3], where all degrees of freedom of the pier bases (of the bridge superstructure model) are fixed in the general frame analysis program. As shown in Fig 2.1, support reactions at the fixed pier ends are extracted from the general frame analysis program and are subsequently used to define the pile head loading conditions in the foundation analysis program. As discussed previously, at the initial design stage, the exact fixities at the pier bases are unknown. Therefore, in the foundation analysis program, the pile head boundary conditions are typically defined as follows:

(a) "Free head" where all six degrees of freedoms are free, or
(b) "Fixed head" where the translational degrees of freedoms are free while the rotational degrees of freedoms are arrested.

In this research, LPILE [6] is selected for demonstration. The same methodology can be applied in other special-purpose foundation analysis programs. Both free head and fixed head assumptions are examined in Chapters 4 and 5. In both cases, LPILE computes the internal forces, displacement (translational and rotational), and soil response over the length of pile. For each degree of freedom, by dividing the applied force (or moment) by the corresponding maximum translational (or rotational) displacement at the pile head, a single stiffness value can be obtained. As the start of a second interaction, these stiffness values can be used to define semi-rigid boundary

conditions of the pier bases (in the form of springs) in the bridge superstructure model in STAAD.Pro. In theory, after an intensive interaction process, reasonably accurate bridge analysis can be achieved when the displacements (in all degrees of freedom) of the pier bases and the pile heads converge. However, this may be deemed impractical in a typical design office considering the large computational effort, especially in the early design stages. Therefore, the internal forces computed from the general frame analysis program after one or two iterations are often used for preliminary sizing of bridge elements, which in some cases can be far from accurate [3]. As discussed in previous sections, such limitation mainly comes from the use of separate programs for the foundation and bridge superstructure analysis. Different from the conventional approach, this research aims to overcome this limitation by running all analysis in a single computer program (e.g., STAAD.Pro) by using SSM 2.0.

2.2 Maximum Allowable Displacement (MAD) approach

Other than force capacity, special attention must also be paid to displacement capacity of bridge elements. Current engineering practice and design standards usually impose criteria on the maximum allowable displacements. Prior to a comprehensive analysis, the recommended maximum allowable displacements serve as a conservative presumptive criterion for bridge analysis. This is in particular convenient for the initial design stage where full details of the bridge superstructure are not yet available. For example, ATC-32 [7] recommends the following tolerable foundation displacements:

(a) Lateral displacement: up to 50 mm, and/or

(b) Rotational displacement: up to 0.008 radian.

However, it should be noted that, the selection of appropriate allowable pile head deflection depends on the bridge type and soil condition and requires engineering expertise and judgement [7][8][9]. Therefore, there is no unified rule on the selection of such values. In this study, no rotational displacement is applied, and for the translational, the following displacements are used:

(a) Lateral displacement: 25 mm

(b) Vertical displacement: 25 mm

As shown in Fig 2.1, the above displacements are applied to the pile head in LPILE. The necessary force/moment to generate such displacements are computed. Similar to the foundation analysis procedures in Section 2.1, by dividing the necessary force/moment by the corresponding pile head displacement, a single stiffness value can be obtained for each degree of freedom. The values are then used to define pier base spring stiffnesses in STAAD.Pro for the bridge superstructure analysis, so that the internal forces in the bridge elements can be computed.

It should be noted that, as stated in ATC-32 [7], the above maximum allowable displacements serve as a conservative presumptive criterion for bridge analysis. Therefore, the maximum allowable displacements should in theory be larger than those in Section 2.1. The details are discussed in Chapter 5. Since LPILE and the other special-purpose foundation analysis program are developed based on finite-difference method and nonlinear force-displacement curves, the spring stiffness values obtained using the MAD method should in theory be smaller than those from the SBC method in Section 2.1.

In conclusion, the MAD method has the same limitation as the SBC method. Reasonable accuracy of bridge analysis can only be achieved after an onerous iteration process, which is not always practical in the early design stages.

2.3 Equivalent Pile Length (EPL) approach

As discussed in the previous sections, the pier base supports in bridge analysis is usually considered to be rigid or semi-rigid. The simplified approach, proposed by Davisson & Robinson [10], can be used to approximate the pier base fixity, by calculating the Equivalent Pile Length (EPL). This approach presents the procedure to calculate depth to fixity for piles with various depths of embedment and unimbedded lengths, and convert it into a cantilever beam. The fixity depth differs according to the flexural stiffness of the pile and the magnitude and variation of soil resistance with respect to depth. The recommendation provided by Davisson & Robinson [10] for the fixity depth expressed in non dimensional terms, in case of cohesive and cohesionless soil is given as following:

(a) For cohesive soil

$$Equivalent\ depth\ to\ fixity = 1.4R \tag{2.1}$$

$$\mathrm{R} = 4\sqrt{(EI/k)} \tag{2.2}$$

where, EI = flexural stiffness of pile (N.m^2)

k = subgrade modulus = $67c_u$ (kN/m^2/m)

c_u = undrained shear strength (kN/m^2/m)

(b) For cohesion less soil,

$$Equivalent\ depth\ to\ fixity = 1.8\text{T} \tag{2.3}$$

$$T = 5\sqrt{(EI/k\ )} \tag{2.4}$$

where, EI = flexural stiffness of pile ($N.m^2$)

k = subgrade modulus ($kN/m^2/m$) = 407.17 for loose sand and over 27145 for dense sand.

In this research, the above method of calculation is used to calculate the fixity depth of piles and the bridge structure with fixed support at the calculated depth below pile cap was modelled, as shown in Fig 2.1, in STAAD.Pro. This method approximates the foundation behaviour, which simplifies the influence of substructure in the analysis.

3 Integrated Analysis Process (IAP)

Integrated Analysis Process (IAP) is an improved analysis method that directly considers the full interaction of soil, foundation, and superstructure elements at the same time. The application of IAP involves the use the computer program [Soil Spring Module (SSM) 2.0] developed in this study. SSM 2.0 can be used in conjunction with a frame analysis program to capture nonlinear load transfer from foundation to soil in different directions simultaneously. STAAD.Pro [4] is selected for demonstration in this study. The same methodology can be applied in other general frame analysis programs. Using the IAP approach, design engineers can complete structural and foundation analysis of pile-supported bridges with good accuracy in a timely manner. When compared with the conventional approaches in current practice, the integrated approach does not involve crude assumptions or intensive iteration since all computation is performed at the same time in only the frame analysis program.

As discussed in Chapter 2, the current approaches (SBC, MAD and EPL) assume the boundary conditions and approximate the foundation or superstructure analysis without fully accounting for soil-structure interaction. In addition, these approaches perform separate analyses for superstructure and foundation in separate software packages. It should also be noted that in general it is very challenging to consider multi-directional nonlinear soil behaviour in the existing commercial structural frame analysis software (e.g., STAAD. Pro). Therefore, SSM 1.0 was developed by Lin et al. [11] to address these issues. The use of SSM 1.0 can:

(1) generate and mesh pile foundations in STAAD.Pro;

(2) add nonlinear springs over the length of pile in the lateral directions based on state-of-the-art literature and procedures; and

(3) launch an integrated analysis in STAAD.Pro including all superstructure elements (e.g., deck, girders and piers) and all substructure elements (e.g., pile caps and piles).

It should be noted that SSM 1.0 only applies lateral soil displacement curves (i.e., p-y curves). As a part of this study, SSM 2.0 is developed to apply also axial load displacement curves (i.e. t-z and q-z curves). Therefore, SSM 2.0 can be used to add nonlinear springs over the length of pile in both lateral and vertical directions in commercial structural frame analysis program. In the current version, SSM 2.0 is developed to work in pair with STAAD.Pro as an extension. The seamless link between the SSM 2.0 and STAAD.Pro was obtained with the help of Open STAAD 2.6 in STAAD.Pro which allows an external program to access its internal graphics and commands.

When using IAP and SSM 2.0 for analysis of the entire structure, the user will first create the super- and sub-structure elements in STAAD.Pro. The user will then select the pile groups and run SSM 2.0. SSM 2.0 has a graphical user interface (GUI) where a series of soil parameters can be selected (or customized), to automatically generate nonlinear soil springs in different directions over the entire lengths of all the piles selected in STAAD.Pro. The STAAD.Pro model can then be analysed in an integrated manner. The background and details of SSM is discussed in this Chapter.

3.1 Soil Spring Module (SSM) and modification

The development of SSM 1.0 is explained in detail in the DOT report by Lin et al. [11]. The program, written in Visual Basic 2010 Express, has many subroutines with specific tasks. There is a subroutine of inputted soil and pile parameters, a subroutine for the generation of elastic and multilinear soil springs, a subroutine for the assignment of those soil springs, as well as a subroutine that performs scour analysis and P-Delta analysis. OpenSTAAD functionality in

STAAD.Pro allows the SSM to fetch pile parameters from a model as well as assign the generated soil spring curves in SSM to pile or pile groups to the model in STAAD.Pro. A graphical user interface of SSM which appears after the program is run, includes various commands described in Section 3.3. These commands allow users to input all the necessary values and soil parameters to generate nonlinear soil springs.

SSM 1.0 enabled users to analyze laterally loaded pile foundations with the help of series of nonlinear springs which are derived from families of p-y where p represents the soil resistance while y is the lateral displacement. The SSM allowed the input of parameters for 7 different types of soil including user input to generate respective lateral soil springs which has now been improved to include axial soil springs (derived from t-z and q-z curves) as well. Hence, the modified SSM also called as SSM 2.0, has additional task for some of the subroutines to allow the input of soil types and corresponding properties for axial curves (t-z and q-z) and generate the elastic and multilinear axial soil springs associated with the curves. Moreover, SSM 1.0 divided a pile or a group of piles modelled in STAAD.Pro into 20 different segments and assigned lateral soil springs in each of them, while SSM 2.0 divides a pile into 40 segments, and each segment is assigned either p-y or t-z soil springs, arranged one after the other and q-z spring at the bottom of the pile. There are additional 5 types of axial curves (t-z and q-z) programmed in SSM 2.0 which are illustrated in the section 3.3 while for all the p-y curves already present in SSM 1.0, DOT report by Lin et al. can be referred. However, illustrations of some of the p-y curves which are used in the case study of this thesis are presented in Section 3.2.

3.2 Soil Models for p-y curves

SSM 1.0 incorporates p-y curves, developed based on full-scale tests, and given by various methods such that laterally loaded pile foundations can be analysed. The soil springs derived from these p-y curves represent the lateral soil resistance provided by the surrounding soil in the embedded length of pile. The p-y curves vary for different soil types, loading types, soil depth and pile parameters. The types of p-y curves generated for the laterally loaded piles in the SSM, are soft clay, stiff clay in the presence of free water, stiff clay above free water, Reese sand, API sand, silt, a c- ϕ soil, strong rock, weak rock, and user defined. The details of the p-y theories for all these soil types can be found in Reese and Van Imp (2001) [12], API (1987) [13] and Lin et al (2011) [11]. Soft clay, stiff clay in presence of free water and API sand were used to model lateral soil behaviour for the parametric study in this thesis. The theories of p-y methods for these 3 soil types are described below.

3.2.1 Soft clay

The p-y curve for soft clay used in SSM is given by Matlock, 1970 [14], and it is represented by the Equation 3.1. The p-y curve is illustrated by the Fig 3.1.

$$p = \frac{p_{ult}}{2}\left(\frac{y}{y_{50}}\right)^{1/3}, y < 8y_{50} \tag{3.1}$$

$$p = p_{ult}, y > 8y_{50}$$

where, y_{50} = lateral displacement at half of $p_{ult.}$

p_{ult} = ultimate soil resistance, smaller of the values given by Equations 3.2 and 3.3

$$p_{ult} = \left[3 + \frac{\gamma'}{C_u} z + \frac{J}{b} z\right] C_u b \tag{3.4}$$

$$p_{ult} = 9 c_u b \tag{3.3}$$

where, γ' = average effective unit weight of the soil,

z = depth from ground surface,

c_u = average undrained shear strength = typical values have been provided in the Table 3.1

J = a constant = determined experimentally to be as 0.5 and

b = pile diameter

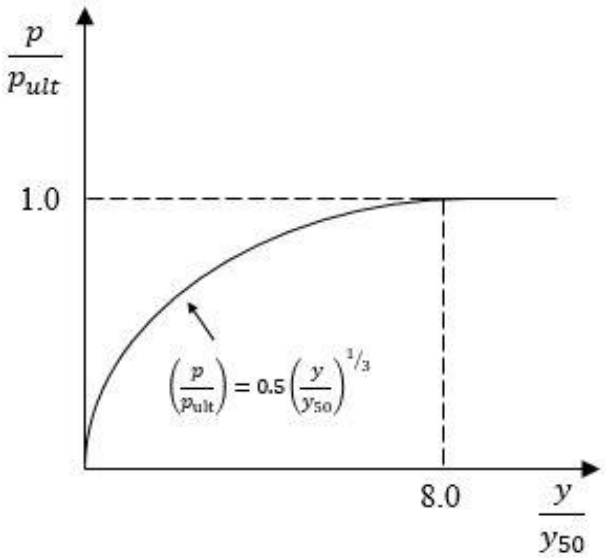

(Source: Reese and Van Impe 2001) [12]

Fig 3.1: Illustration of p-y curves in Soft Clay

Table 3.1 Representative values of cu and ε_{50} for normally consolidated clays

Consistency of clay	Undrained shear strength* , c_u (kPa)	Principal Strain @ 50 % (ε_{50})
Soft	<48	0.02
Medium	48-96	0.01
Stiff	96-192	0.005

*(Peck et al. 1974) [15]

(Source: Reese and Van Impe 2001) [12]

3.2.2 Stiff clay in the presence of free water

The p-y curves for stiff clay in presence of free water was proposed by Reese et al. (1975) [16] which was developed based on lateral load tests on two 0.6 m diameter steel piles embedded in stiff clay under water table at Manor, Texas. The curve composed of five portions (Equation 3.4 - 3.11) and is presented by Fig 3.2. The illustrations of the p-y curves for short term static loading is given below.

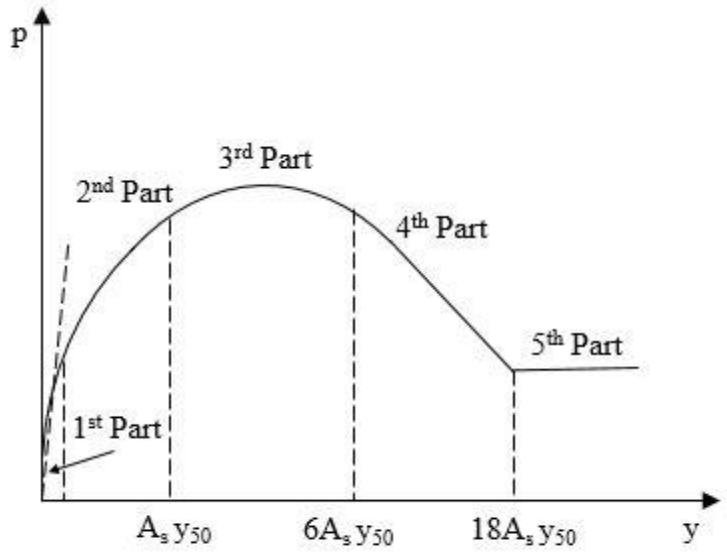

(Source: Reese and Van Impe 2001) [12]

Fig 3.2: Illustration of the p-y curves for stiff clay in the presence of free water

The first linear portion of the p-y curve, is given by the Equation 3.4

$$p = (k_s z)y \tag{3.5}$$

where, k_s = coefficient of subgrade reaction and the appropriate values are shown in Table 3.2.

Table 3.2 Representative values of cu, ε_{50} and ks for over consolidated clays

Average undrained shear strength*, c_u (kPa)	Principal Strain @ 50 %, ε_{50}	Coefficient of subgrade reaction, k_s (MN/m^3) (static loading)
50-100	0.007	135
100-200	0.005	270
300-400	0.004	540

*The average undrained shear strength should be computed from the shear strength of the soil to a depth of five pile diameters.

(Source: Reese and Van Impe 2001) [12]

The initial parabolic portion of the p-y curve is established by equation 5. The equation defines the portion of the p-y curve from the point of intersection with equation 4 to a point where y is equal to $A_s y_{50}$.

$$p = \frac{p_{ult}}{2}\left(\frac{y}{y_{50}}\right)^{1/2} \tag{3.6}$$

where, p_{ult} =ultimate soil resistance whose value is taken as the smaller of the values given by the Equations 3.6 and 3.7.

$$p_{ult} = \left[2 + \frac{\gamma'}{c_u} z + \frac{2.83}{b} z\right] c_u b \tag{3.6}$$

$$p_{ult} = 11c_u b \tag{3.7}$$

y_{50} = lateral displacement at one half the p_{ult} and can be computed from the Equation 3.8,

$$y_{50} = \varepsilon_{50} b \tag{3.8}$$

where, ε_{50} = principal strain @ 50% and it can be used from Table 3.1 in the absence of results of laboratory tests.

Similarly, the second parabolic portion or the 3rd part of the p-y curve is given by Equation 3.9

$$p = \frac{p_{ult}}{2}\left[\frac{y}{y_{50}}\right]^{0.5} - 0.055 p_{ult}\left[\frac{y - A_s y_{50}}{A_s y_{50}}\right]^{1.25} \tag{3.9}$$

where, A_s = a constant for y_{50}, whose value can be determined from the Fig 3.3.

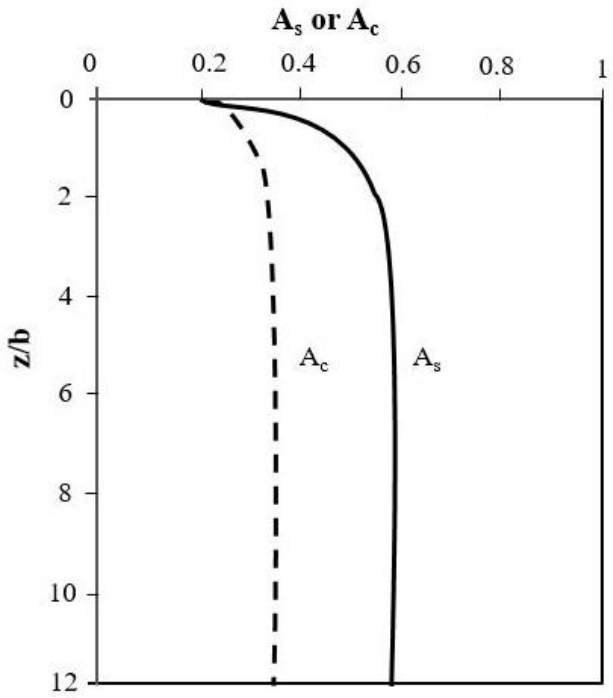

(Source: Reese and Van Impe 2001) [12]

Fig 3.3: Values of constants A_c and A_s

Equation 3.10 establishes the next straight-line portion of the p-y curve.

$$p = \frac{p_{ult}}{2}\sqrt{6A_s} - 0.411p_{ult} - \frac{0.0625}{y_{50}}p_{ult}(y - 6A_s y_{50}) \tag{3.10}$$

This defines the portion of the of the p-y curve from the point where y is equal to $6A_s y_{50}$ to a point where y is equal to $18A_s y_{50}$

The final straight line portion of the p-y curve is established by the Equation 3.11.

$$p = \frac{p_{ult}}{2}\sqrt{6A_s} - 0.411p_c - 0.75p_c A_s \tag{3.11}$$

It defines the portion of the p-y curve from the point where y is equal to $18A_s y_{50}$ and for all larger values of y.

3.2.3 API sand

The lateral soil resistance- deflection (p-y) relationship for sand in case of short term static loading recommended by American Petroleum Institute (API), 1987 [13] is given by the following expression:

$$p = Ap_{ult}tanh\left(\frac{kz}{Ap_{ult}}y\right) \tag{3.12}$$

where, A= a factor to account for static or cyclic loading and for static loading it is given by Equation 3.13.

$$A = \left(3 - 0.8\,\frac{z}{b}\right) \geq 0.9 \tag{3.13}$$

k =the initial modulus of subgrade reaction, (kN/m^3), and is determined from Fig 3.4

p_{ult} = ultimate soil resistance, and is taken as smaller of the values computed by Equations 3.14 and 3.15.

$$p_{ult} = \gamma' z\left[\frac{K_0\, z \tan\phi\ \sin}{\tan(\beta-\phi)cos\alpha} + \frac{\tan\beta}{\tan(\beta-\phi)}(b + z\tan\beta\tan\alpha)\right.$$
$$\left. + K_o z\tan\beta(\tan\phi\sin\beta - \tan\alpha) - \quad K_A\, b\right] \tag{3.14}$$

$$p_{ult} = K_A b\gamma z(tan^8\beta - 1) + K_o b\gamma z tan\phi tan^4\beta \tag{3.15}$$

where, $a = \frac{\phi}{2};\ \beta = 45 + \frac{\phi}{2}; K_o = 0.4;\ K_A = tan^2(45^o - \frac{\phi}{2})$

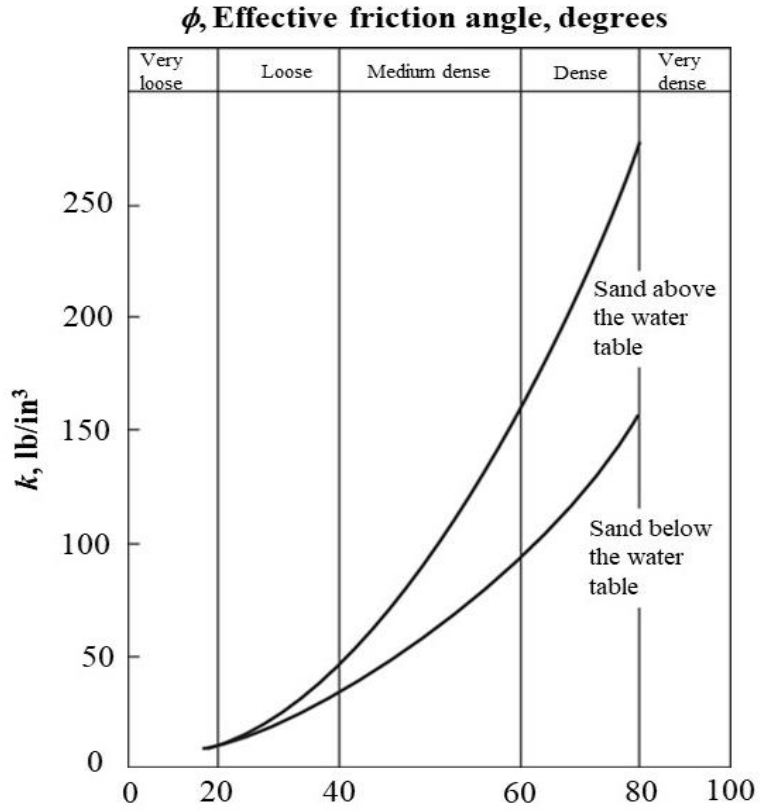

(Source: API 1987) [13]

Fig 3.4: Value of coefficient of subgrade reaction k, used for API sand criteria

3.3 Soil models for t-z and q-z curves

As discussed earlier in Chapter 3, SSM 1.0 only applies lateral soil displacement curves (i.e., p-y curves). As a part of this study, SSM 2.0 is developed to apply also axial load displacement curves (i.e., t-z and q-z curves). Therefore, SSM 2.0 can be used to add nonlinear springs over the length of pile in both lateral and vertical directions in commercial structural frame analysis program. The addition of these curves in SSM 2.0 simulates the nonlinear behaviours due to soil skin friction and end bearing resistance respectively.

Specifically, the t-z and q-z curves recommended by the API [13], and Reese O' Neil [17], were incorporated in SSM 2.0 for cohesive and cohesionless soils in case of driven pile and drilled shaft, to account for the axial loads. For the input, development and validation of axial soil springs, generated in SSM 2.0, the user manual of Tzpile (2014) [18] as well as the STAAD. Pro manual 2007 [4] were used.

The ultimate axial load capacity of piles in compression is given by the following equation

$$Q_c = Q_s + Q_p = \int_0^L f(z)p(z)dz + qA_p \tag{3.16}$$

where, q_s = shaft friction capacity in compression, in force units and is obtained by integrating the shaft friction between the pile and the soil along the pile's imbedded length (L)

q_p = tip end bearing capacity, in force units,

f(z) = unit shaft friction in stress units,

p(z) = pile perimeter,

q = unit end bearing at the pile tip, in stress units,

A_p = gross end area of the pile

z = depth below the ground surface.

3.3.1 API clay (driven pile)

Driven piles are prefabricated piles which are driven into the ground using a pile driving hammer. The SSM employs the recommendation provided by American Petroleum Institute (API)

for the calculation of ultimate skin friction, ultimate end bearing resistance, skin friction (t-z) load transfer curves and end bearing curves (q-z) curves for driven piles in cohesive soil. [13] The unit shaft friction, f(z) at depth z, for pipe piles in cohesive soil can be calculated using the given Equation 3.17.

$$f(z) = \alpha c_u \tag{3.17}$$

where, α = dimensionless shaft friction factor, for clays which is calculated from the Equations 3.18 and 3.19

c_u = undrained shear strength of the soil at the calculation point.

$$\alpha = \frac{1}{2}\psi^{\frac{-1}{2}} \qquad for\ \psi \leq 1, \quad \alpha \leq 1 \tag{3.18}$$

$$\alpha = \frac{1}{2}\,\psi^{\frac{-1}{4}} \qquad for\ \psi > 1, \quad \alpha \leq 1 \tag{3.19}$$

where, $\psi = \frac{c_u}{\sigma_v\,(Z)}$

$\sigma_v(z)$ = effective vertical stress at depth z.

The t-z curves recommended by API for non-carbonated cohesive and cohesion less soils is given in Fig 3.5.

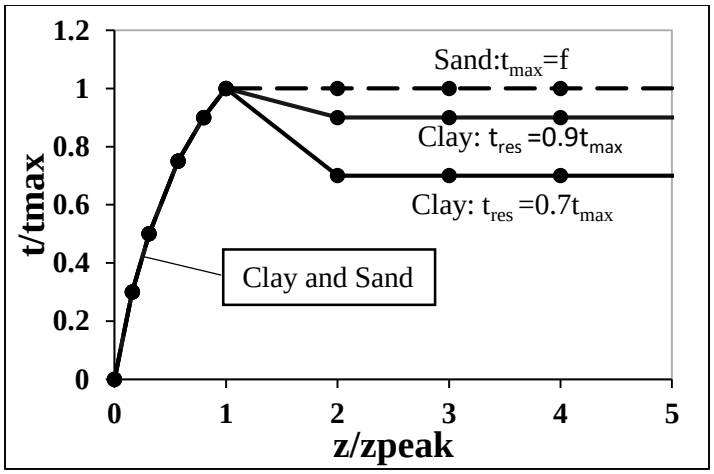

(Source : API 1987) [13]

Fig 3.5: Typical load-axial displacement (t-z) curves in cohesive and cohesionless soil

In the Fig 3.5, t is the mobilized soil-pile friction; t_{max} is the maximum soil pile friction or the unit shaft friction computed by Equation 16; t_{res} is the residual soil pile friction or unit shaft friction and the value of residual friction for cohesive soil ranges from $0.7t_{max}$ to $0.9\ t_{max.;}$ z is the local pile axial deflection, z_{peak} is the displacement of pile corresponding to maximum soil pile friction or unit shaft friction and its typical value is recommended to be 0.01 percent of the pile outer diameter (D) for routine design purposes. In case of non- circular pile cross section, an equivalent diameter is used which is computed by equating the cross- sectional area with the area of a circle. Table 3.2 illustrates the API tz curves for clay and sand used in the SSM.

Table 3.3 Definition of t-z curves recommended by API

Soil Displacement (z) / Pile Diameter (D)	mobilized shaft friction (t)/ maximum or unit shaft friction (t_{max})	
	Clay	**Sand**
0.0016	0.3	0.3
0.0031	0.5	0.5
0.0057	0.75	0.75
0.008	0.9	0.9
0.01	1	1
0.02	0.7 to 0.9*	1
∞	0.7 to 0.9*	1

*SSM employs the residual strength of API clay to be 0.9 times the maximum unit skin friction

Similarly, the unit end bearing, q, in cohesive soil can be computed using the Equation 3.20.

$$q = 9c_u \tag{3.20}$$

where, c_u = undrained shear strength at the pile tip.

The end bearing transfer (q-z) curves recommended by API is same for both the cohesive and cohesion less soil which is shown in Table 3.3 and Fig 3.6.

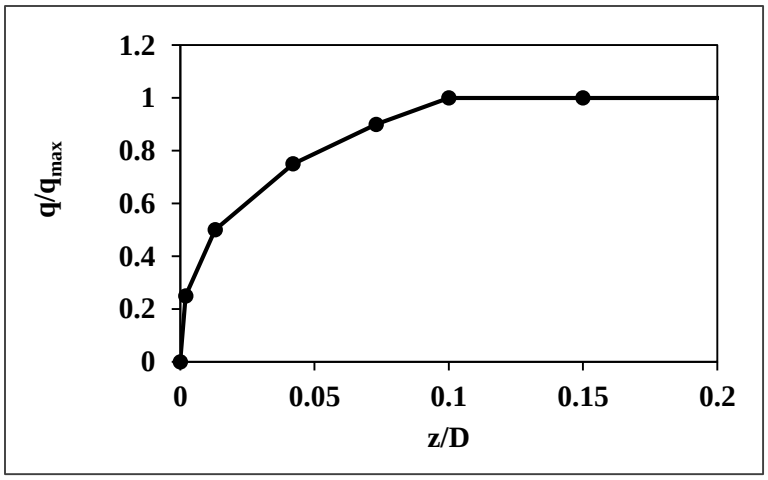

(Source: API,1987) [13]

Fig 3.6: API sand and clay end bearing (q-z) load transfer curve

Table 3.4 Definition of the API q-z curve

Soil Displacement/ Pile diameter (z/D)	Unit end bearing / maximum end bearing (q/q_{max})
0	0
0.002	0.25
0.013	0.5
0.042	0.75
0.073	0.9
0.1	1
∞	1

(Source: API, 1987) [13]

3.3.2 API sand (driven pile)

The unit shaft friction, f(z) at a depth z, for pipe piles in cohesion less soil can be calculated using the following equation:

$$f(z) = \beta \sigma_v(z) \tag{3.21}$$

where, β = dimensionless shaft friction factor, for sands whose values in case of open ended driven unplugged pipe piles is recommended in Table 3.4;

σ_v(z) = effective vertical stress at depth z.

The typical t-z curve recommended by API for cohseionless soil is given in Table 3.2 and Fig 3.5

The unit end bearing of piles, q, in cohesionless soils, in stress unit is computed using Equation 3.22

$$q = N_q \sigma_v \tag{3.22}$$

where, N_q = dimensionless bearing capacity factor whose recommended values are in Table 3.4.

SSM also has limited the value of q in case it exceeds the maximum unit end bearing values provided in the Table 3.4. Typical API q-z curve is given in Table 3.3 and Fig 3.6.

Table 3.5 Design parameters for cohesionless siliceous soil

Relative Density	**Soil Description**	**Shaft Friction Factor, β***	**Maximum Shaft friction values, kPa**	**End Bearing Factor, N_q**	**Maximum Unit End Bearing Values, MPa**
Very Loose	Sand				
Loose	Sand				
Loose	Sand-silt**				
Medium Dense	Silt				
Dense	Silt	N/A***	N/A***	N/A***	N/A***
Medium dense	Sand-silt**	0.29	67	12	3
Medium dense	Sand				
Dense	Sand-silt**	0.37	81	20	5
Dense	Sand				
Very Dense	Sand-silt**	0.46	96	40	10
Very Dense	Sand	0.56	115	50	12

*The shaft friction factor, β is given by K tan (δ) where δ is the soil pile friction angle and K is the coefficient of lateral earth pressure, whose API recommended value is 1 for full displacement piles and 0.8 for non displacement piles

**Sand-silt includes those soils with significant fractions of both sand and silt.

*** Design parameters for these soil combinations may be unconservative. So, it is recommended to use CPT-based methods

[The parameters listed in this table are intended as guidelines only]

.

3.3.3 Clay in drilled shaft pile

Drilled shaft foundations are formed by drilling a borehole into a ground and then filling a cast in place reinforced concrete piles into the borehole. SSM employs the method provided by Reese and O Neil, 1999 [17] for the computation of side resistance, base resistance and hence the axial load pile capacity of the drilled piles.

The unit side resistance for compression loading in cohesive soil is given as:

$$f(z) = \alpha c_u \tag{3.23}$$

where, α = dimensionless correlation coefficient whose value is considered 0 at exclusion zones.

Exclusion zone includes a depth of 1.5 m from the ground and a distance of B (the diameter of the shaft base) above the base of the pile or periphery of bell in case of belled shaft. Elsewhere the value of α is 0.55.

The base resistance for compression loading in cohesive soil is given as,

$$q(z) = 9c_u \qquad If\ c_u \geq 96\ kPa \tag{3.24}$$

$$q(z) = N_c^*\, c_u = \left(\frac{4}{3}\right)[ln(I_r + 1)]c_u \qquad If\ c_u < 96\ kPa \tag{3.25}$$

The values of N^*_c and I_r are given in Table 3.5. Linear interpolation is used for the values between those tabulated.

Table 3.6 Values of Ir and Nc*

c_u	I_r	N^*_c
24 kPa	50	6.5
48 kPa	150	8
≥96 kPa	250–300	9

(Source: Reese and O Neil, 1999)[17]

The normalized load transfer curves given in Fig 3.7 and Fig 3.8 developed by Reese and O Neil based on the study of tests of drilled shafts has been used for the generation of t-z and q-z curves in the SSM.

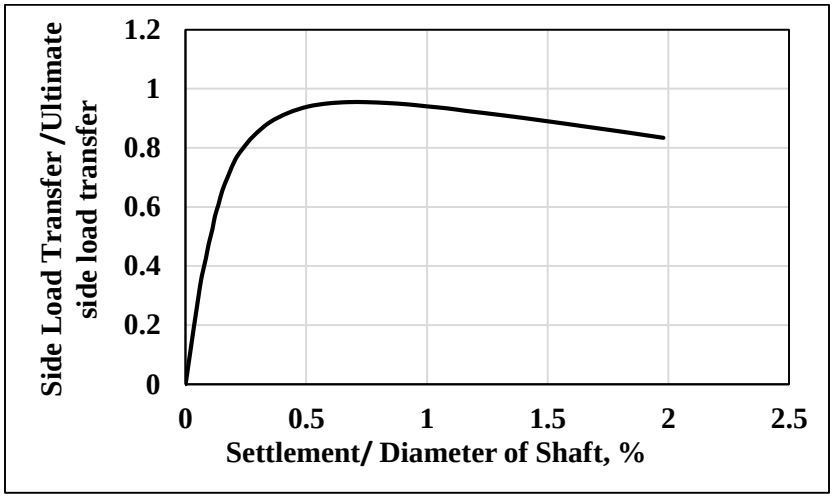

(Source: Reese and O'Neil, 1988) [17]

Fig 3.7: Normalized t-z curve for drilled shaft in clay*

*The Fig only includes the trend line of the curve which has been used in SSM 2.0.

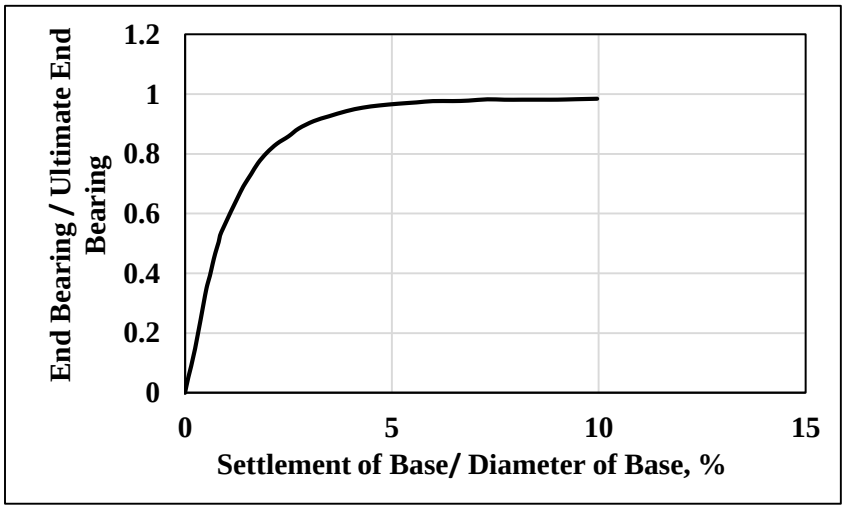

(Source: Reese and O' Neil, 1988) [17]

Fig 3.8: Normalized base load transfer (q-z) curve for drilled shaft in clay*

*The Fig only includes the trend line of the curve which has been used in SSM 2.0

3.3.4 Sand in drilled shaft pile

The unit side resistance for compression loading in cohesionless soil is given by Equation 3.26.

$$f_{max} = \beta \sigma'_v \qquad f_{max} \leq 200\ kPa \tag{3.26}$$

where, β = dimensionless correlation factor, whose value is given in Equation 3.26 and 3.27

σ_v = vertical effective stress at the point of calculation.

In sands,

$$\beta = 1.5 - 0.245 z_i^{0.5} \qquad 0.25 \leq \beta \leq 1.2\ and\ SPT\ 50 > N60 \geq 15\ blows/0.3m \tag{3.27}$$

$$\beta = \left[\frac{N_{60}}{15}\right]\left\{1.5 - 0.245 z_i^{0.5}\right\} \qquad 0.25 \leq \beta \leq 1.2\ and\ SPT\ N60 < 15\ blows/0.3m \tag{3.28}$$

In gravelly sands,

$$\beta = 2 - 0.15 z_i^{0.75} \qquad 0.25 \leq \beta \leq 1.8 \text{ and } SPT\ N60 \geq 15\ blows/0.3\ m \tag{3.29}$$

where, N_{60} = mean uncorrected standard penetration test (SPT) blow count at the point of when 60% of the hammer energy is transferred to the drill string, which should not exceed 50 blows/0.3 m

z_i = vertical distance from the ground surface.

The unit base resistance for compression loading in cohesionless soil is given as,

$$q_{max} = 57.5\ N_{60} \qquad q_{max} \leq 2.9\ MPa \quad N60 \leq 50\ blows/0.3\ m \tag{3.30}$$

The normalised load transfer curves (t-z and q-z) are given in Fig 3.9 and Fig 3.10.

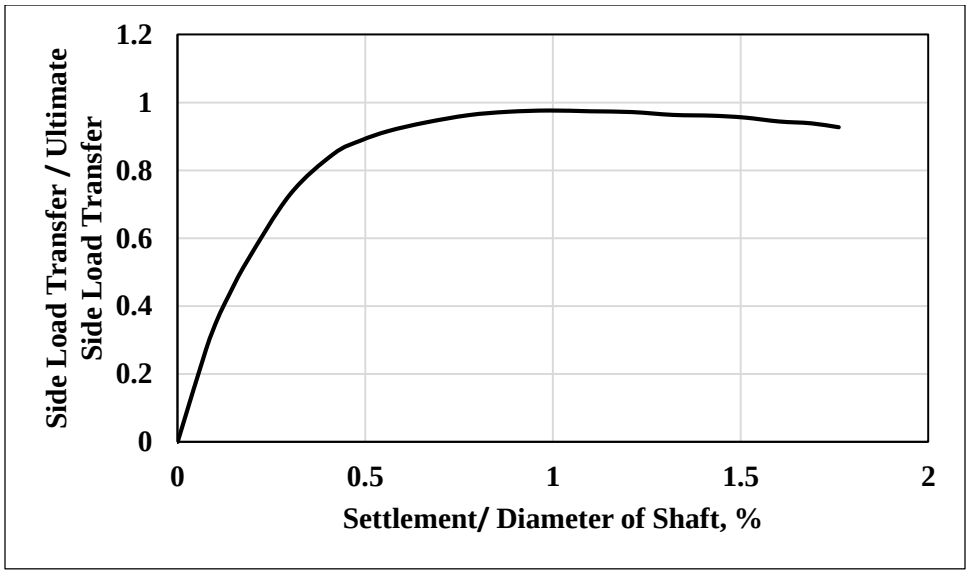

(Source: Reese and O'Neil, 1988) [17]

Fig 3.9: Normalised side load transfer (t-z) curve for drilled shaft in cohesionless soil*

*The figure only includes the trend line of the curve which has been used in SSM 2.0.

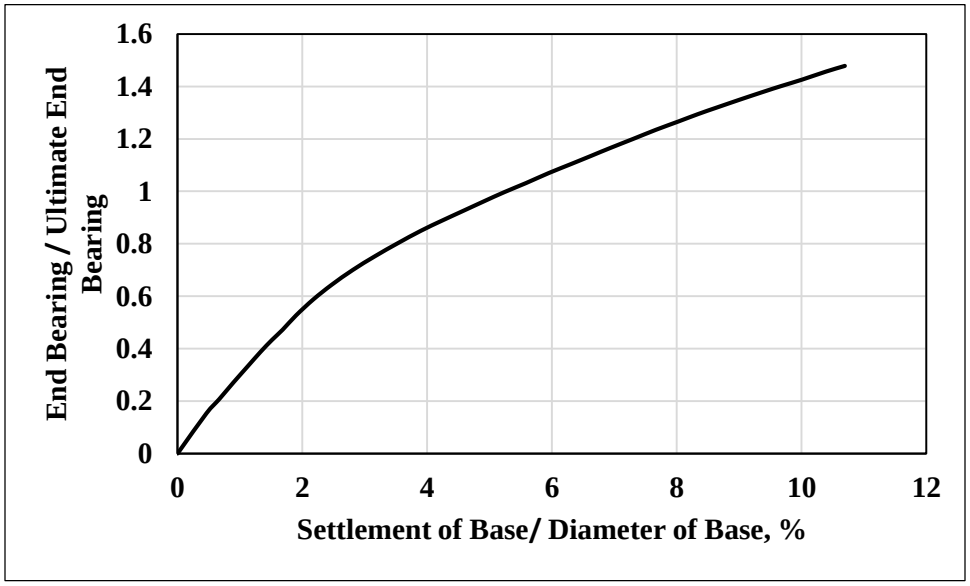

(Source: Reese and O'Neil, 1988) [17]

Fig 3.10: Normalised base load transfer (q-z) curve for drilled shaft in cohesionless soil*

*The figure only includes the trend line of the curve which has been used in SSM 2.0.

3.3.5 User input

SSM 2.0 facilitates the input of any axial (t-z and q-z) curves directly, which allows the user to generate the soil spring stiffness for any type of soil or method of soil spring generation which is not defined in the program. It is equally useful for the user to directly put the values when the information is available from field tests. For t-z curves, the user needs to input a family of side load transfer (t), and settlement or axial displacement at a depth, z. Once, the t-z input is finished, user is prompted to input a family of end bearing (q), and settlement of base at a depth, z for the q-z curve.

3.4 Elastic and Multilinear soil springs

The SSM generates elastic and multilinear soil springs and these are assigned along the pile length in structure model to represent the soil behaviour. Section 3.2 and Section 3.3 describe about the types of soil, as well as different methods and illustrations used in SSM for the generation of p-y, t-z and q-z soil springs. In SSM, thus programmed various methods calculate lateral (p-y), and axial (t-z, q-z) curves which are used to develop elastic and multilinear soil springs.

Elastic soil springs represent the initial slope of the p-y, t-z or q-z curves and its unit is Force per unit length (F/L). The slope of any given curve in SSM is calculated using Secant method of slope calculation. For the calculation of p-y elastic soil spring in SSM, initial slope of a given p-y curve is multiplied by the length of element which is given in equation 3.31.

$$K_{py} = k_{i,\ py} \times L_i \tag{3.31}$$

where, $k_{i,\ py}$ = initial slope of the given p-y curve at a given soil depth z_i and zero displacement,

and its unit is Force per unit length squared (F/L^2)

L_i = length of the element at the point of calculation.

Similarly, in case of t-z curve, elastic soil spring is calculated by multiplying the initial slope of given t-z curve by surface area of the element and is given in Equation 3.32. While in case of q-z curve, the elastic soil spring is the initial slope of programmed q-z curve, which is given in equation 3.33, as q in q-z curve is load at the pile tip.

$$K_{tz} = k_{i,\ tz} \times A_{ci} = k_{i,\ t} \times \pi d L_i \tag{3.32}$$

$$K_{qz} = k_{i,\ qz} \tag{3.33}$$

where, $k_{i,\ tz}$ =initial slope of t-z curve at a given depth z_i and zero displacement, and its unit is F/L^3.

A_{ci} = surface area of the pile segment which is in contact with the soil in shear,

whose unit is L^2.

$k_{i,\ qz}$ = initial slope of q-z curve at a given depth z_i and zero displacement. Its unit is Force per unit length (F/L).

The surface area of the pile is calculated in the SSM programme assuming the pile to be a circular one. However, if the pile is not circular in shape, one of the bigger lengths of the pile cross-section is considered to be the diameter (d) and the area is calculated for the particular element with length L_i.

The illustration of the generation of elastic soil springs in case of p-y, t-z and q-z curves is given in the Fig 3.11.

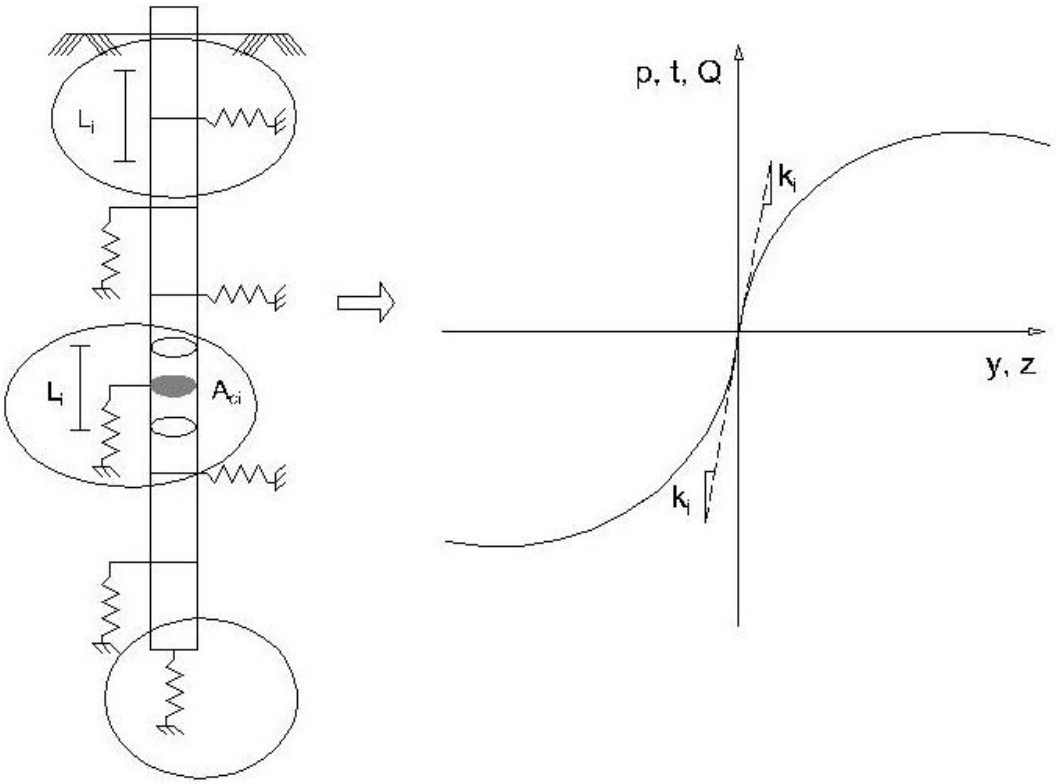

Fig 3.11: Illustration of generation of elastic soil springs

After the generation of initial elastic springs, SSM generates multilinear springs. At each given depth of pile or point of calculation, we have a nonlinear axial (t-z, q-z) or lateral (p-y) load displacement curve programmed in SSM. A piecewise sloped line is formed, as shown in Fig 3.12 to approximate the nonlinear curves. These piece wise sloped lines, calculated from the secant method, approximate the non-linearity of the soil spring curves which are obtained using various methods of p-y, t-z and q-z curves generation that are programmed in the SSM. The illustration of the generation of multilinear soil spring is given in Fig 3.12.

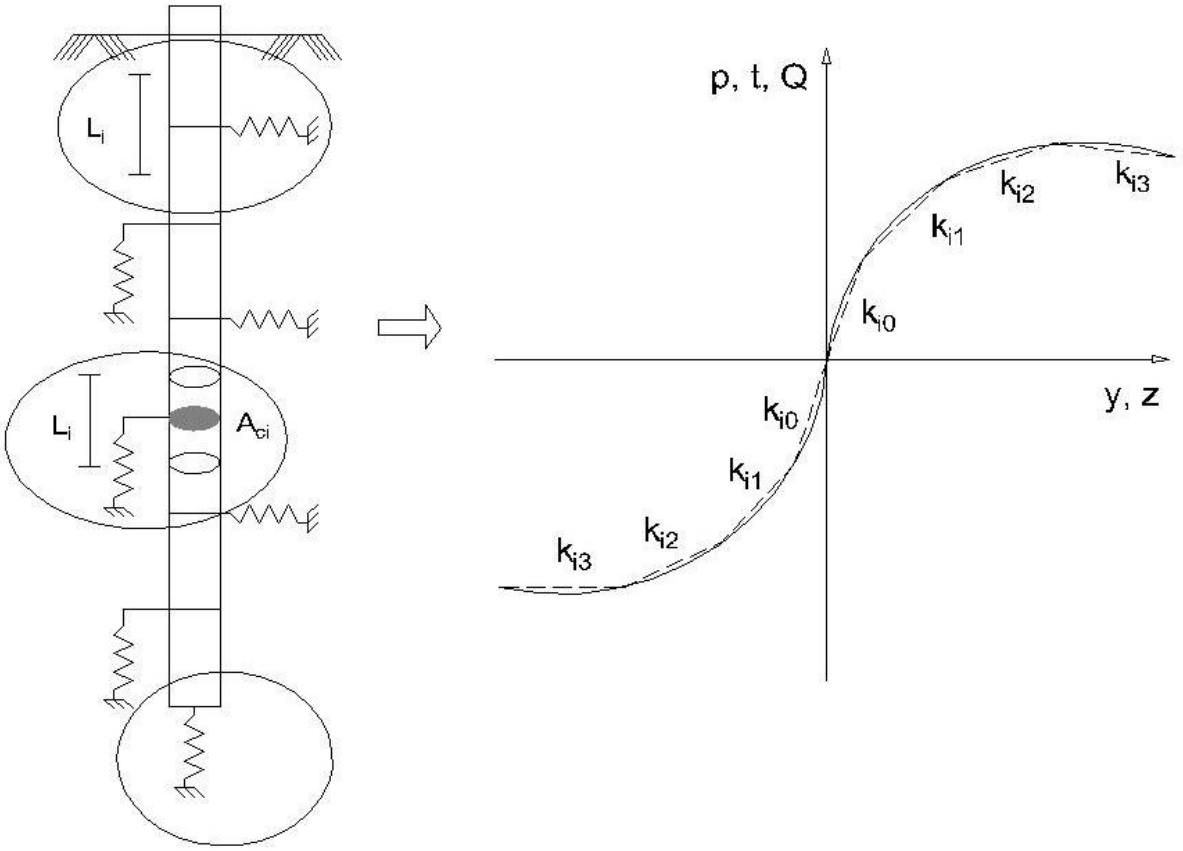

Fig 3.12: Approximation of multilinear soil springs of p-y, t-z and q-z curves

Multilinear springs in case of nonlinear p-y curves are calculated by multiplying those slopes at different point of the nonlinear p-y curves by length of the pile segment as given in the Equation 3.34.

$$K_{ij,\ py} = k_{ij.\ py} \times L_i \tag{3.34}$$

where, $K_{ij,\ py}$ = multilinear soil spring stiffness of a p-y curve at given point of calculation, z_i, and lateral soil displacement y_j, and the unit is F/L

$k_{ij,\ py}$ = slope of the p-y curve at y_j. and point of calculation, z_i

L_i = elemental length at soil depth z_i. and the unit is F/L^2

Similarly, for t-z and q-z curves multilinear springs are calculated as shown in the Equation 3.35 and 3.36 respectively.

$$K_{ij,\ tz} = k_{ij,\ tz} \times A_{ci} \tag{3.35}$$

$$K_{ij,\ qz} = k_{ij,\ qz} \tag{3.36}$$

where, $K_{ij,\ tz}$ = multilinear soil spring stiffness of a t-z curve at a given soil depth or point of calculation, z_i and axial soil displacement, zj, and the unit is F/L.

$k_{ij,\ tz}$ = slope of the t-z curve at z_i and z_j, and the unit is F/L^3

A_{ci} = corresponding elemental surface area at the point of calculation with the length L_i.

$K_{ij,\ qz}$ = multilinear soil spring of a q-z curve at given soil depth, z_i and axial soil displacement, z_j, and the unit is F/L.

$k_{ij,\ qz}$ = slope of the q-z curve at z_i and z_j, the unit is F/L.

3.5 Operation of Soil Spring Module (SSM)

Integrated Analysis Process comprise of using SSM and STAAD.Pro for the modelling and analysis of a pile-supported structure. In order to run SSM, STAAD.Pro is opened in advance, as the location of an opened STAAD file can be automatically searched by the SSM. When run, GUI interface of SSM appears, as shown in Fig 3.13 to input pile and soil parameters. Users can fill in the soil and pile parameters in the SSM in two ways. SSM input file can be built and saved with a name of SSM_input.txt in the same address as that of STAAD file. When user clicks "**open**" under the "**File**" menu, it opens the saved file and all the soil and pile parameters in the file will be read. Additionally, in absence of saved input file, when user selects pile foundation from the model built in STAAD. Pro and runs the SSM, all the pile parameters are retrieved from the model and soil parameters can be entered manually to generate lateral and axial soil springs. There are various commands that can be performed in the SSM with the help of SSM user interface which are described below.

"**Select Piles**" option is clicked in the interface for the selection of pile models from STAAD.PRO to be assigned with soil spring supports. The piles having same dimensions (length, width and depth) can only be selected together otherwise they have to be selected and applied with the soil springs separately. Pile width and depth refers to the width and depth of the pile cross section respectively, both of which, in case of circular or hollow pile is taken as the value of the outside diameter.

The button **"Strata, Vertical Axis, Loading Directions"** lets users to select the axis corresponding to vertical soil strata, global vertical axis in STAAD. Pro, and lateral direction in global axis.

"Load Types" button is used for specifying either the load is static or cyclic. In the current SSM, t-z and q-z soil curves are not available for the cyclic loading.

The desired unit input is made by clicking the **"Unit"** button. P-multiplier is a group effect reduction factor which is defined as the ratio of soil resistance of a pile within a group to that of an identical single pile.

There is a **"p-multiplier"** button in the SSM user interface with the default value of 1 for a single pile. However, for a group of piles, SSM programme assigns p-multiplier values in pile groups row-by-row, relative to the loading direction and spacing between the pile rows, developed by Mokwa et al. (2000) [19]. This p- multiplier value is also suggested by current design recommendations, such as those in FHWA (2016) [20], AASHTO (2012) [21] , and FEMA P-751 (2012) [22]. "Leading-row" piles have larger *p*-multipliers than "trailing rows" since the soil in front of trailing piles has been weakened by the movement of the leading piles away from the soil mass. For t-z curve, no reduction factor has been employed in the current version, SSM 2.0.

"The increment number" defines the number of equal divisions of a pile into small segments and each segment is assigned the soil spring. The current version, SSM 2.0 by default divides the SSM into 40 segments.

"Total Layers" refers to the total numbers of soil layers penetrated by the selected pile(s). After assigning total numbers of soil layers, the users can select the available layer in **"Soil Layer"** drop box. The depth of each layer can be specified in the section: Depth from Pile Head, where we have **"Top of Layer"** and **"Bottom of Layer"** to input the top and bottom distance of the selected soil layer from pile head. Once we input the depth of the soil layer, in soil type option, there is a

drop box where we can select the soil type. There are two boxes each to put the soil parameters for the generation of lateral (p-y) and axial (t-z and q-z) soil springs.

The **"TZ Soil Type"** was added in the new version i.e. SSM 2.0 to input the soil parameters to generate the corresponding t-z and q-z soil springs. The users can select among the following soil types in the section: (a) **driven pile in clay (API),** (b) **driven pile in sand (API)**, (c) **drilled shaft in clay (Reese & O' Neil)**, (d) **drilled shaft in sand (Reese O' Neil)**, and (e) **input t-z and q-z curves.** After the selection of the soil type, clicking **"Edit"** button beside each soil type opens an interface where users can input or change different parameter values for the selected soil type. SSM 2.0 uses API t-z and q-z curves for the soils in driven pile while Reese & O'Neil t-z and q-z curves in case of drilled shaft. API clay requires the input of effective unit weight, undrained shear strength, and principal strain corresponding to 50% of the maximum stress (e_{50}). API sand requires the input of effective unit weight and effective friction angle. For Reese & O' Neil clay, effective unit weight, undrained shear strength, principal strain corresponding to 50%, ultimate unit side friction and ultimate unit tip resistance are the required input parameters. Similarly, the input parameter for sand in drilled shaft which are effective unit weight, effective friction angle, ultimate unit side resistance, ultimate unit tip resistance.

In **"p-y Soil Type"** input dropdown box there is an option of selecting following soil types to generate p-y curves: (a) **soft clay**, (b) **stiff clay in presence of free water**, (c) **stiff clay without free water**, (d) **Reese sand**, (e) **API sand**, (f) **silt**, (g) **strong rock**, (h) **Reese weak rock**, (i) **user input.** The required parameter for the above soil type is given in DOT report. If any changes have to be made in any soil parameter, soil layer, elevation, the users can click on the **"Edit"** button as it helps SSM to recognize the changes.

After all the parameters has been put, clicking the **"Profile"** allows the users to view profile of the pile, soil and ground level as well the scour if the scour value has been assigned. Once all the soil, pile parameter is put well, next step is the generation of p-y and t-z curves in corresponding to the assigned parameters.

The **"Generation"** button calculates the initial elastic spring stiffness and nonlinear spring for each soil layer and stores the values. Once the values are calculated, they can be assigned along the pile length and the **"Elastic Soil Springs"** button will be automatically activated. Clicking on the button will divide the selected pile in the STAAD.Pro into the number of divisions in increment number. For the SSM, we have assigned 40 as increment number in the program. And the same click on the button functions to assign the initial elastic soil springs to those discretized elements. The SSM 2.0 has been programmed in such a way it assigns p-y and t-z springs in the order of one after another and q-z spring at the tip of the pile. Completion of this activity automatically activates **"Multilinear Soil Spring"** button. Clicking on the **"Multilinear Soil Springs"** button assigns the multilinear soil springs to the discretized elements in the pile. This function replaces the elastic springs previously assigned in the structure model with multilinear springs. Multilinear soil springs are the non liner springs and represent the soil behaviour.

SSM also allows the performance of scour analysis which can be achieved by inputting the scour depth below the ground surface where the program recalculates the soil springs for the structure model in STAAD. Pro rather than simply removing the existing soil springs. For the analysis in this thesis, we have not considered scour but this tool can be very effective in case of scour analysis of the pile-supported structures.

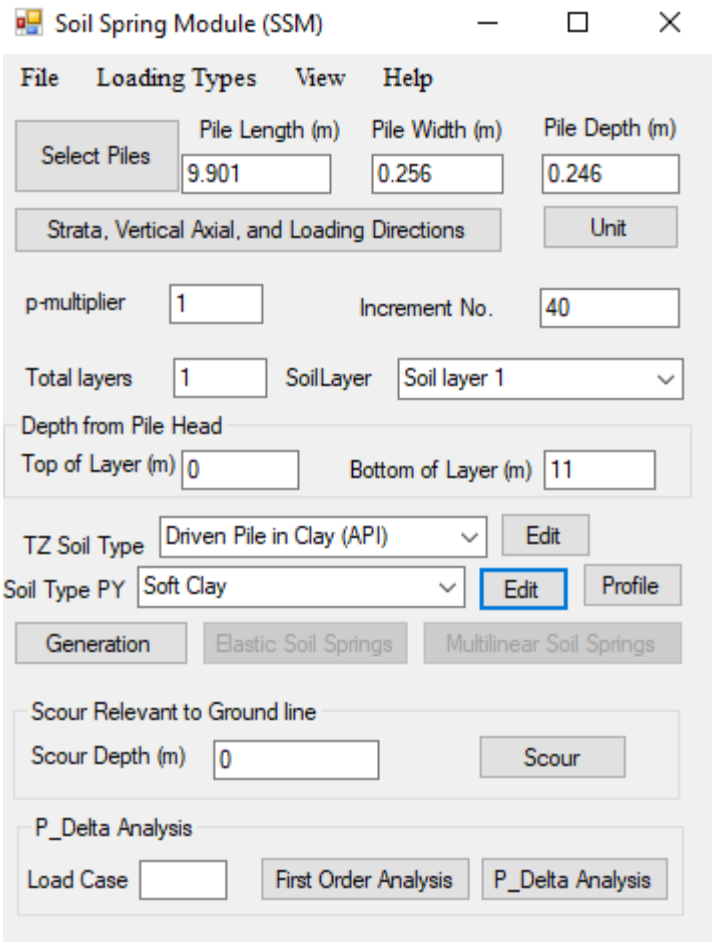

Fig 3.13: The SSM interface

4 Case Study

4.1 Bridge description

Kansas Bridge 45 (Jewell County, KS, USA) is examined in this research for a case study. The bridge superstructure and one of the eight pile foundations are shown in Fig 4.1(a) and Fig 4.1(c), respectively. As shown, the 112-m bridge has five spans. The superstructure is composed of a concrete deck on top of four W33×141 steel girders. The superstructure is supported by four bents. Each bent has two concrete piers and each pier is supported by a pile group including eight HP10×42 steel piles. A more detailed discussion on the geometric and material properties of various bridge elements can be found in [3]. Frame elements are used in STAAD.Pro to model the girders, piers and piles. The tapered piers are discretized into frame elements with different cross-sectional sizes, as seen in Fig 4.1(b). Shell elements are used to model the pile caps. At the abutment locations, the translational degrees of freedom are arrested while the rotational degrees of freedom are set free.

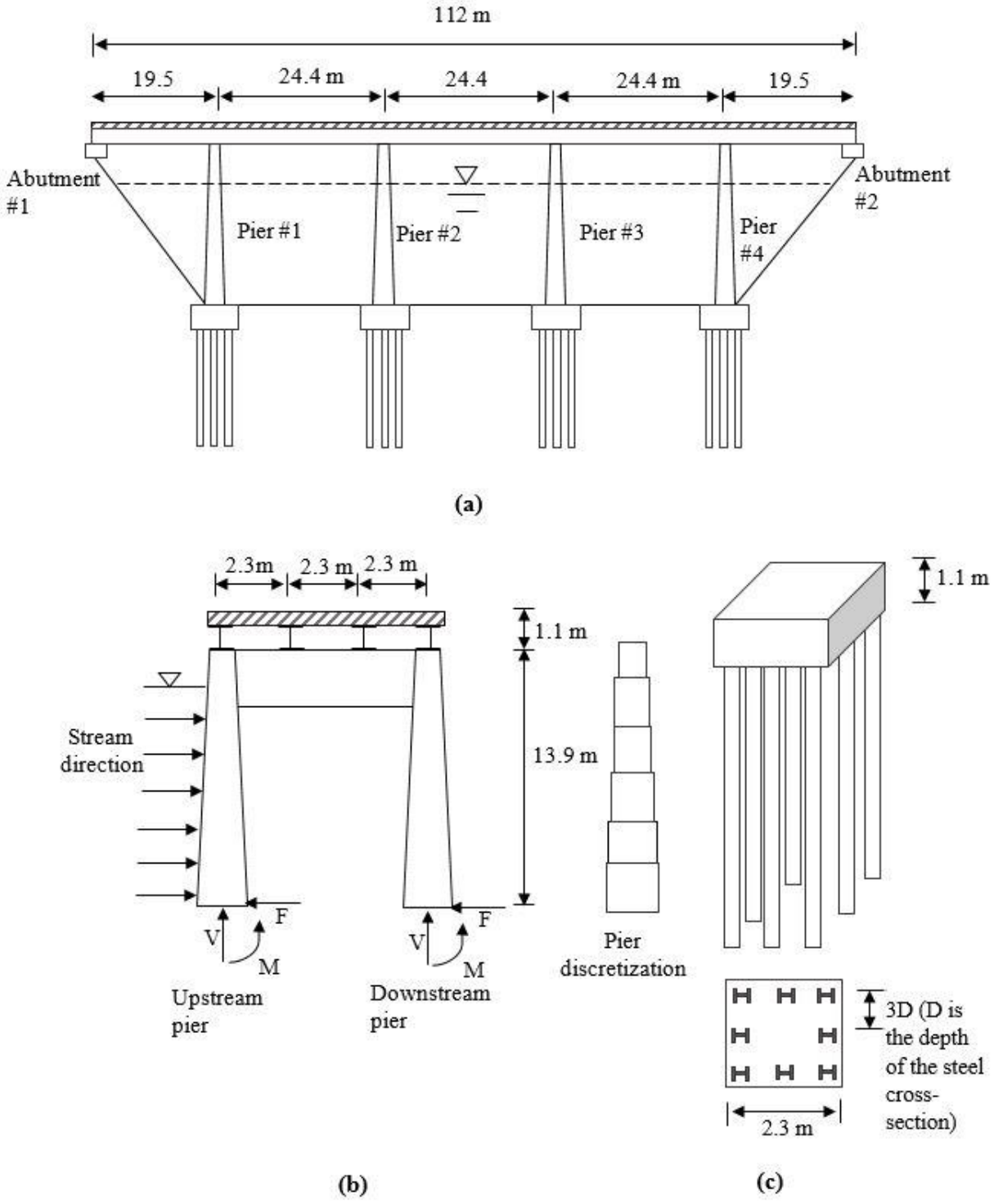

Fig 4.1: Bridge K45(a) front view from the upstream; (b) superstructure side view; (c) group pile and cross section

4.2 Load calculation and Application

The loads considered in the bridge analysis are a combination of vertical and lateral where self weight accounts for the vertical load while flood loads with debris and wind loads are included in the lateral loads. The bridge self weight is considered by specifying the materials unit weights in STAAD.Pro where the unit weight of concrete element = 24 kN/m^3 and unit weight of steel element = 77 kN/m^3. Wind loads were calculated as concentrated loads by multiplying the tributary area of the bridge deck and fascia girder normal to wind loads by wind pressure. The wind pressure was calculated using the provisions specified in AASHTO-LRFD Bridge Design Specifications [21]. The concentrated wind loads of 57 kN, 129 kN, and 143 kN were applied to the bridge girder at the location of abutment, outside piers and inside piers respectively. The design 100-year flood for the bridge was taken at the design elevation of 12.5 m above the base of piers for the hydraulic load calculation. Both the water and debris were calculated based on the AASHTO-LRFD Bridge Design Specifications [21]. Uniformly distributed water loads of 6.6 kN/m, 6.3 kN/m, 6.1 kN/m, 5.8 kN/m, 5.5 kN/m, 5.4 kN/m and 5.1 kN/m from the base of pier and each with a depth of 1.55 m were applied at all the 8 piers. Above the water loads, concentrated debris load of 196 kN was applied only to the upstream piers A detailed discussion on the load calculation and application can be found in the KDOT report by Lin et al.[11]. A load factor of 1.0 was applied to all load cases.

4.3 Modelling of soil layers

In this study, the bridge model is analysed using three conventional approaches (from Chapter 2) and the IAP (from Chapter 3) under the following cases: (a) stiff clay, (b) soft clay, (c) dense sand, (d) loose sand, and (e) multiple soil layers. The soil properties are listed in Table 4.1. In all cases, the top surface of the first soil layer is flush with the top surface of the pile cap (see Fig 4.2 for an example). For the cases with a single soil layer, the layer has a depth of 11 m. For the case with multiple soil layers, the sequence and depths are shown in Fig 4.2.

As discussed in Chapter 3, after entering the pile dimensions and configuration in the user interface of SSM 2.0, for the case study bridge, all piles are automatically generated and meshed in STAAD.Pro. The soil properties and depths are also entered in the user interface of SSM 2.0, after which nonlinear springs (in various directions) are automatically generated over the entire length of piles in STAAD.Pro to simulate the load transfer. An example is shown in Fig 4.3.

Table 4.1 Properties of soil layers used in the case study

Case no.	Soil Types	γ' (kN/m^3)	c_u (kPa)	ε_{50}	k (kN/m^3)	ϕ (degree)
1.	**Soft Clay**	8.2	35	0.01	-	-
2.	**Stiff Clay**	10	120	0.005	220000	-
3.	**Loose Sand**	8.5	-	-	10000	30
4.	**Dense sand**	10	-	-	40000	40
5.	**Multilayered soil**					
	Soft clay (0 m -4 m)	8.2	35	0.001	-	-
	Sand (4 m -7.5 m)	10	-	-	34000	33
	Stiff clay (7.5 m – 11 m)	10	70	0.007	136000	-

Note: γ' = effective unit weight, C_u= Undrained shear strength, ε_{50} = Principal strain, k= coefficient of subgrade reaction, ϕ = effective friction angle. (Source: KDOT, Lin et al, 2011) [11]

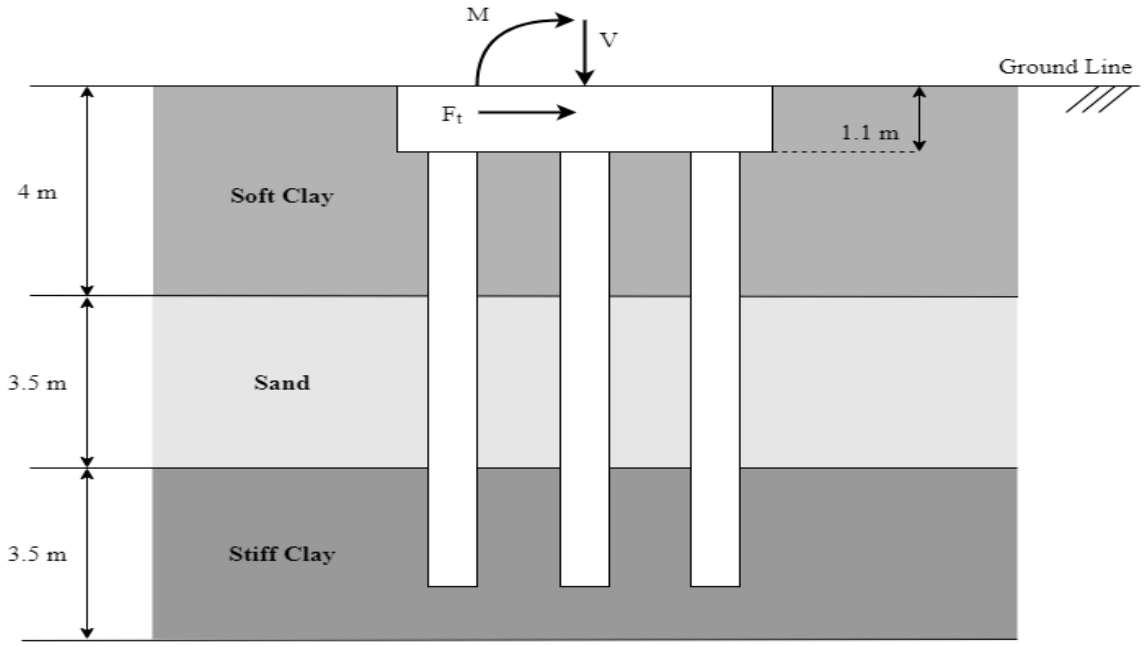

Fig 4.2: Pile foundation with multiple soil layers

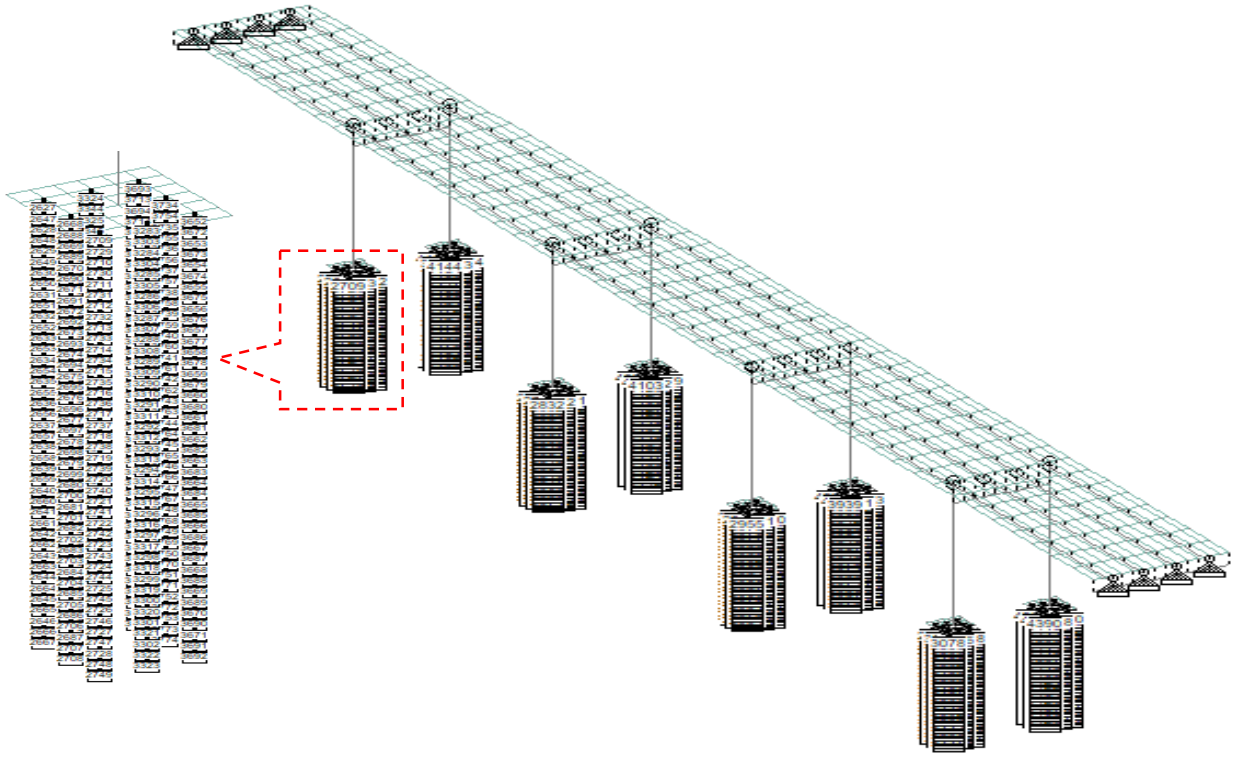

Fig 4.3: Typical model of the bridge superstructure and foundation in STAAD.Pro

5 Results and Discussions

The Kansas Bridge 45 is analysed using the conventional approaches (SBC, MAD and EPL) discussed in Chapter 2 and the IAP approach discussed in Chapters 3. For the SBC and MAD approaches, the bridge is analysed in both pile free head and file fixed head conditions, as discussed in Chapter 2. This totals six analysis approaches. For each approach, the five different soil conditions in Table 4.1 are applied. This totals 30 analysis cases. The responses of the super- and sub-structures are included in Appendices A and B, respectively. This chapter includes only the key comparisons.

By comparing the upstream and downstream piers in the responses in the appendix, it was found that the internal forces in upstream piers are in general larger than those in downstream piers. Since all piers are typically of the same sizes, the upstream piers are selected for further comparison in this chapter. Fig 5.1 shows the shear forces at the bottom of the four upstream piers in loose sand for the free head and fixed head conditions. It can be seen from the figure that internal forces in Piers 2 and 3 (i.e., the two middle piers of the bridge) are the greatest. In addition, the differences of internal forces obtained by various analysis approaches are larger for the two middle piers. The same was observed in the other types of soil conditions in Table 4.1, as shown in the appendices. Since both the load application and bridge geometry are symmetric about the centerline, Pier 2 is selected for further comparison in this chapter.

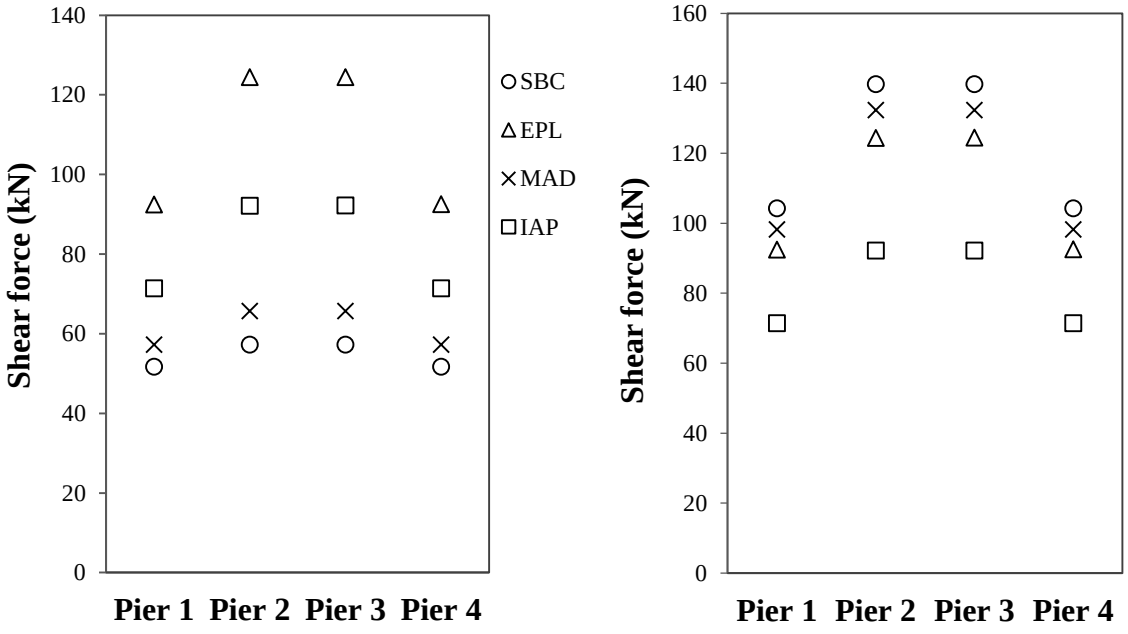

(a) (b)

Fig 5.1: Distribution of shear force at the bottom of upstream piers in loose sand; (a) free head pile, (b) fixed head pile

5.1 Superstructure Responses

Superstructure response of the bridge has been represented by the shear force, bending moment and the lateral deflection of pier #2 of the bridge under various methods, pile head, and soil conditions, which are shown in Fig 5.2 to Fig 5.7.

5.1.1 Comparative study of conventional and IAP methods in a single soil type

The comparative study between the integrated superstructure- foundation model using IAP and various other methods in current practice i.e. SBC, MAD and EPL, accounts for the effect of the design analysis approach in a pile-supported structure.

Fig 5.2 depicts the distribution of bending moment (with respect to z axis in the standard coordinate system) along the pier #2 in loose sand for 3 conventional methods and the IAP. As mentioned above, we have the analysis for both free head and fixed head pile condition. Fig 5.2(a) illustrates that equivalent pile length method (EPL) which is also called as Davisson and Robinson method, generates a greater lateral pile response when the pile head is free in simplified boundary condition (SBC) and maximum allowable displacement (MAD) methods. SBC and MAD, when the pile head is free, have a negligible bending moment at the bottom of pier whereas SBC has the highest bending moment at the top. Similarly, Fig 5.2(b) shows that in fixed head condition, the bending moment in these two conventional methods are very similar to each other both at the top as well as bottom of the pier. At the top, they are slightly smaller than IAP, while at the bottom, their value increases significantly than IAP. The most significant difference in the bending moment in all these methods can be seen towards the bottom of the pier. SBC has the largest bending moment, when the pile head is fixed which is followed by MAD. This shows that in these two conventional method of bridge analysis, with the change of pile head boundary condition, the load borne by pier at different locations is significantly affected with pier bearing most of the load at the top in free head pile condition and bearing more load at bottom in fixed head pile condition. The fixed head pile condition increases the lateral resistance capacity of the pier by increasing stiffness and also through the development of pile axial forces which contributes to resistance indirectly through frame action. This indicates the SBC and MAD methods overestimate the load

borne by pier in fixed head pile condition and underestimates in case of free head pile condition. The difference in bending moment in pier do not seem much significant in SBC and MAD. Considering this fact, we can say that the IAP method has bending moment somewhere in between the free head and fixed head pile condition analysis of SBC and MAD. Additionally, EPL method, also called as "Davisson and Robinson method" which is more conservative than other two conventional methods have similar bending moment as IAP at the top of pier and it gradually increases throughout the pile and finally is much larger than IAP at the bottom. At pier length 11.6 m, the kink in the bending moment in the figure reflects concentrated debris load in the bridge model which is applied only in the upstream pier.

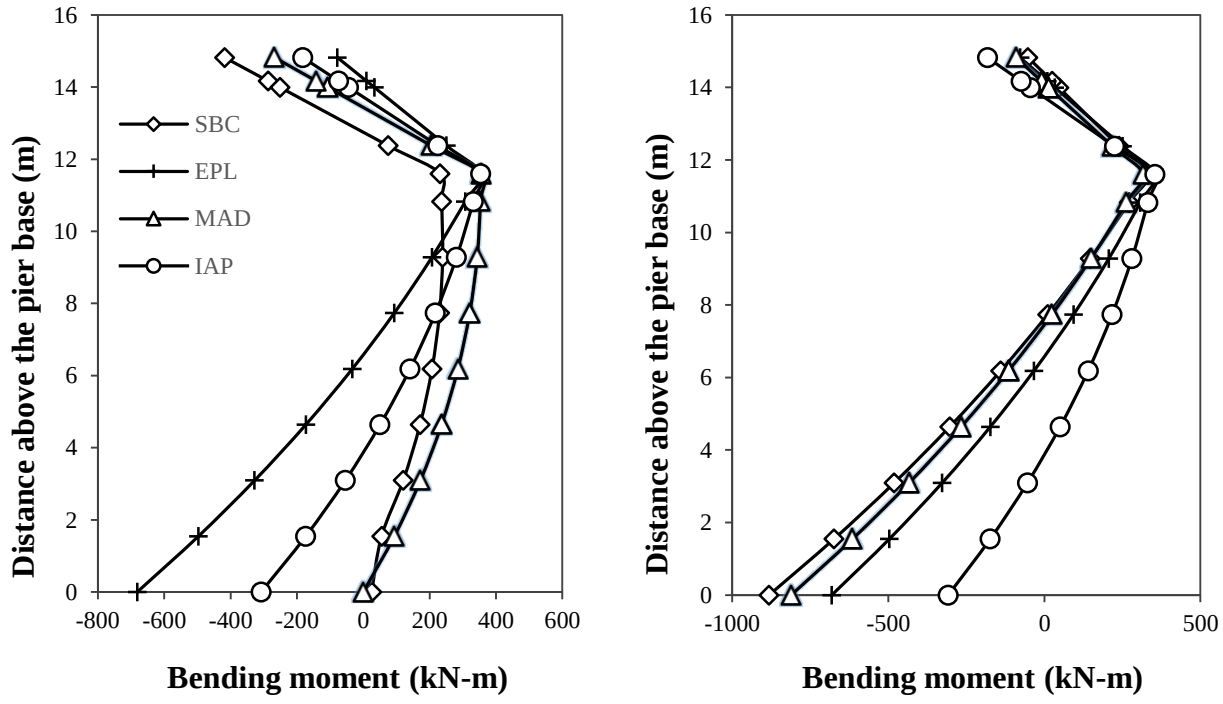

Fig 5.2: Distribution of bending moment along the pier #2 in loose sand; (a) free head pile, (b) fixed head pile

Distribution of shear force also illustrates the effect of these various design approaches on the lateral response of a pile-supported structure. Fig 5.3 compares the distribution of shear force throughout the pier in loose sand for both the pile head fixity conditions. The shear forces along the pier length in SBC and MAD are smaller than IAP when pile head is free. Similarly, the shear forces along the pier length in SBC and MAD are higher than IAP when the pile head is fixed. But the results in SBC and MAD are very close to each other in both the cases**.** In case of fixed head pile, the shear force along the pier is almost same in case of 3 conventional methods ie. SBC, MAD and EPL as observed from Fig 5.3(b). The result suggests that the SBC and MAD generate greater lateral pile response in fixed head.

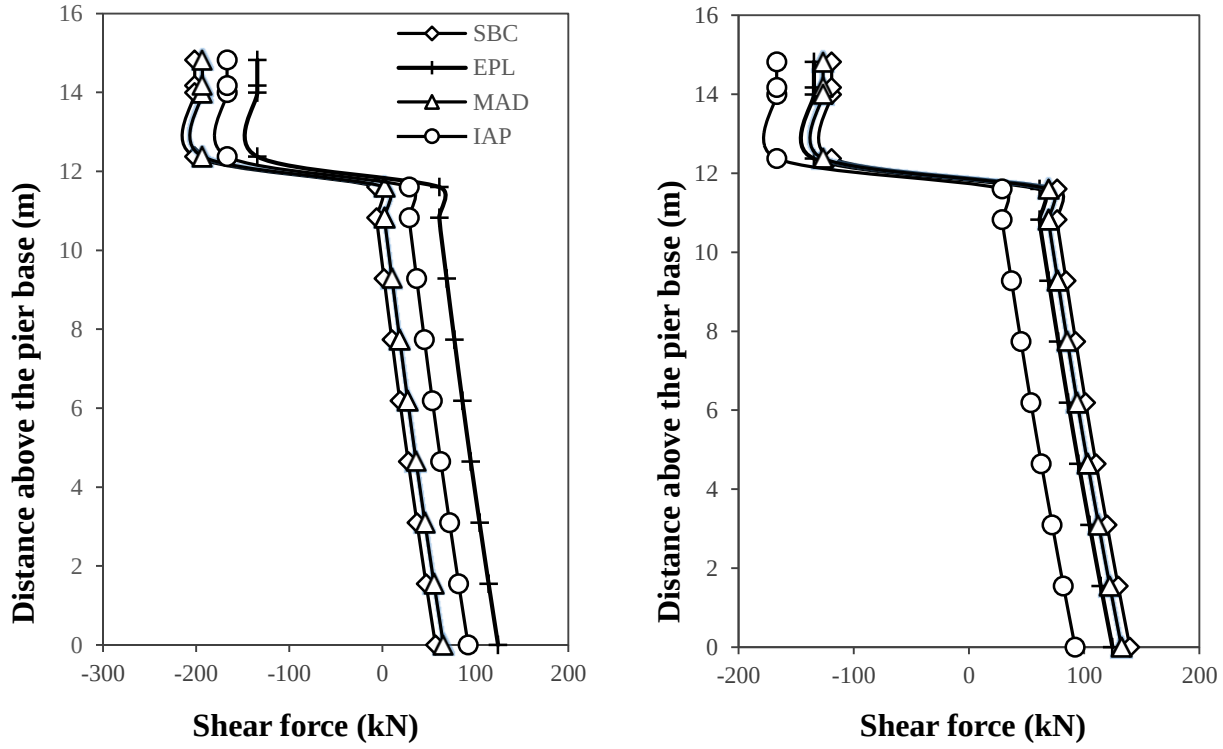

Fig 5.3: Distribution of shear force along the upstream pier #2 in loose sand (a) free head pile (b) fixed head pile

The lateral displacement of piers is also one of the important responses that signifies the differences among IAP and other conventional methods. Fig 5.4(a) shows that the highest deflection along the pier for free head pile occurs in case of SBC, followed by MAD, IAP and then EPL. Also, the lateral deflection at the top of pier reduces significantly at the bottom in all the cases except SBC. The figure illustrates that MAD most likely have similar deflection as that of IAP. Fig 5.4(b) illustrates that in case of fixed head, the deflection along the pier while going from the top to bottom reduces in all the cases including SBC, which has the lowest lateral displacement. IAP has the highest lateral deflection throughout the pier.

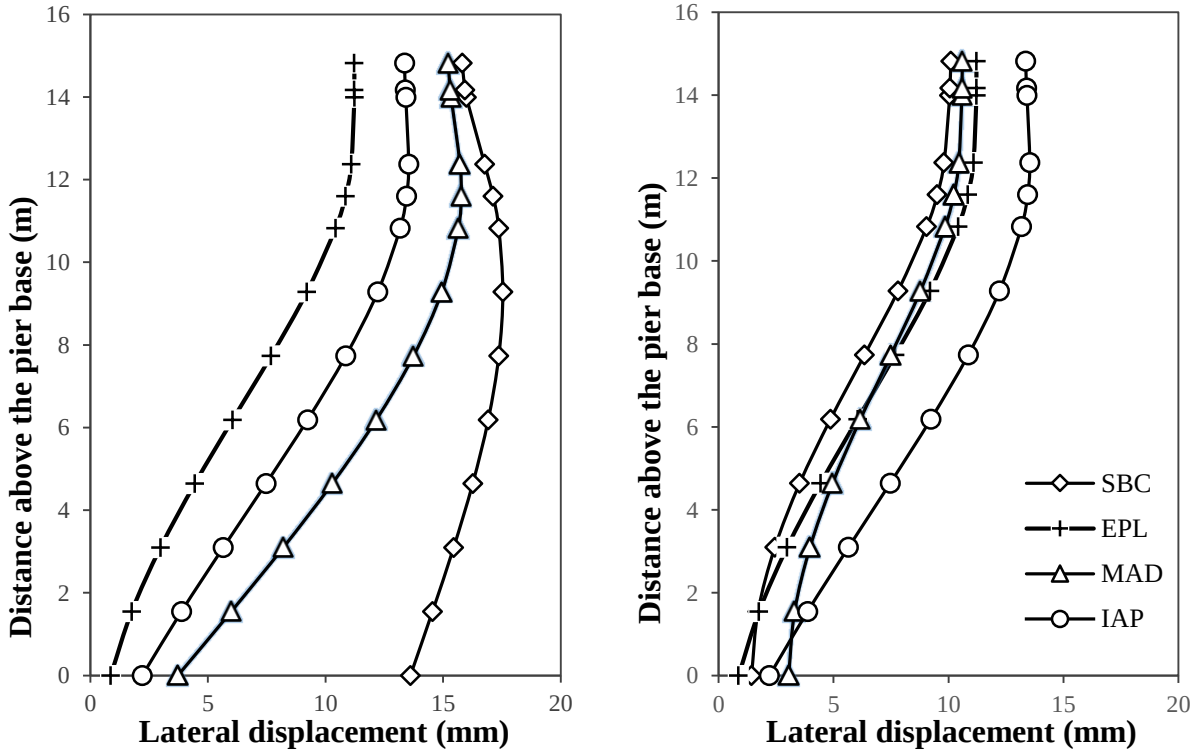

Fig 5.4: Lateral displacement of the pier #2 in loose sand for different methods (a)free head pile, (b) fixed head pile

5.1.2 Comparative study of conventional and IAP methods in different soil conditions

The five different types of soil cause the bridge structure and sub structure to respond differently and affect the soil foundation stiffness. As seen from the appendix A, though the trend of figures is similar, we can see differences in how the response values at different locations change significantly due to change in soil parameters and stiffness values. The comparative study of the superstructure responses in 4 different methods affected by soil types is presented in Fig 5.5 to Fig 5.7, which show the bending moments, shear forces and lateral deflections at the top and bottom of the bridge pier #2. The purpose of this study is to analyse how the response values at these locations vary as per the change in soil conditions and how do these soil types corresponds to the change in method of bridge analysis.

Bending moment at the top and bottom of pier in 4 different methods of analysis and 5 different soil types is depicted by the Fig 5.5. We can see the differences in direction of the bending moments in different methods, hence, absolute values are taken into consideration for the comparative study.

Fig 5.5(a) illustrates that in free head pile condition, the absolute values of the bending moments at the top of pier, are highest in SBC, followed by MAD, IAP and then finally EPL. In EPL, the differences in soil types do not seem to make much difference as the absolute values of bending moments for all the soil types are very close to each other. However, in SBC, soft clay and loose sand have the similar and maximum absolute bending moment, followed by multilayered soil, dense sand and finally stiff clay. And, at the bottom of the pier, as seen from Fig 5.5(c), the absolute value of bending moments in different soil types in SBC is just in a reverse order as that

of the pier head which means that the stiffer the soil, higher the absolute bending moment at the bottom of the pier. Again, Fig 5.5(a) shows that, for MAD in free head pile, at the top of pier, the trend is similar to that of the SBC but the values are more close to each other. However, at the bottom of the pier, all the values are zero as seen from Fig 5.5(c). This zero bending moment is due to the release of rotational moment along z axis, which can also be seen in the stiffness values in Table 5.1. These observations suggest that, among these conventional approaches, when the pile head is free, SBC seems to respond better to the difference in soil type. Similarly, in IAP method, while going from the top to bottom of the pier, the value of absolute bending moment increases. Also, at the bottom of the pier, stiffer the soil higher the absolute bending moment and vise versa at the top, which reflects the contribution of soil stiffness to the distribution of lateral loads in the bridge structure. Moreover, in IAP, the general pattern in all the different soil types, is that more lateral loads were borne by the pier bottom than the top. However, in case of MAD and SBC, the pier bottom bore lesser load than the top. This shows the foundation structure interaction is significant in case of IAP. Also, the effect of soil type seems to have no significant difference in case of MAD, and EPL while the responses in SBC and IAP seem to correspond to the change in soil type more.

Fig 5.5(b) illustrates that when the pile head is fixed, absolute bending moment at top of pier, is highest in case of IAP method which means bending moment values at the top of pier decrease in SBC and MAD when going from free head to fixed head. At the bottom, as shown in Fig 5.5(d), the values in SBC and MAD become very large compared to the IAP method because of the high stiffness values at the pier base as seen in Table 5.1. Also, based on the observations, the lateral response of SBC and MAD, in fixed head pile, increases from top of the pier to the bottom. This is similar to EPL and IAP. Additionally, in case of fixed head pile, MAD also corresponds to the

change of soil condition. And if we have to pick one of the conventional methods which is closer to the IAP in terms of lateral response, we could go for MAD, when the pile head is fixed.

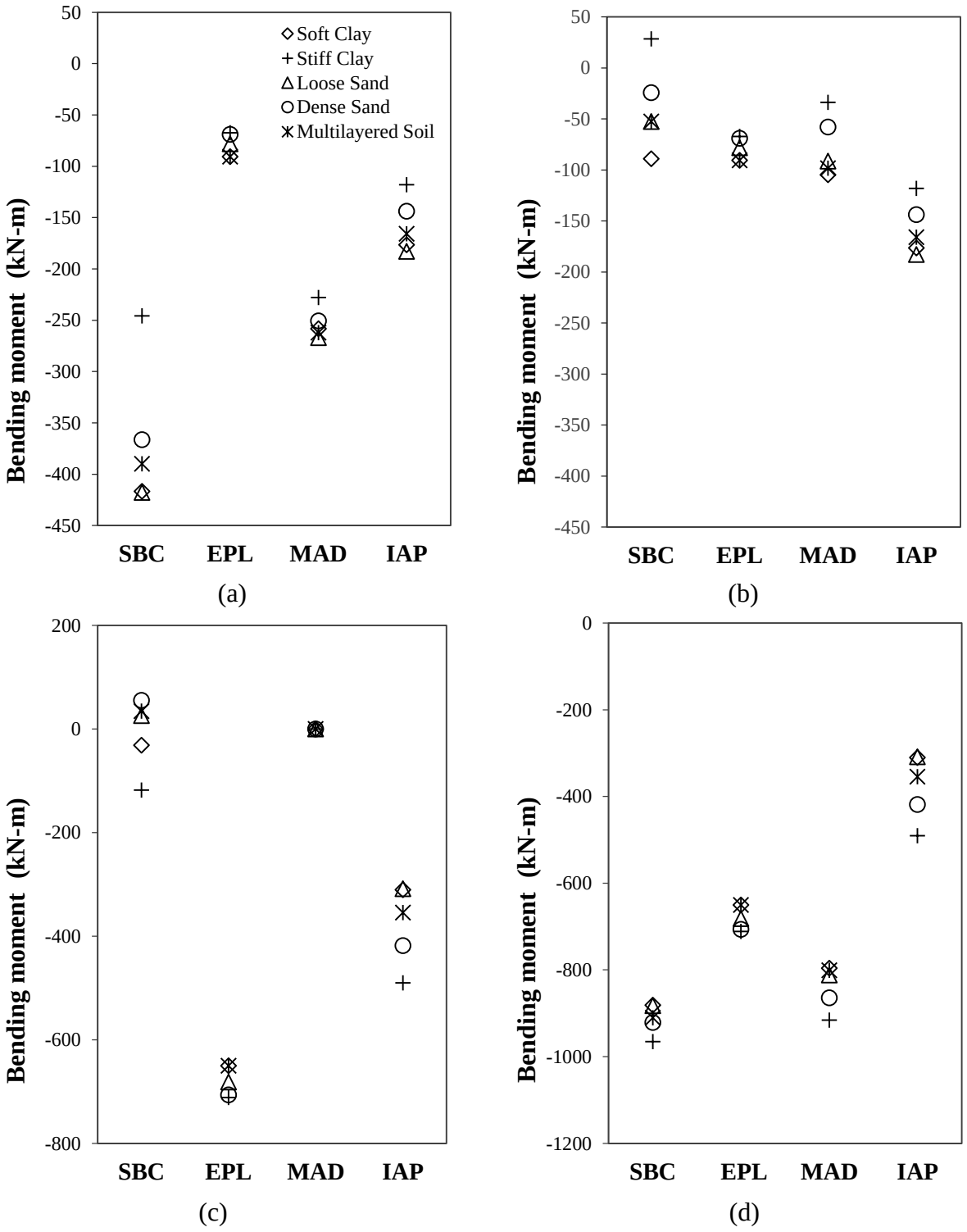

Fig 5.5: Bending moment of the upstream pier #2 for different methods using 5 different soil types (a) top free head, (b) top fixed head, c) bottom free head, (d) bottom fixed head

Shear force at the top and bottom of pier, in free and fixed head condition in 4 different methods and 5 different soil types is depicted by the Fig 5.6. We can see the differences in direction of the shear force in different methods. But the comparative study is made on the absolute values. Fig 5.6(a) shows that the shear force at the top of pier, for pile head condition, is relatively higher in case of SBC and MAD methods followed by IAP and then EPL. At bottom of the pier, the shear force value reduces for SBC and MAD and is smaller than IAP, as shown in the Fig 5.6(c). However, the values in each method decrease at bottom than their respective values at the top of the pier. Also, direction of the forces is reversed in all the methods from top to bottom of the pier. Additionally, SBC and IAP have visible soil effect on the lateral pier response. These two figures illustrate that, at the top of pier, in case of free head, soft clay has the maximum shear force, followed by loose sand, multilayered soil, dense sand and stiff clay. It can be observed that higher the flexural soil stiffness, lower the shear values at top of the pier and vice versa at the bottom. EPL and MAD do not have significant difference in shear values due to soil as all the values can be seen overlapping.

For the fixed head condition, as shown in Fig 5.6(b), the shear force values at the top of pier in SBC and MAD is lower than that of free head condition and become similar to EPL method. Unlike free head condition, MAD also shows some significant soil effect in this case, where dense sand has the highest shear force, and soft clay, multilayered soil and loose sand have shear force values overlapping and stiff clay has the lowest value. This order of the shear value is same for the SBC as well but differs from that of IAP as mentioned above. At the bottom of pier, Fig 5.6(c) illustrates that SBC, and MAD generate greater lateral response than that of IAP but the shear value pattern as per the soil type in these two is similar to that of IAP.

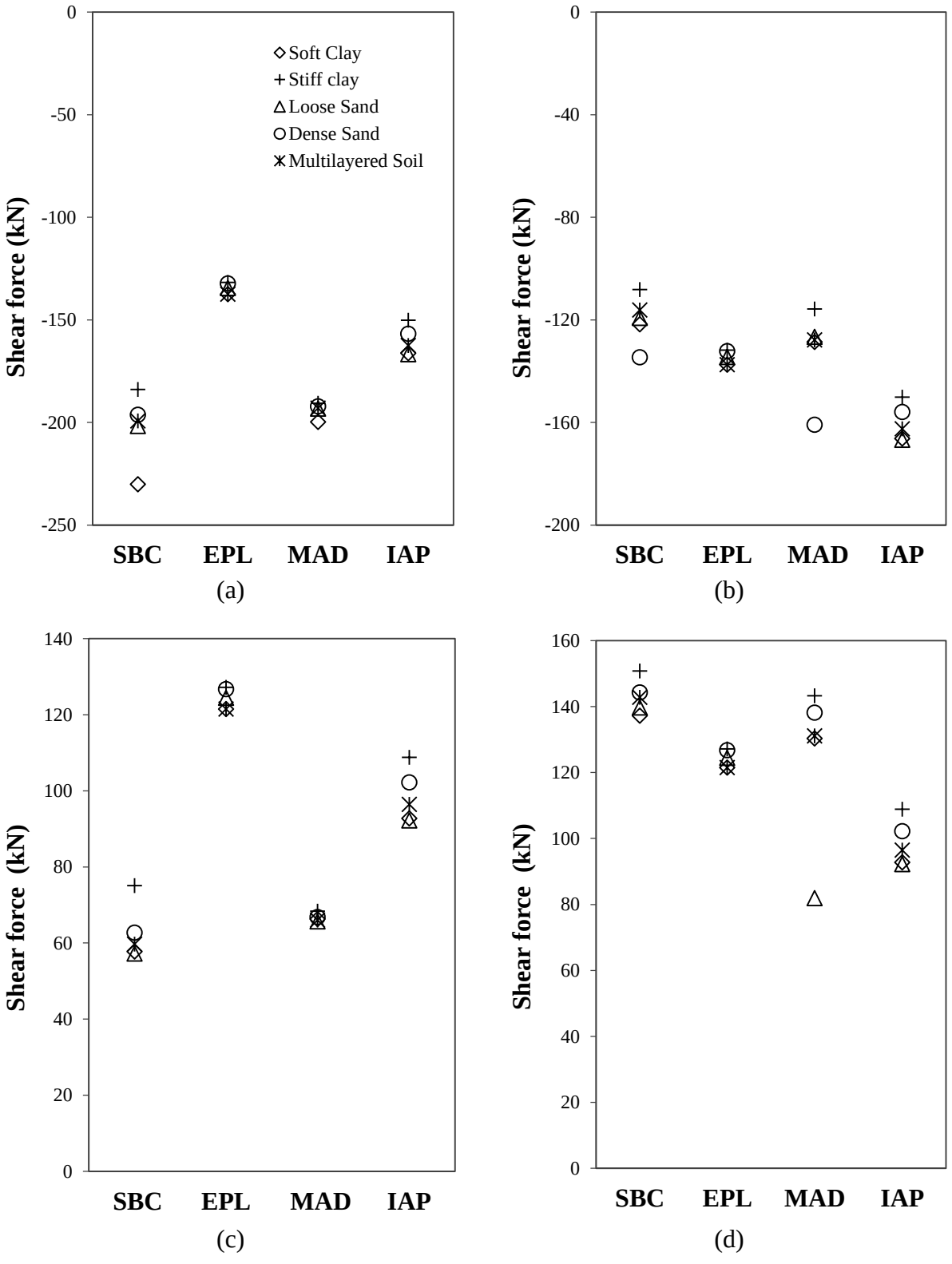

Fig 5.6: Shear Force of the upstream pier #2 for different methods in different soil types (a) top free head, (b) top fixed head, (c) bottom free head, (d) bottom fixed head.

Fig 5.7 compares the lateral displacement of the top and bottom pier for different soil types each in case of SBC, MAD, EPL and IAP. From Fig 5.7(a) and Fig 5.7(c), it can be observed that, for the free pile head condition, at the top of pier, EPL and MAD have, lateral displacement values for all the soil types almost overlapping one another, but SBC and IAP show a small difference in the values due to the soil profiles. While, at the bottom, lateral displacement values for different soil types in case of SBC are significantly different from each other, showing a strong soil effect, while EPL, MAD and IAP methods also show some difference in the values with the change in soil stiffness but the discrepancies are comparatively smaller than that of SBC.

Fig 5.7(b), shows that when the pile head is fixed, the lateral displacement at the top of pier in SBC and MAD, is almost same regardless of the soil type. While at bottom of the pier, both SBC and MAD seems to reflect the effect of soil type in lateral displacement values, as shown in Fig 5.7(d). Additionally, at the bottom, SBC is seen having closer results to the IAP method in terms of soil displacement values and the extent of soil effects. Despite MAD reflecting the soil effect, it has the largest deflection for stiff clay while in case of other methods stiff clay has the smallest deflection.

From these observations, it can be seen that in free head pile, only SBC and IAP corresponds to the difference in soil stiffness which is reflected in shear force values at the top and bottom of the pier while in fixed head both MAD also corresponds to the different soil types

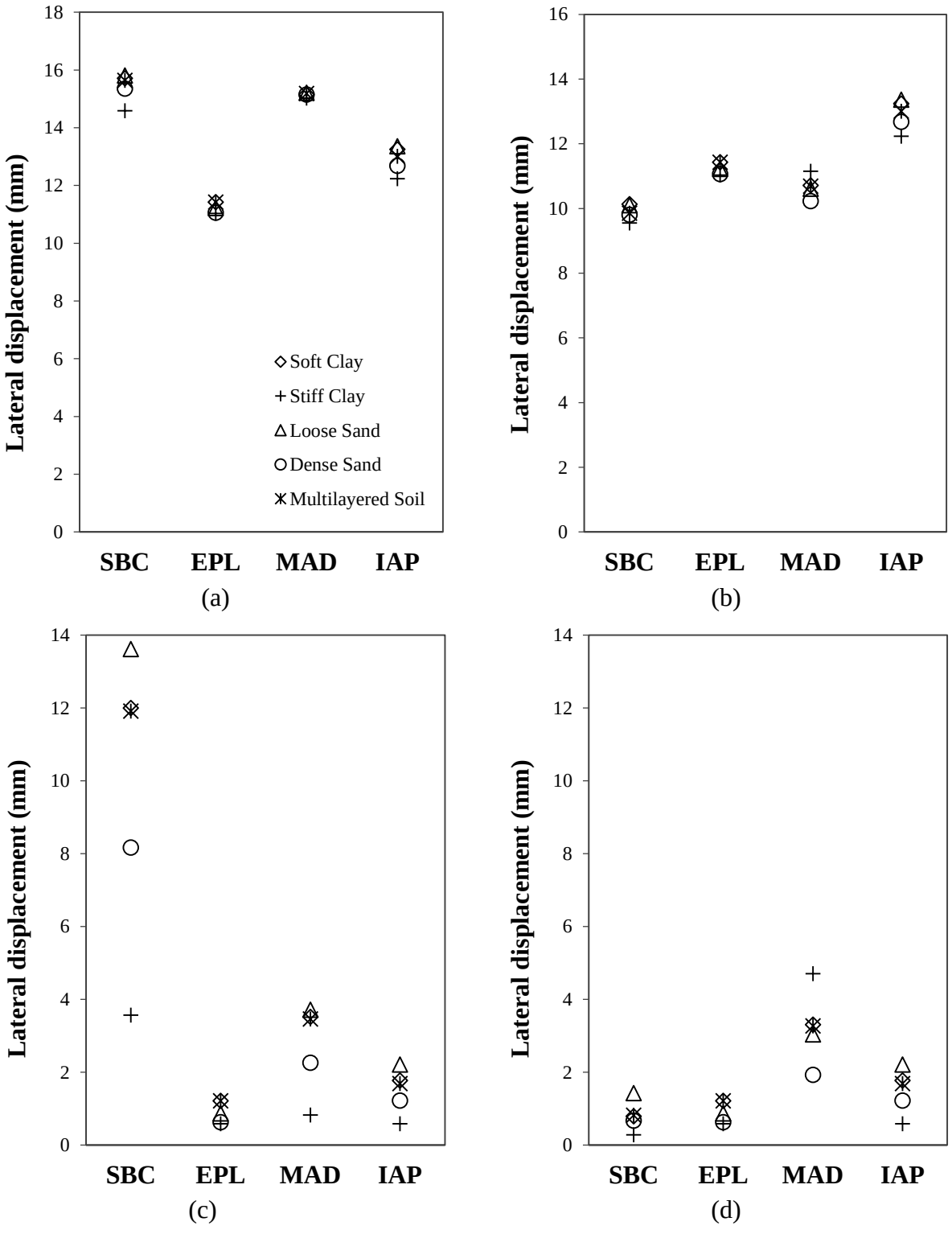

Fig 5.7: Lateral displacement of the upstream pier #2 for different methods in 5 different soils (a) top free head, (b) top fixed head, (c) bottom free head, (d) bottom fixed head

5.2 Foundation Responses

The foundation response of the pile groups in SBC, MAD and IAP methods are depicted by the bending moment, shear force and the lateral deflections in a single and multiple soil types and they account for the transfer of lateral loads from the superstructure to foundation.

In IAP method, the superstructure-foundation model built in STAAD.Pro using SSM, was analysed and the foundation response for the pile groups under pier #2 was considered for the representation. The bending moment and shear force of individual piles were added to be the equivalent to that of the pile group while, the lateral displacement of only an individual pile was taken. There is no EPL method for the foundation analysis because this method considers the bottom of the piles at the calculated equivalent depth to be fixed. And this depth is usually very small to be considered as a pile for the representation of foundation response. For the foundation analysis of other two conventional methods, i.e. SBC and MAD, a single pile was modelled in the STAAD.Pro and soil springs generated using SSM, and this pile was analysed twice for free head and partially rigid head condition. The loads employed for each of the methods are discussed in Section 2.1 and Section 2.2. The bending moment and shear force of the modelled piles were multiplied by the total number of piles in the group to present the foundation response.

5.2.1 Comparative study of conventional and IAP method in a single soil type

Fig 5.8 depicts the bending moment along the pile length in both free head and fixed head pile group under pier#2 in loose sand. From Fig 5.8(a), it can be observed that in free head, the SBC method have highest bending moment at the top of the pile head. In MAD method, the bending

moment at the pile head when it is free to rotate is almost zero. In IAP method, the bending moment is very small compared to the SBC and MAD throughout the pile. And the location of the maximum bending moment in MAD is slightly deeper than that of SBC and IAP whereas they are almost similar in case of these latter two methods.

When the pile head is fixed, the value of bending moment for SBC method, at the top of pile or ground level is observed to be similar to that of IAP which is very small, as shown in Fig 5.8(b). While in case of MAD, the maximum bending moment occurs at the top of pile. This observation suggests SBC seems to have closer foundation response to IAP than MAD in case of fixed head.

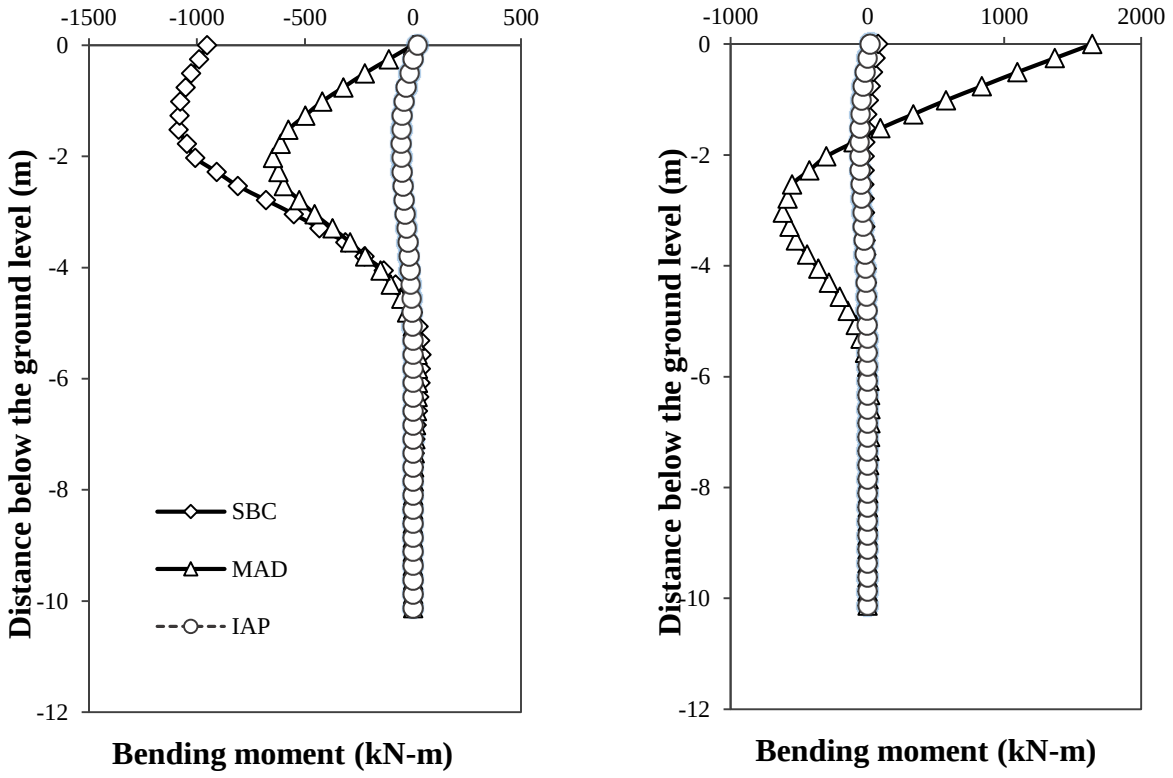

Fig 5.8: Distribution of bending moment along group of piles under pier#2 in loose sand (a) free head, (d) fixed head

Fig 5.9 depicts the shear force diagram throughout the pile in case of free head and fixed head soil in loose sand. IAP has smaller shear force throughout the pile while SBC and MAD have much larger values in free head pile, as seen from Fig 5.9(a). Also, in SBC, the value gradually increases from the ground level towards depth of the pile while in MAD, the highest shear force is at the top of the pile or ground level. Fig 5.9(b) shows that the shear force at the top of pile in MAD increases and becomes even higher when the pile head is fixed. While in case of SBC, when the pile is fixed head, the shear force reduces significantly than that of free head pile and becomes almost same as that of IAP. From the observations, it can be said that use of conventional methods for the foundation analysis exert much higher shear force on the piles compared to the IAP method.

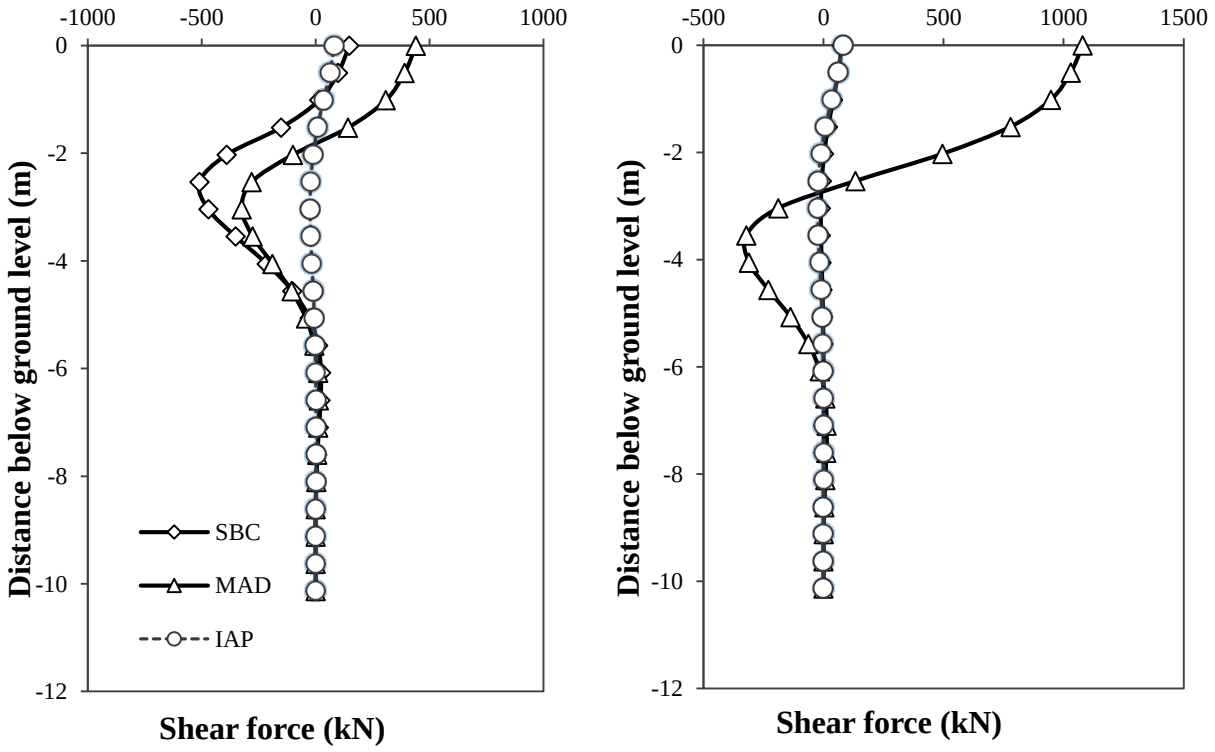

(a) (b)

Fig 5.9: Distribution of shear force in along group of piles under pier#2 in loose sand (a) free head, (b) fixed head

Lateral deflections of the pile groups anticipate the displacements that occur in the pile due to the applied lateral loads which is shown in the Fig 5.10. From Fig 5.10(a), it can be observed that lateral deflection of IAP is very small compared to MAD and SBC in free head condition. And SBC has the highest lateral deflection. Similarly, for MAD method, the allowable lateral deflection of 25 mm was applied for the analysis, as well as the translational direction was released in case of both the free and fixed head, and hence, the maximum deflection value is same in both the of these pile head conditions. However, if we look at SBC method, the lateral deflection is reduced and becomes same as IAP when the pile head is fixed, as seen from Fig 5.10(b). The significant reduction in pile deflection in SBC from free head to fixed head shows the higher contribution for the lateral displacement provided by rotational load, as rotational movement is restrained in latter case.

Comparing the lateral deflection at pile head, Fig 5.10 to the lateral deflection at pier base, Fig 5.4, it can be seen that the deflection values in SBC and MAD vary from each other, however, in case of IAP the displacement values are similar which shows the continuity of the structure in IAP.

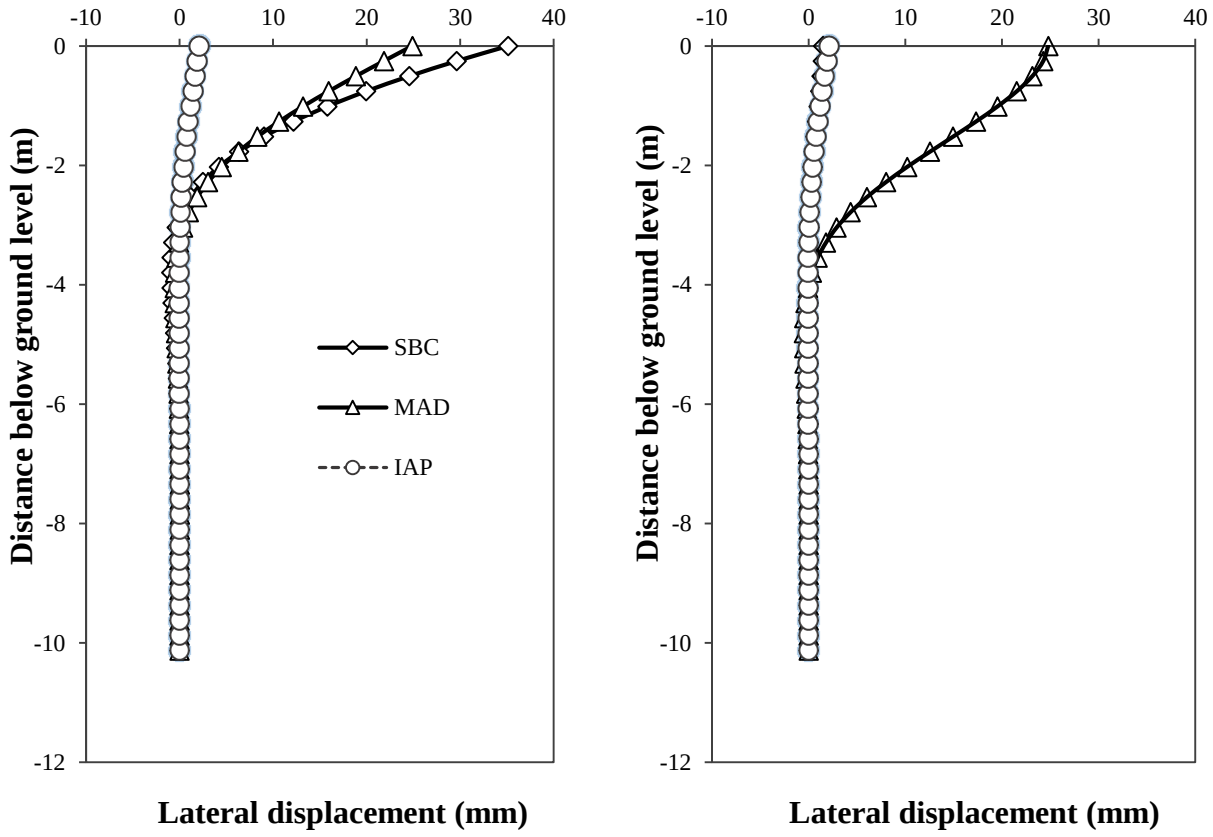

Fig 5.10: Lateral displacement along piles under pier #2 in loose sand (a) free head, (b) fixed head

5.2.2 Comparitive study of conventional and IAP methods in different soil conditions

Soft clay, stiff clay, multilayered soil, loose sand and dense sand with parametric properties as mentioned in the Table 4.1, were used for the pile group analysis under the IAP and 2 different conventional methods i.e. SBC and MAD. We have considered the maximum bending moment, the location of maximum bending moment, maximum shear force, and axial and lateral deflection at pile head in all these soil types, as shown in Fig 5.11-Fig 5.15 , to evaluate and compare the responses of different design approaches and also to study the effect of soil conditions on these responses.

From Fig 5.11(a) and (b), it can be seen that the maximum bending moment values were almost same in all the soil types in case of SBC and IAP. While in case MAD, for both free and fixed head pile condition, the maximum bending moment values vary with the change in soil type. In MAD, when the pile is free head, absolute value of the maximum bending moment is for the dense sand, followed by stiff clay, loose sand, multilayered soil, and soft clay while for the fixed head pile condition the order is same except the maximum bending moment value of stiff clay is reduced and becomes smallar than that of loose sand. This seem to have occurred because of the stiff clay not being able to reach the maximum lateral displacement of 25 mm employed in case of MAD method, which is also reflected in the stiffness values at the pier base along x direction in Table 5.1.

In Fig 5.11(c) indicates that the location of maximum bending moment changes with different soil types in SBC, when the pile is free head while in MAD, except the stiff clay, all other soil types have the maximum value at the almost same location. In IAP, stiffer the soil, the location of

maximum bending moment is closer to the ground surface, and hence, stiff clay lies in the top of the order for having maximum bending moment at 0.25 m from the ground surface which is followed by dense sand, multilayered soil, soft clay and the loose sand which are at the location of 1.26 m, 1.5 m, 1.5 m and 1.7 m below the ground surface respectively. In SBC and IAP, we can see the effects of soil in the location of maximum bending moment while MAD does not reflect the effect much in terms of location.

Fig 5.11(d) shows that in fixed head pile condition, both of the conventional methods, i.e. SBC and MAD, have their maximum bending moment at the pile head regardless of the soil condition

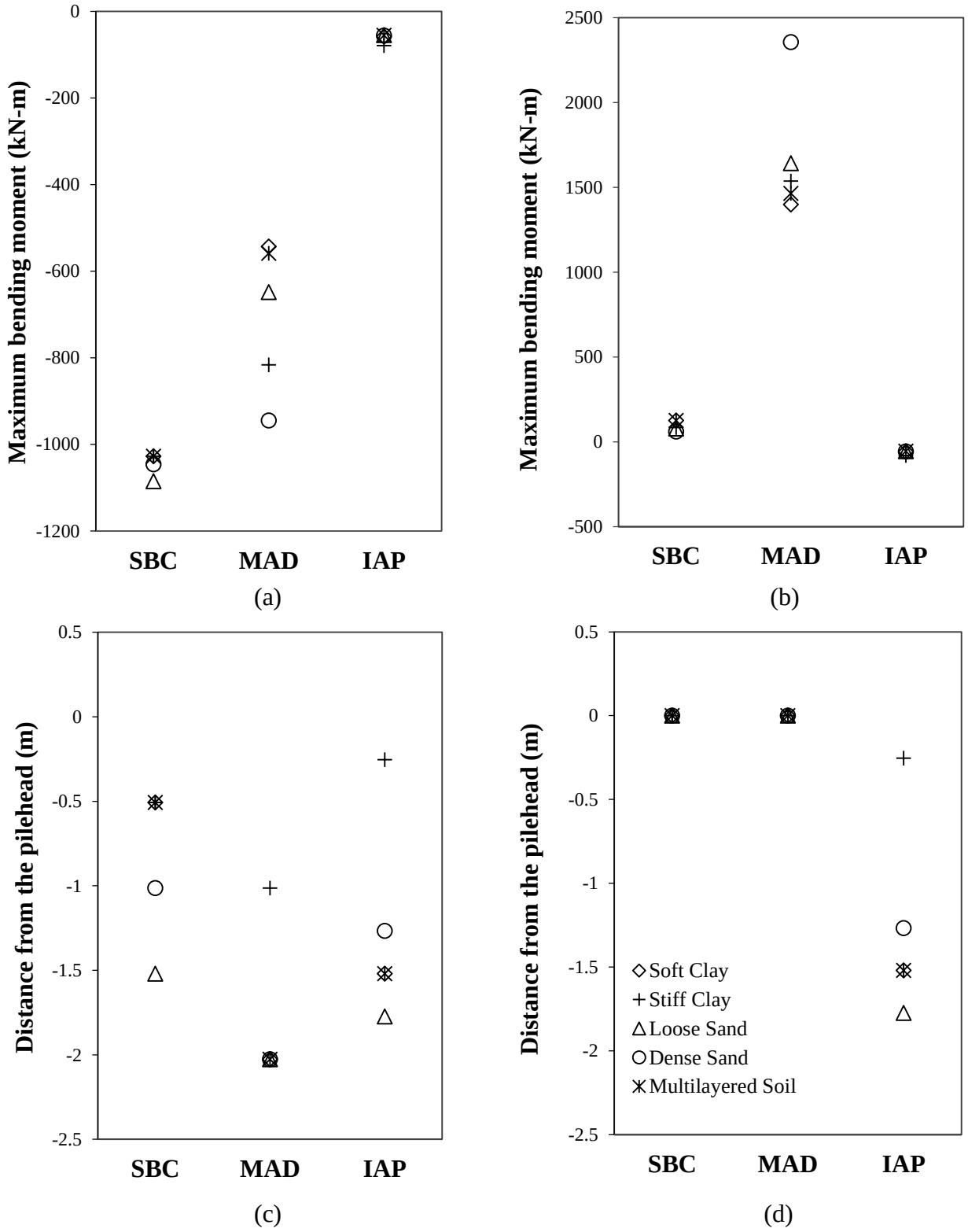

Fig 5.11: Maximum bending moment in piles groups under pier #2 in different soil types a. free head b. fixed head; Location of maximum bending moment c. free head d. fixed head

Fig 5.12 compares the maximum shear forces along the equivalent pile group in SBC, MAD and IAP, for different soil and pile head fixity conditions. Fig 5.12(a) demonstrates that the soil effect in maximum shear force for SBC and MAD, when the pile head is free, are more visible than IAP. Additionally, the values of are also higher than that of IAP suggesting the increase in lateral reponse of pile in the conventional methods. Morever, MAD and SBC in different soil conditions have their respective shear values in opposite direction.

Fig 5.12(b) indicates that in fixed head pile condition, SBC, has maximum shear force value much reduced than that of free head pile and almost same regardless of the soil condition. This lateral response of SBC is similar to that of IAP, where all the soil types have same shear force except for stiff clay, which is smaller and in the opposite direction than the rest. However, for MAD, the shear values are much higher than that of these two methods, and there also a visible soil effect.

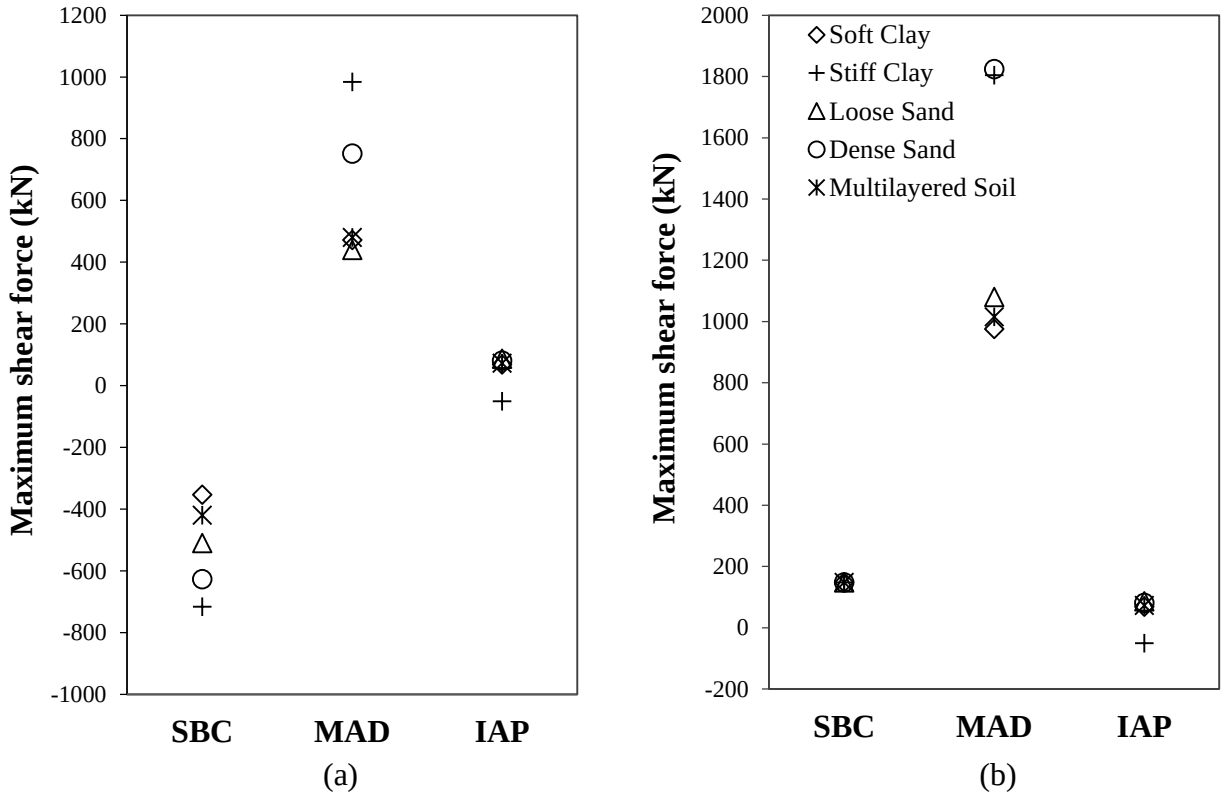

Fig 5.12: Maximum shear force in pile group under pier #2 in different methods in case of soil types; (a) free head, (b) fixed head

Lateral deflections of pile foundation in IAP, SBC and MAD in case of different soil type is compared by the Fig 5.13. It can be seen that in case of IAP, the maximum lateral deflection is very small regardless of the soil type. Fig 5.13(a) shows that in case of free head pile, SBC shows significant difference in the deflection values for each soil type where loose sand has the highest deflection followed by soft clay, multilayered soil, dense sand and stiff clay. Similarly, in case of MAD, maximum allowable lateral deflection was assumed to be 25 mm and hence, all the soil types except stiff clay, have 25 mm lateral deflection. Comparing between SBC and MAD, it can be observed that in SBC, for soil types like soft clay and loose sand, the maximum lateral deflection value is more than 25 mm. It was a general assumption that, the lateral deflection would not reach more than the presumptive value but the above observation suggests that it might not be true.

Similarly, in case of fixed head pile, MAD has same maximum allowable lateral deflection applied to it while in case of SBC, the deflection values in each soil types are reduced from that of free head pile condition. The values are almost same in all the soil types and the results look similar to that of IAP.

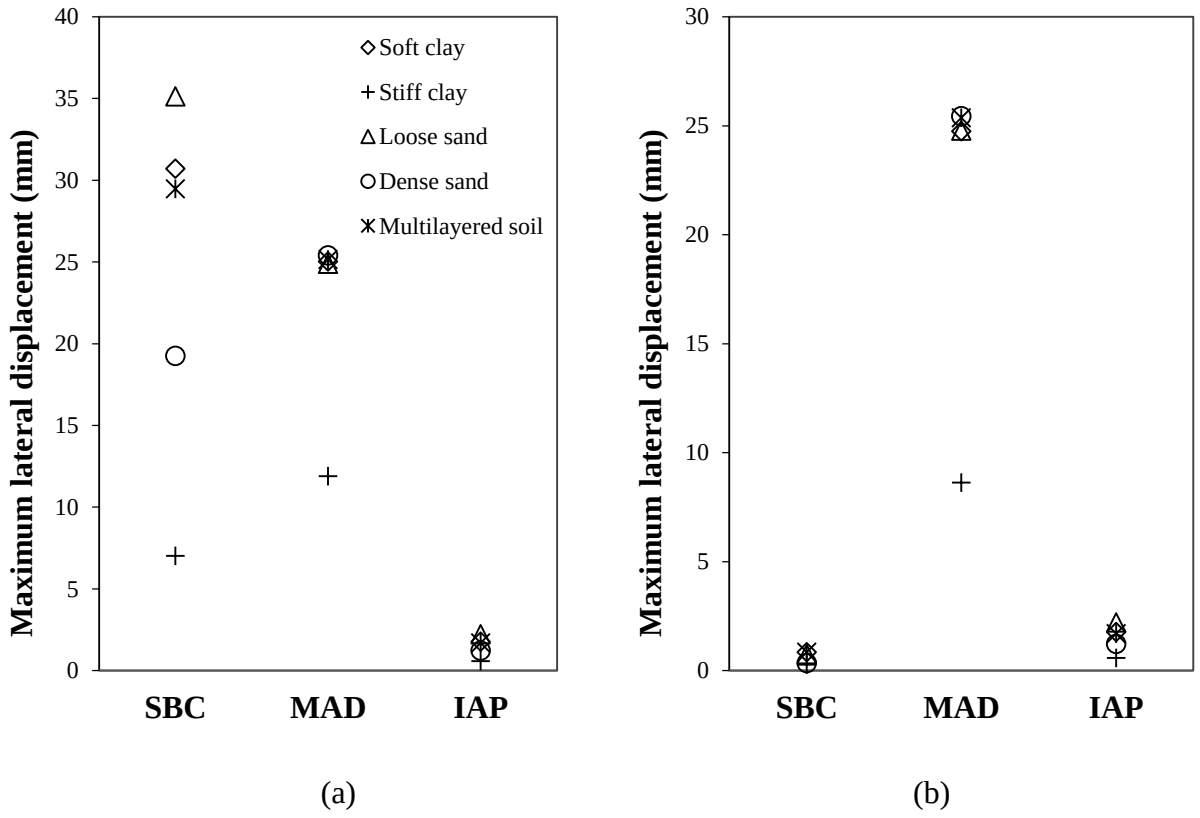

Fig 5.13: Maximum lateral displacement in pile #2 in different methods in case of different soil types; (a) free head (b) fixed head

SSM 2.0 has axial soil springs along with the lateral springs and hence, the IAP method accounts in the axial behaviour of the pile groups. The bridge foundation contains 8 pile caps with each containing a group of 9 individual pile arranged in 3 rows, as shown in Fig 4.1(c), and the average value of axial displacement in each row was calculated. Fig 5.14 represents the axial displacement of the each row of pile groups, named as leading row, middle row and back row, for

the above mentiones 5 different types of soil in IAP method to facilitate the comparitive effects of these different soils. It is observed that among these different soils, soft clay has the maximum axial displacement, while is followed by loose sand, multilayered soil, stiff clay and dense sand, where stiff clay and dense sand have similar values and the least comared to others. Moreover, back row have more axial desplacement that the other two rows.

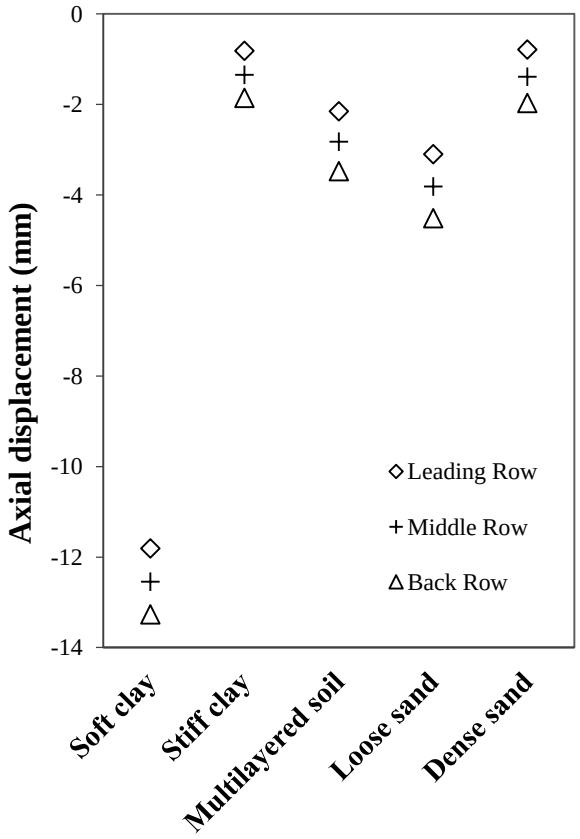

Fig 5.14: Axial displacement of the pile head in all soil types in IAP (average of the displacement in each row)

Fig 5.15 compares the maximum axial displacement in SBC, MAD and IAP in case of different soil types. It can be observed that, displacement values in SBC and MAD for both free head and fixed head pile conditions are the same, suggesting no effect of pile head boundary condition on

the settlement values in these two conventional methods. This is in consistent with the values of translation stiffness along Y direction, in Table 5.1, which shows same stiffness values in SBC and MAD for both free and fixed head. Fig 5.15 illustrates that MAD, as usual has presumptive deflection values and all of these do not reach the maximum limit while IAP and SBC have similar results.

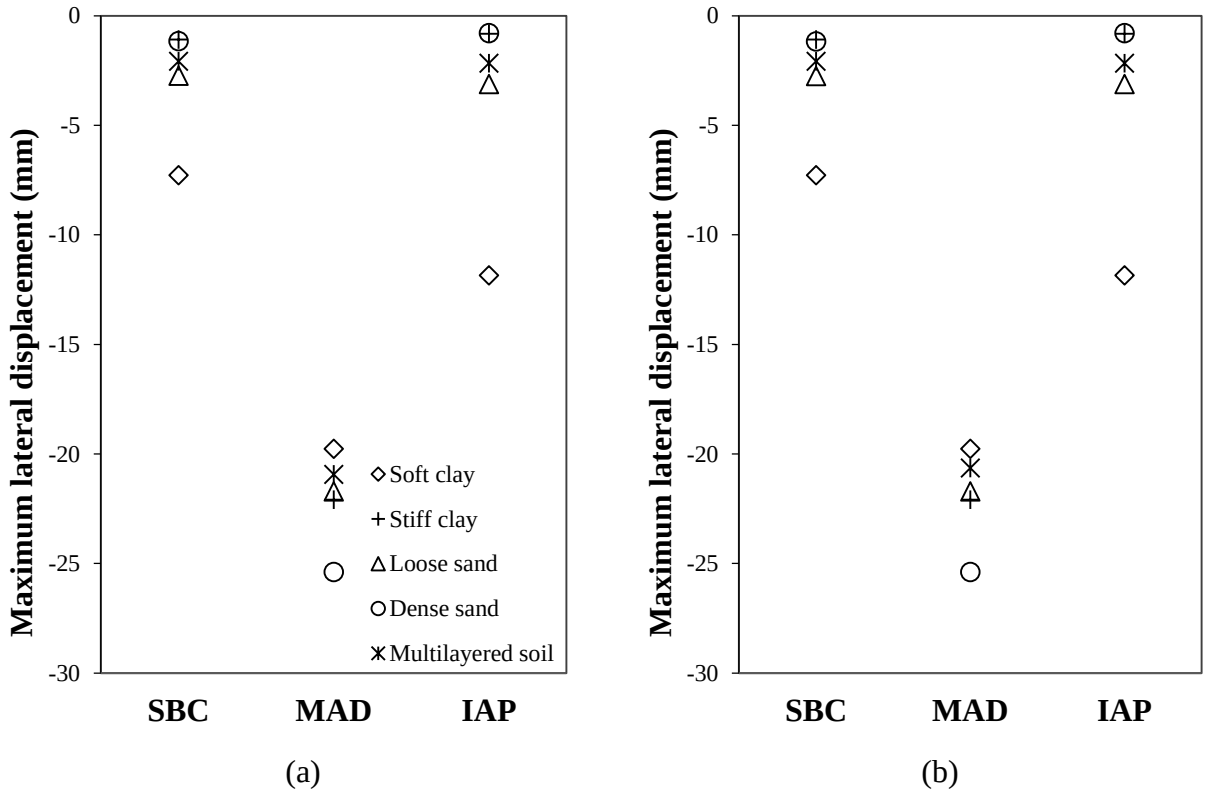

Fig 5.15: Maximum axial displacement of the pile in case of different soil types for different methods; (a) free head (b) fixed head

5.3 Spring Stiffness for superstructure

Spring stiffness values at the base of superstructure account for most of the superstructure and foundation responses and is one of the important factors to consider in structure design analyses and soil structure interaction. In case of conventional method SBC, the reaction forces at the base of superstructure obtained after assigning the fixed support, was then divided by the deflection at the pile head along corresponding directions generated from the single pile analysis in case of both free head and fixed head boundary condition. And, in another conventional method, MAD, we assumed maximum lateral and axial displacement at the pile head of 25 mm each. The spring stiffness value along these two directions is then obtained by diving the corresponding loads generated in pile analysis by the applied maximum displacement. Whereas, for IAP, the shear force, axial force, bending moment and forces in other directions obtained from the integrated structure analysis at the base of a pier were divided by deflections at the pile head in the corresponding directions.

Table 5.1 shows the spring stiffness values at the base pier #2 of K45 bridge in case of various bridge analysis methods i.e. SBC, MAD and IAP under various soil conditions. The table shows stiffness values along 3 degree of freedoms i.e. translational X (K_{FX}), Y (K_{FY}) and rotational Z (K_{MZ}). In MAD method, for the pile analysis, only the maximum allowable lateral displacement (dx) and vertical displacement (dy) is applied, and hence, we get stiffness along X (K_{FX}), and Y (K_{FY}) direction only. Moreover, due to lack of rotational displacement in the pile analysis, the moment along Z direction (K_{FZ}) is released in case of MAD analysis, which can be seen in Table 5.1. Besides, the spring stiffness used in all the pier bases is same in case of MAD method. Similarly, SSM was used for the analysis of single pile foundation in case of SBC and MAD, and

SSM does not have provision for the torsional soil springs, because of which we don't have any significant stiffness values along rotational Y (K_{MY}) in SBC, and hence it is not mentioned here. Additionally, in SBC, only piers 3 and 7 have forces along translational Z in the bridge, that leaves no K_{FZ} for pier #2. As per the value of $K_{MX,}$ we have some value in SBC along rotational X, but is not shown in the table to make it uniform with MAD for comparison.

Table 5.1 compares the stiffness values in IAP, and SBC and MAD in different pile head boundary condition. For free head, K_{FX} value in SBC is smaller than K_{FX} value in MAD for all the given soil conditions whereas in fixed head pile condition, K_{FX} value in SBC is larger than that of MAD. It can also be observed that the K_{FX} values in MAD, in fixed pile head condition, are similar to that of IAP. This seems to have contributed to the lateral response of superstructure in MAD, when the pile is fixed head, having closer results to that of IAP than SBC. Similarly, K_{FY} value in SBC is larger than those in MAD in case of both free and fixed head pile under all the given soil condition. Also, K_{FY} values of SBC are more agreeable to that of IAP than MAD. This observation aligns with the observations from Fig 5.15 where the maximum axial deformation in case of IAP and SBC are similar. Furthermore, SBC have some value for K_{MZ} which is small compared to IAP but in MAD, it is released. This contributes to having zero and a very small bending moment at the base of pier in free head MAD and SBC respectively.

The table also illustrates the difference in superstructure base stiffness values in different soil types. It can be seen that stiffer the soil, higher is the stiffness values. In SBC, translational stiffness along X direction, K_{FX} is highest in case of stiff clay followed by dense sand, multilayered soil, soft clay and loose sand in case of both free and fixed head condition. IAP and MAD also follows the similar pattern. For $K_{FX,}$ In MAD, dense sand has the highest stiffness, followed by stiff clay, loose sand, multilayered soil and soft clay while in case of SBC, the value for stiff clay is the

highest which is followed by dense sand, multilayered soil, soft clay and loose sand. This pattern of SBC is as that of IAP. From the above observations, it can be concluded that along lateral response MAD have results closer to IAP than SBC while in case of axial response, IAP and SBC have more similar results.

Table 5.1 Stiffness values at the bottom of pier #2 in upstream

Soft Clay					
	SBC		**MAD**		**IAP**
	Free head	**Fixed head**	**Free head**	**Fixed head**	
K_{Fx} (kN/m)	4810	174384.9	18855.86	39450.28	52396.045
K_{Fy} (kN/m)	175310.03	175310	89289.15	89289.15	104595.2
K_{Mz} (kNm/deg)	796.69	Fixed	Released	Fixed	5263.56
Stiff Clay					
	SBC		**MAD**		**IAP**
	Free head	**Fixed head**	**Free head**	**Fixed head**	
K_{Fx} (kN/m)	21037.46	541401	82716.88	209159.4	185398.63
K_{Fy} (kN/m)	1175191	1170564	239097.9	239097.9	913592.43
K_{Mz} (kNm/deg)	1637.17	Fixed	Released	Fixed	10661.17
Loose Sand					
	SBC		**MAD**		**IAP**
	Free head	**Fixed head**	**Free head**	**Fixed head**	
K_{Fx} (kN/m)	4203.78	98207.45	17684.89	43569.47	41671.79
K_{Fy} (kN/m)	465617.3	465617.3	174714.3	174714.3	338828.2
K_{Mz} (kNm/deg)	738.06	Fixed	Released	Fixed	5316.91
Dense Sand					
	SBC		**MAD**		**IAP**
	Free head	**Fixed head**	**Free head**	**Fixed head**	
K_{Fx} (kN/m)	7675.726	216574.8	29615.63	71715.02	83656.3
K_{Fy} (kN/m)	1095500	1095500	493224.1	493224.07	8911656.3
K_{Mz} (kNm/deg)	126.04	Fixed	Released	Fixed	8205.12
Multilayered soil					
	SBC		**MAD**		**IAP**
	Free head	**Fixed head**	**Free head**	**Fixed head**	
K_{Fx} (kN/m)	5010.822	175004.7	19088.52	40052.04	57100.7
K_{Fy} (kN/m)	614175.6	614175.6	144815.1	146540	452855.5
K_{Mz} (kNm/deg)	827.11	Fixed	Released	Fixed	6448.16

6 Conclusions and Recommendations

The thesis has presented modifications and the use of Integrated Analysis Process (IAP) and a comparative study between the IAP and other conventional methods currently in use i.e. SBC, MAD and EPL for a pile-supported framed structure. Substructure and superstructure elements were analysed in a holistic approach in IAP, through the use of STAAD.Pro and SSM 2.0 that utilized p-y, t-z and q-z soil springs. Whereas other methods analyzed the superstructure and foundation separately. The IAP method is believed to ease the job of engineers involved in the design of pile-supported structures by bridging the gap between the foundation and superstructure analysis, as well as incorporating the soil structure interaction in the design to make it more realistic. The IAP method can also be extended to include more features in the analysis. The Soil Spring Module (SSM) program used in the IAP can be updated for more soil spring curves, as well as other features as per the need. Moreover, the scour analysis which can predict the susceptibility of pile-supported structures to the scour can also be done to make a realistic structure response analysis for a hazardous situation.

A case study was carried out to demonstrate the use of various pile-supported structure analysis methods and the IAP method. A comparative study was also conducted among the IAP method and these traditional methods such as SBC, MAD and EPL with some crude assumptions for the analysis of Kansan 45 bridge. The analysis was made under various soil and pile head boundary (free and fixed in case of MAD and SBC) conditions. Responses of the structure and foundation were evaluated, and the spring stiffness values at the base of pier was also studied. Based on the study, following conclusion were drawn:

- The bending moment distribution for superstructure given by IAP lies somewhere in between free head and fixed head conditions of SBC and MAD. However, in general SBC method shows some comparable result as that of IAP in free head, and for fixed head pile condition MAD shows more agreeable response to that of IAP.
- In the lateral response of the structure, the change in soil condition is well approximated by the IAP method. EPL shows little to no soil effect, MAD corresponds to the soil change only in case of fixed head pile condition, whereas SBC shows soil effect both in case of free and fixed head pile condition.
- The maximum lateral displacement of superstructure in IAP is most agreeable with MAD. Besides, in case of fixed head pile, SBC, MAD and IAP all have similar deflection values.
- The lateral load borne by the structure in SBC and MAD, in free head condition, is higher at the top of pier and reduces towards the bottom or closer to the foundation, But in IAP, the structure bears mode load towards the bottom than the top. Whereas, when the boundary condition is changed in SBC and MAD, the load borne by the structure increases by a large amount. This suggests that SBC and MAD may have more comparable results to that of IAP in fixed head condition.
- The foundation and superstructure responses are converged in case of IAP, as the lateral deflection in superstructure base is almost same as that of lateral deflection in the pile head while there are huge discrepancies in these two deflections in case of MAD and SBC.
- The lateral response of the foundation given by IAP, aligns more with the response given by SBC, in fixed head pile condition.
- The axial response in a foundation is not affected by the pile head boundary condition.

- In weaker soils like soft clay and loose sand, the maximum lateral displacement in pile head given by SBC exceeds the presumptive maximum allowable displacement value provided by MAD.

The thesis has worked as a first step towards the implementation of IAP method through the use of SSM for achieving integrated analysis of a pile-supported framed structure and comparative study with current approaches. The results presented here are based only on the parameter changes of soil types and boundary conditions in these approaches. For the further comparison, other parameters such as change of pile configuration, and material type for the pile and structure could give better insight into the differences in responses of these approaches. Besides, IAP used in this thesis, is based on state-of-the art procedures and it has a lot of potential for further development and update as per the need. For example, some of the areas in SSM that can be updated for better analysis could be the addition of torsional soil spring (t-θ) curves, pile group effects, and scour hole analysis.

References

[1] "The deadliest bridge collapses in the US in the last 50 years," *CNN*, Mar. 15, 2018.

[2] C. Lin, C. Bennett, J. Han, and R. Parsons, "Scour effects on the response of laterally loaded piles considering stress history of sand," *Comput. Geotech.*, vol. 37, no. 7–8, pp. 1008–1014, 2010.

[3] C. Lin, C. Bennett, J. Han, and R. L. Parsons, "Integrated analysis of the performance of pile-supported bridges under scoured conditions," *Eng. Struct.*, vol. 36, pp. 27–38, Mar. 2012, doi: 10.1016/j.engstruct.2011.11.015.

[4] "Technical Reference Manual for STAAD. Pro," Bentley System Inc., Exton, PA, 2007.

[5] A. Aviram, K. R. Mackie, and B. Stojadinović, "Guidelines for Nonlinear Analysis of Bridge Structures in California," Pacific Earthquake Engineering Research Center, University of California Berkeley, CA, USA, 2008/03, 2008.

[6] W. M. Isenhower, S.-T. Wang, and L. G. Vasque, "LPILE User's Manual: A Pragram for the Analysis of Deep Foundations Under Lateral Loading," Ensoft Inc, Apr. 2019.

[7] "Improved Seismic Design Criteria for California Bridges : Provisional Recommendations," California Department of Transportation, Applied Technology Council, Redwood City. CA, USA, ATC-32, 1996.

[8] S. G. Paikowsky *et al.*, "Load and resistance factor design (LRFD) for deep foundations," Transportation Research Board, National Research Council, Washington, USA, National Cooperative Highway Research Program Report 507, 2004.

[9] C. Lin and R. Wu, "Evaluation of vertical effective stress and pile lateral capacity considering scour-hole dimensions," *Can. Geotech. J.*, vol. 56, no. 1, pp. 135–143, 2019.

[10] Davisson MT, Robinson KE, "Bending and buckling of partially embedded piles," Canada, 1965.

[11] C. Lin, C. Bennett, J. Han, R. Parsons, and A. D. Parr, "Capacity of Scour-Damaged Bridges, Part 2: Integrated Analysis Program (IAP)—A Program for the Analysis of Lateral Performance of Pile-Supported Structures under Scour Conditions," Art. no. K-TRAN: KU-10-2, Nov. 2013, Accessed: Jun. 22, 2021. [Online]. Available: https://trid.trb.org/view/1320051

[12] Reese, L. C. and Van Impe, W. F., Single Piles and Pile Groups under Lateral Loading. Leiden, the Netherlands: A.A. Balkema Publishers, 2001.

[13] *Recommended Practice for Planning, Designing and Constructing Fixed Offshore Platforms*, 17th ed. Washington, D.C.: American Petroleum Institute (API), 1987.

[14] H. Matlock, “Correlation for Design of Laterally Loaded Piles in Soft Clay,” presented at the Offshore Technology Conference, Apr. 1970. doi: 10.4043/1204-MS.

[15] R. B. Peck, W. E. Hanson, and T. H. Thornburn, *Foundation Engineering*. New York: Wiley, 1974.

[16] L. C. Reese, W. R. Cox, and F. D. Koop, “Field testing and analysis of laterally loaded piles in stiff clay,” presented at the Offshore Technology Conference, 1975.

[17] M. W. O’Neill and L. C. Reese, “Drilled shafts: Construction procedures and design methods,” FHWA, Washington, D.C., FHWA-IF-99-025, 1999.

[18] L. C. Reese, T. S. Wang, and J. A. Arrellaga, “TZPILE 2014- User’s Manual, Analysis of Load Versus Settlement for an Axially - Loaded Deep Foundation,” Ensoft Inc, Austin, TX, 2014.

[19] R. L. Mokwa, J. M. Duncan, and E. V. Charles, “Investigation of the Resistance of Pile Caps and Integral Abutments to Lateral Loading,” Virginia Transportation Research Council, Charlottesville, Virginia, FHWA/VTRC 00-CR4, 2000.

[20] “Design and construction of driven pile foundations – volume 1,” National Highway Institute U.S. Department of Transportation, Federal Highway Administration, Washington, D.C., FWHA-NH-16-009.

[21] “AASHTO LRFD bridge design specifications,” American Association of State Highway and Transportation Officials (AASHTO), Washington, D.C., USA, LRFDBDS-9, 2020.

[22] “NEHRP recommended seismic provisions: design examples,” Federal Emergency Management Agency (FEMA). National Institute of Building Sciences, Building Seismic Safety Council, Washington, D.C., USA, FEMA P-751, 2012.

Appendix A

Structural Response of SBC, MAD, EPL and IAP in soft clay, stiff clay, multilayered soil, and dense sand.

Soft Clay

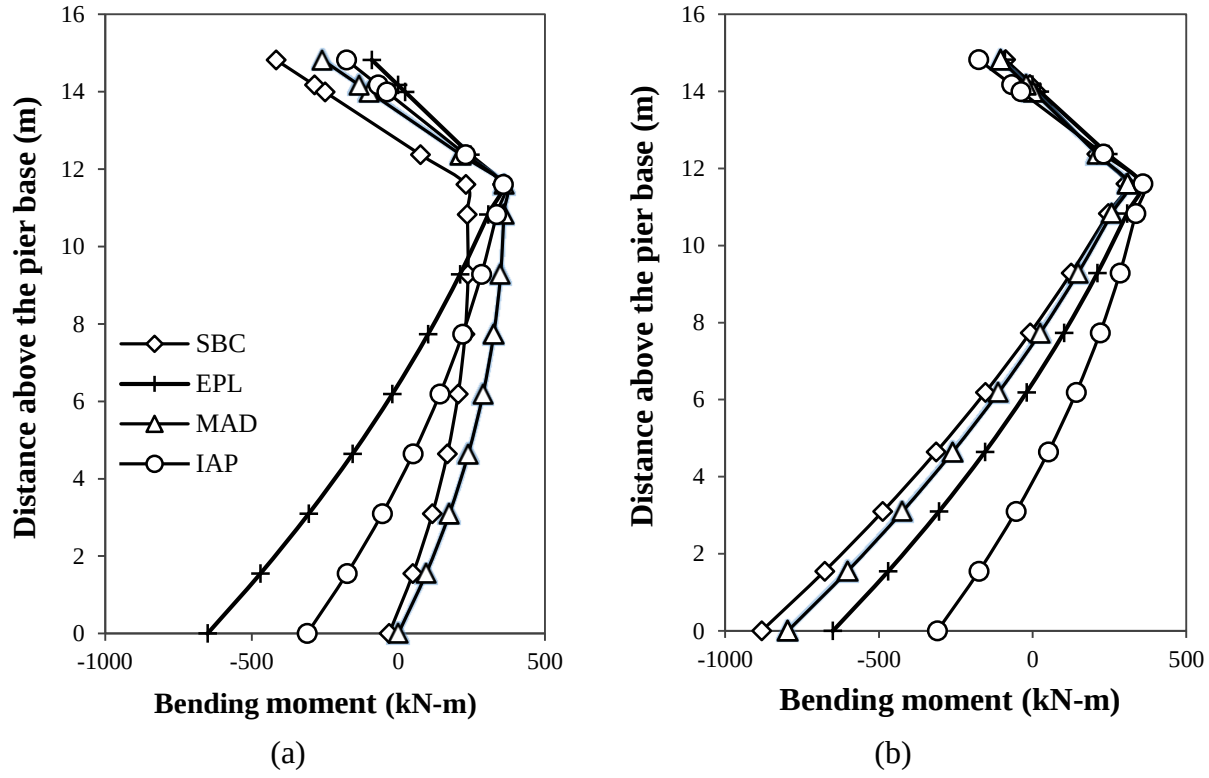

Fig A1: Bending moment along pier #2 in soft clay (a) Free pile head; (b) Fixed pile head

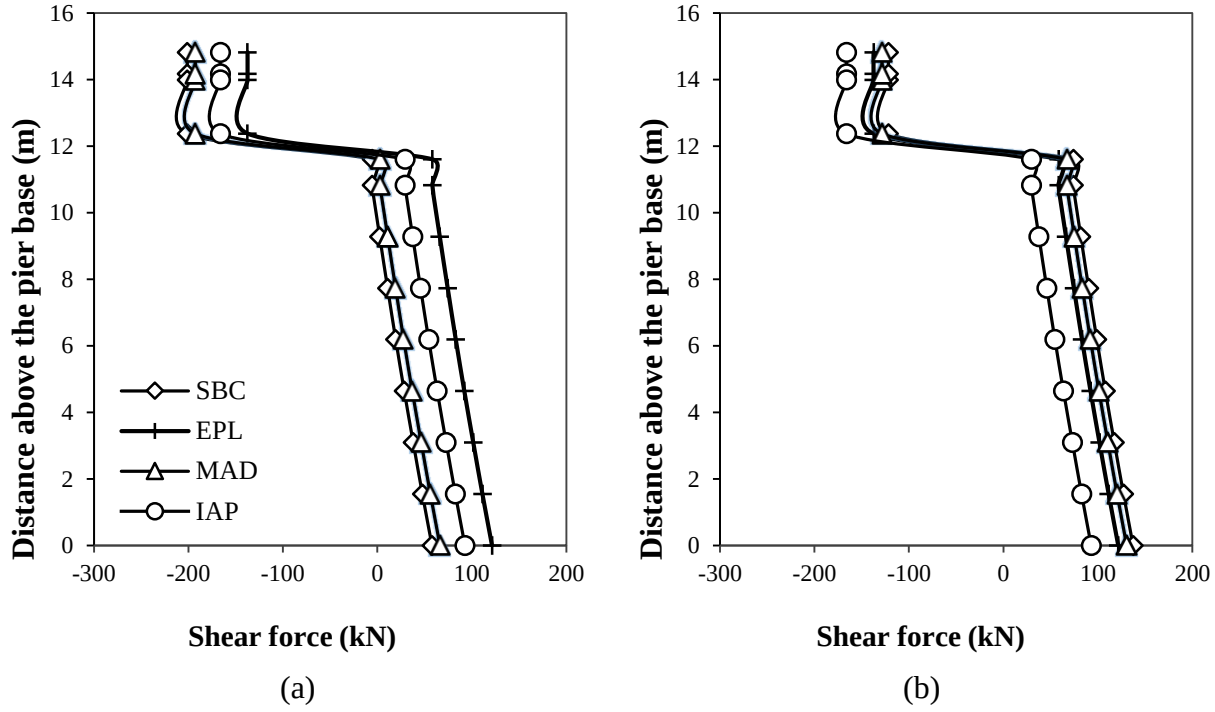

Fig A2: Shear force along pier #2 in soft clay (a) Free pile head; (b) Fixed pile head

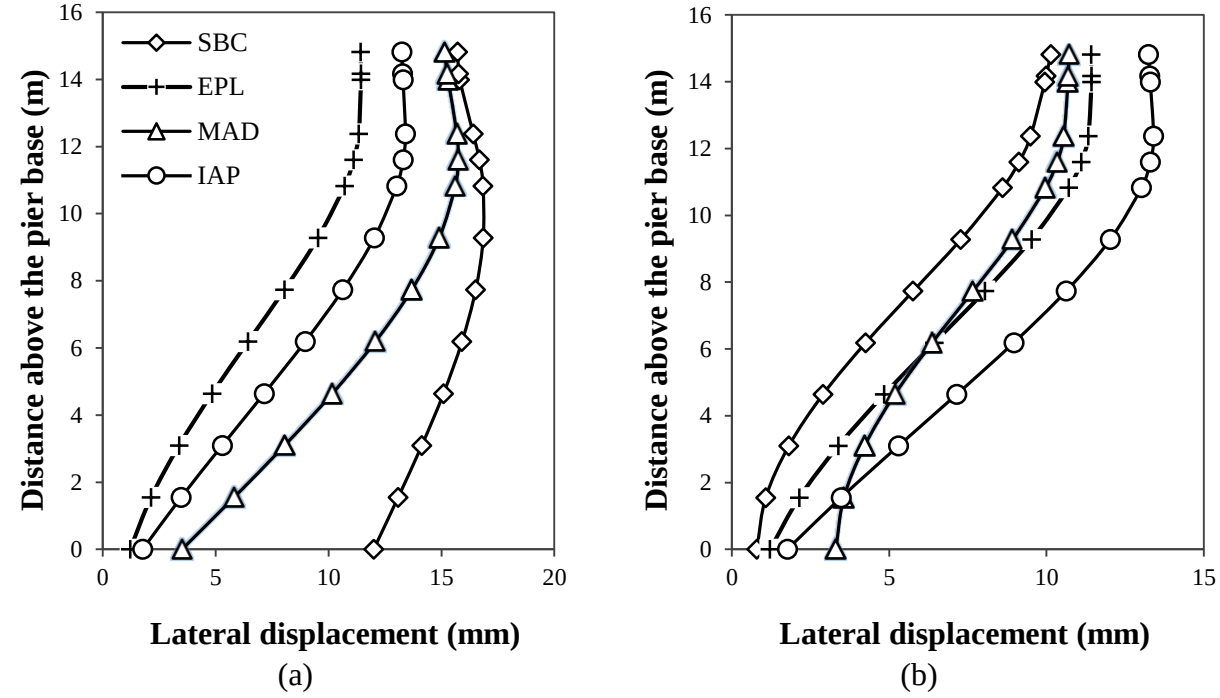

Fig A3: Lateral displacement along pier #2 in soft clay (a) Free pile head; (b) Fixed head pile

Stiff Clay

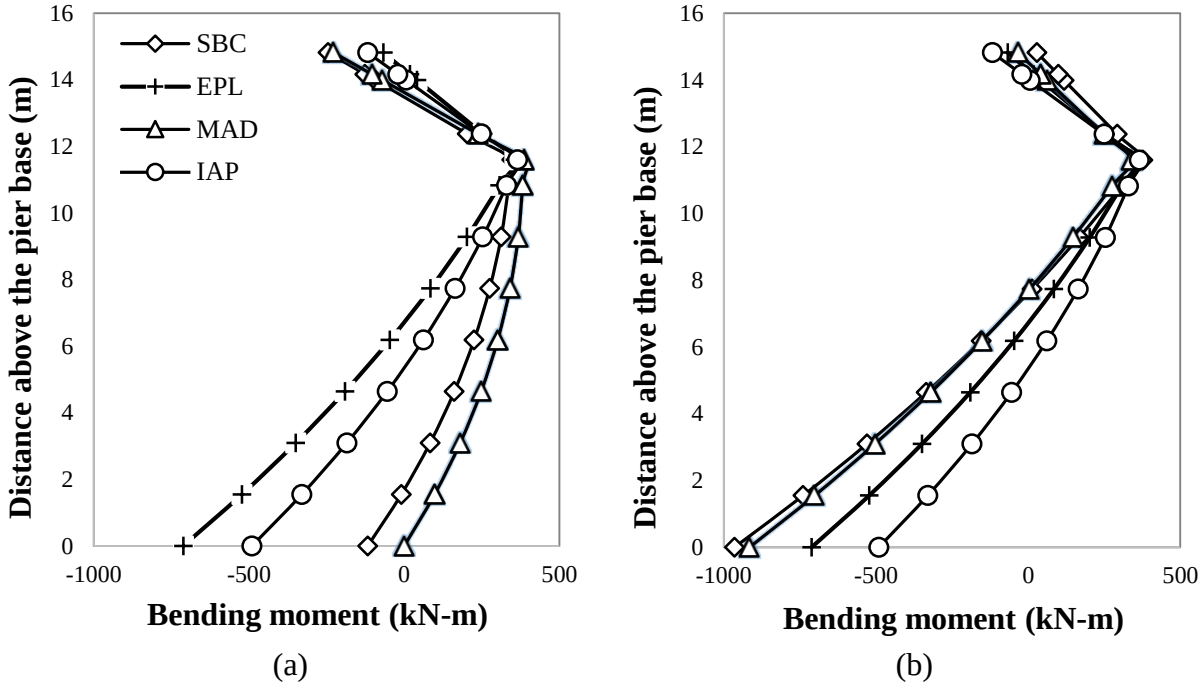

Fig A4: Bending moment along pier #2 in stiff clay (a) Free pile head; (b) Fixed pile head

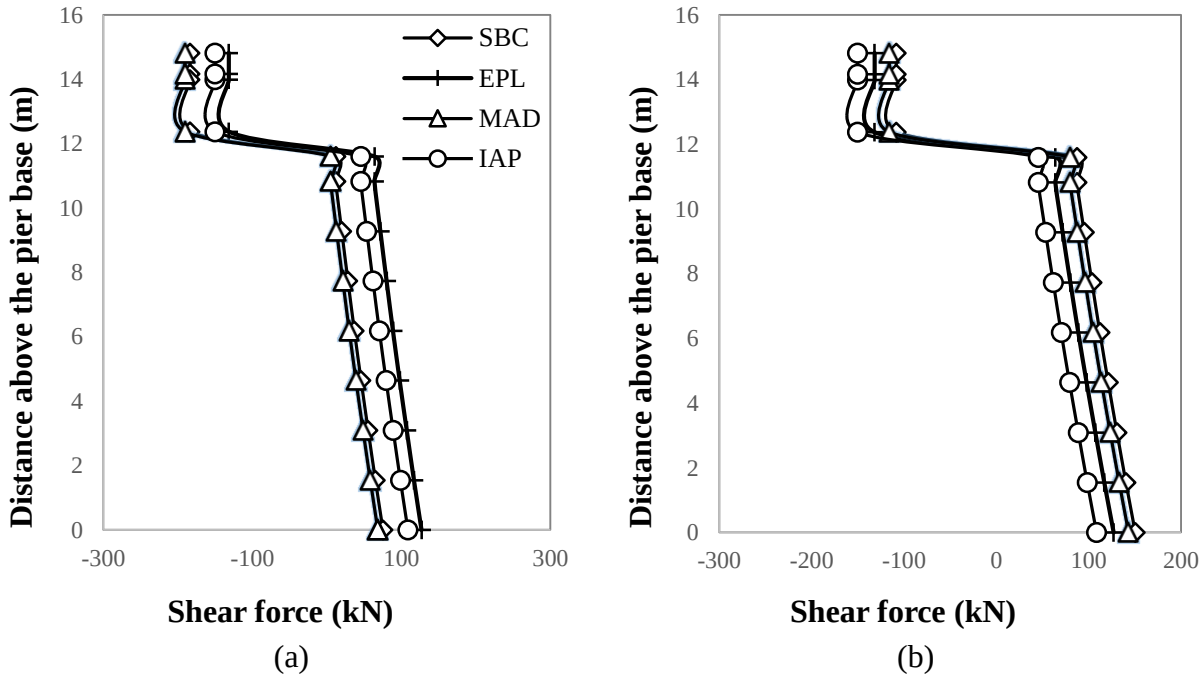

Fig A5: Shear force profile along pier #2 in stiff clay (a) Free pile head; (b) Fixed pile head

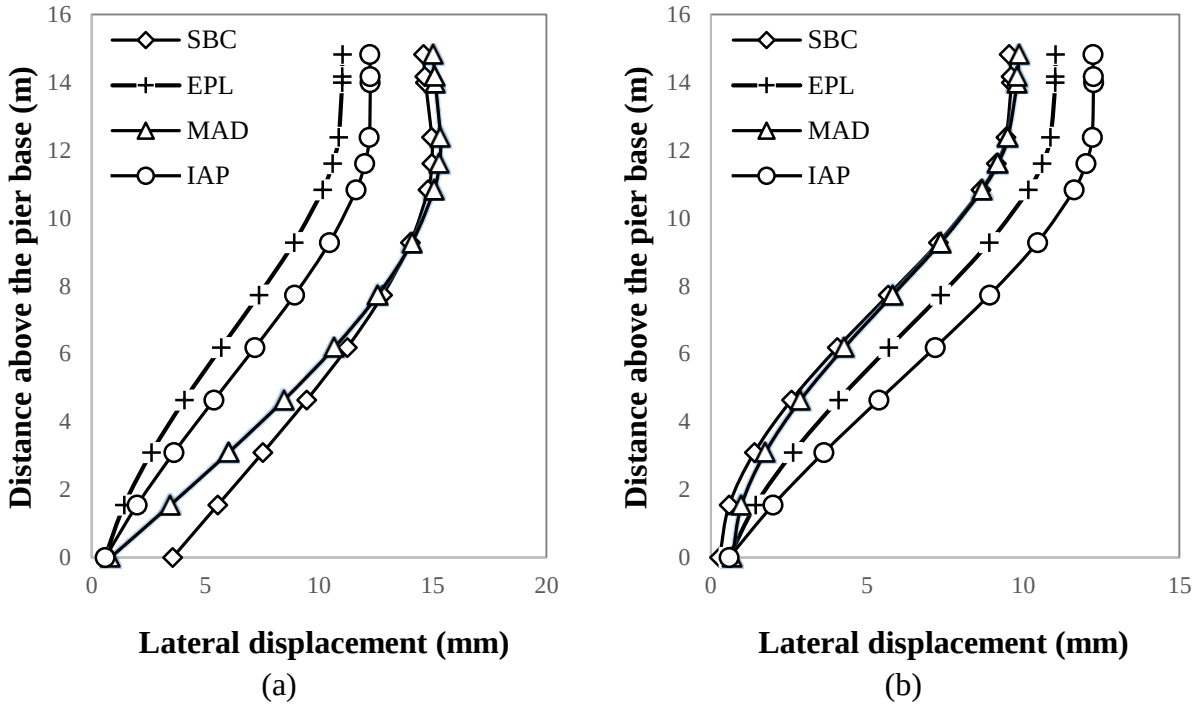

Fig A6: Lateral displacement along pier #2 in stiff clay (a) Free pile head; (b) Fixed pile head

Multilayered Soil

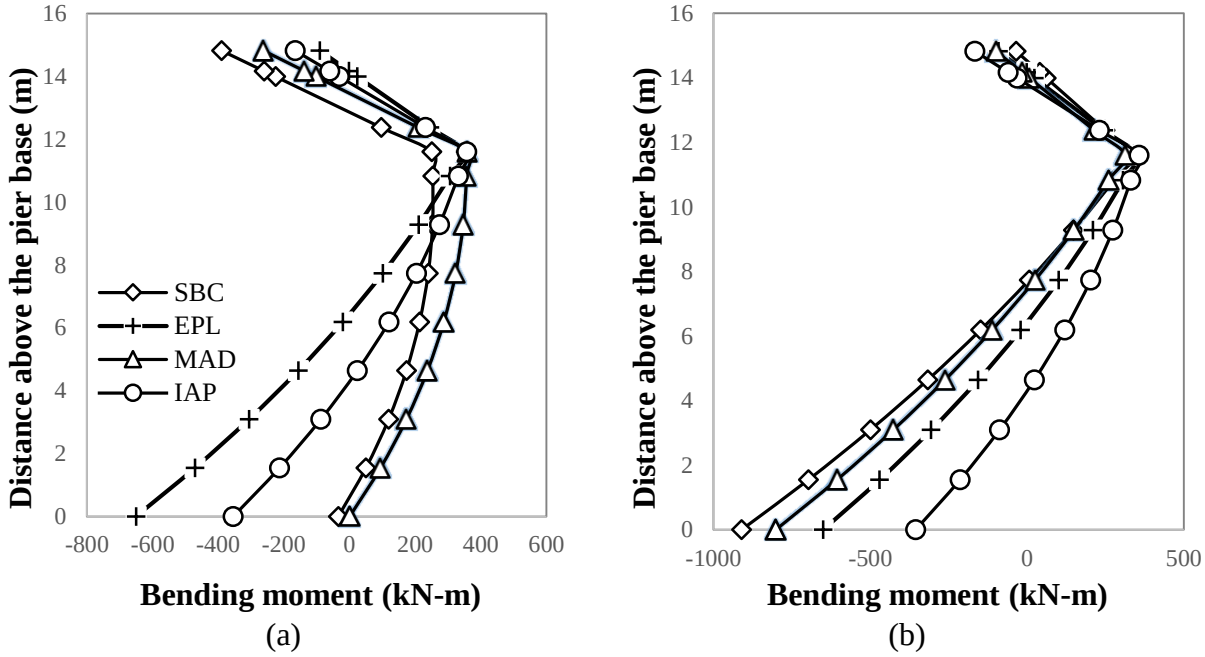

Fig A7: Bending moment along pier #2 in multilayered soil (a) Free pile head; (b) Fixed pile head

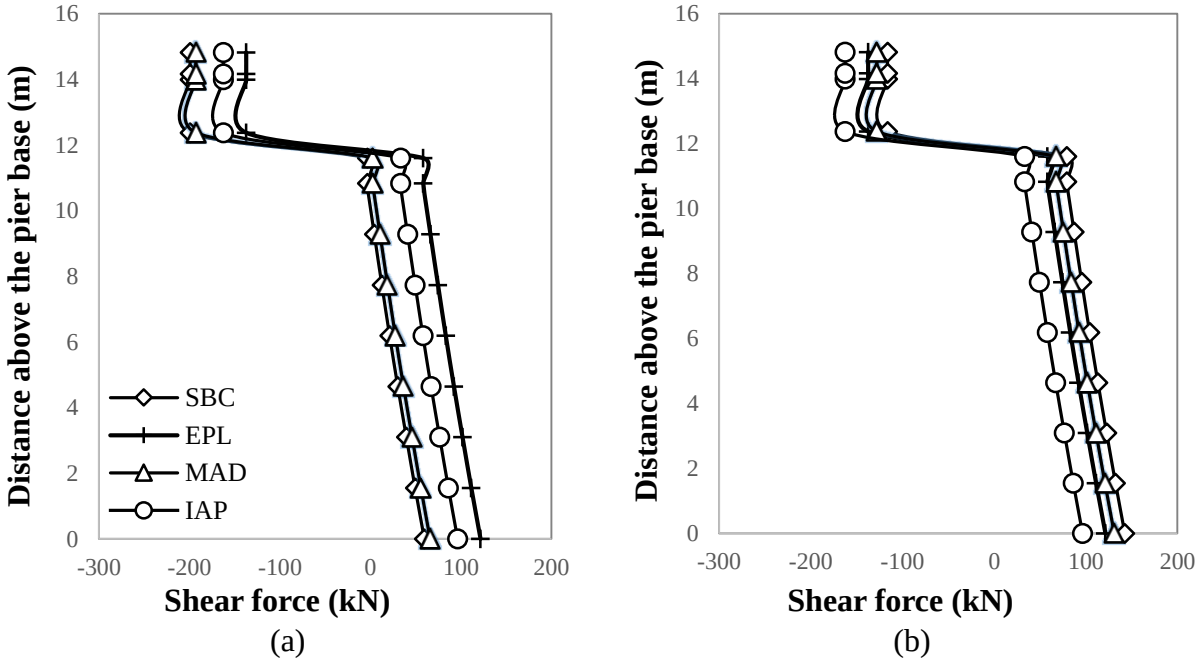

Fig A8: Shear force along pier #2 in multilayered soil (a) Free pile head; (b) Fixed pile head

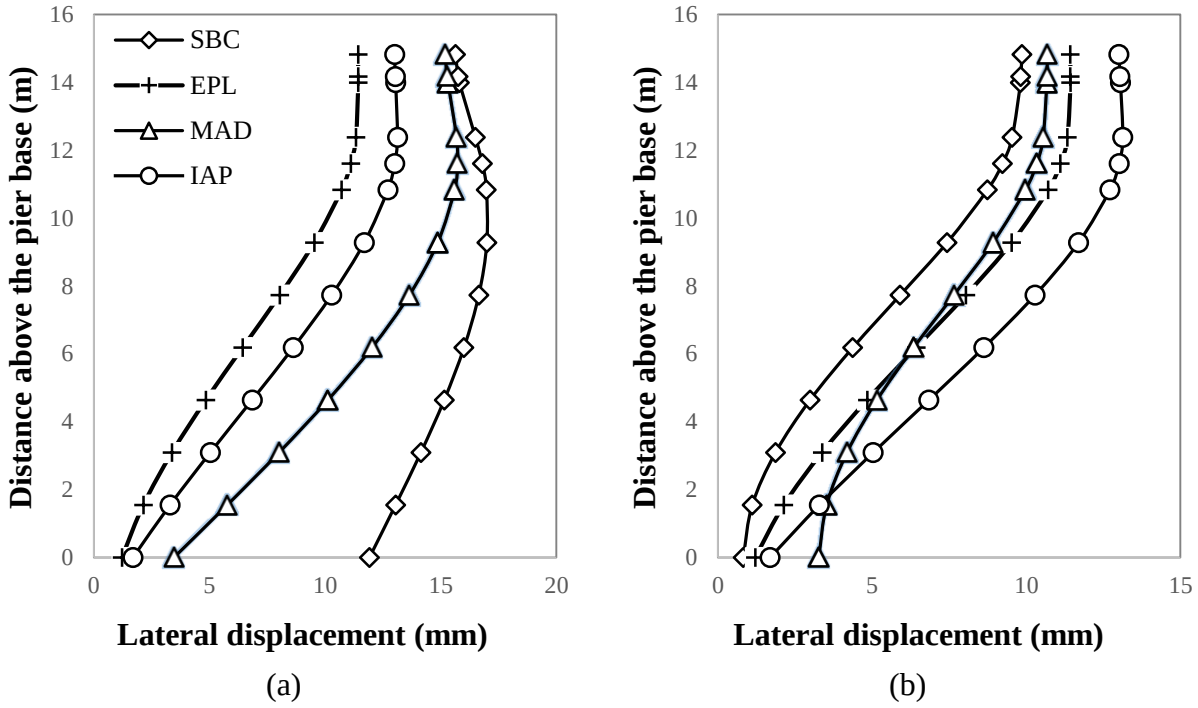

Fig A9: Lateral displacement along pier #2 in multilayered soil (a) Free pile head; (b) Fixed pile head

Dense Sand

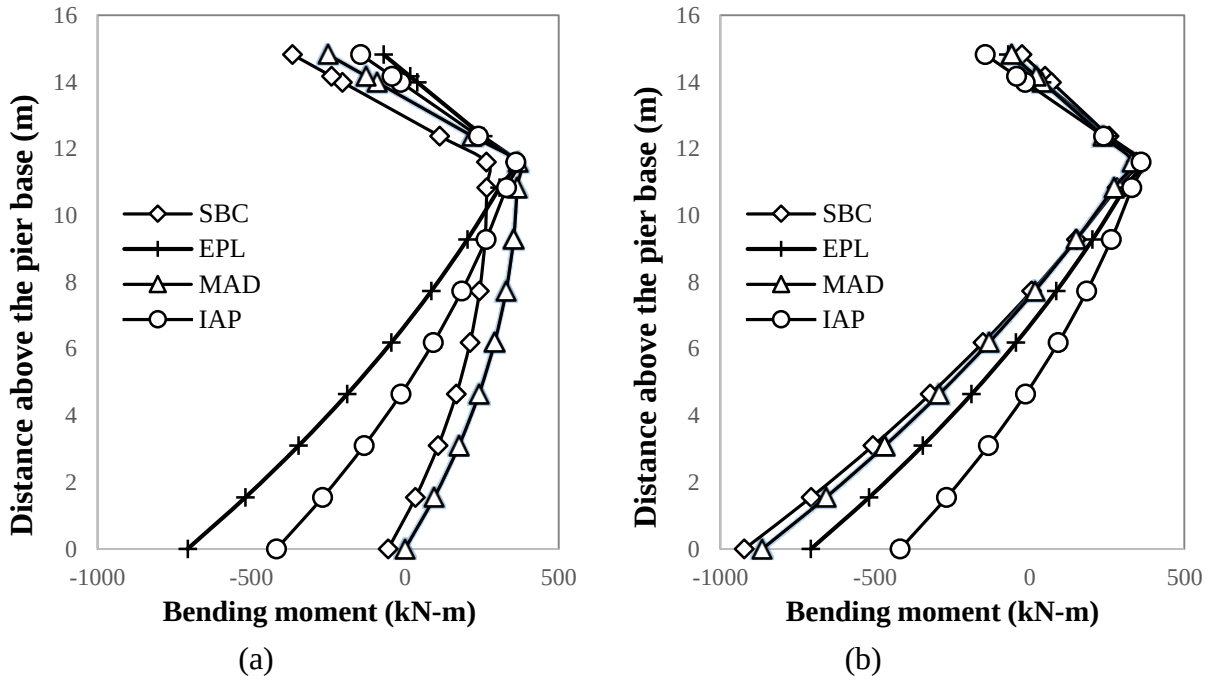

Fig A10: Bending moment along pier #2 in dense sand (a) Free pile head; (b) Fixed pile head

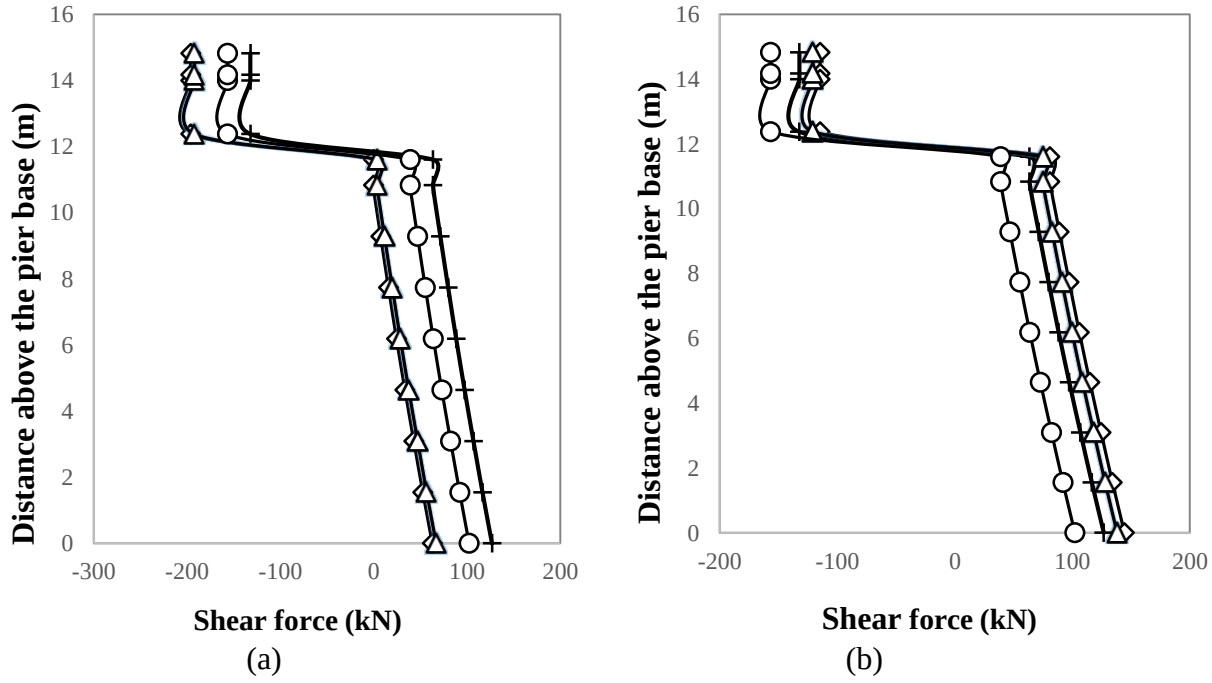

Fig A11: Shear force along pier #2 in dense sand (a) Free pile head; (b) Fixed pile head

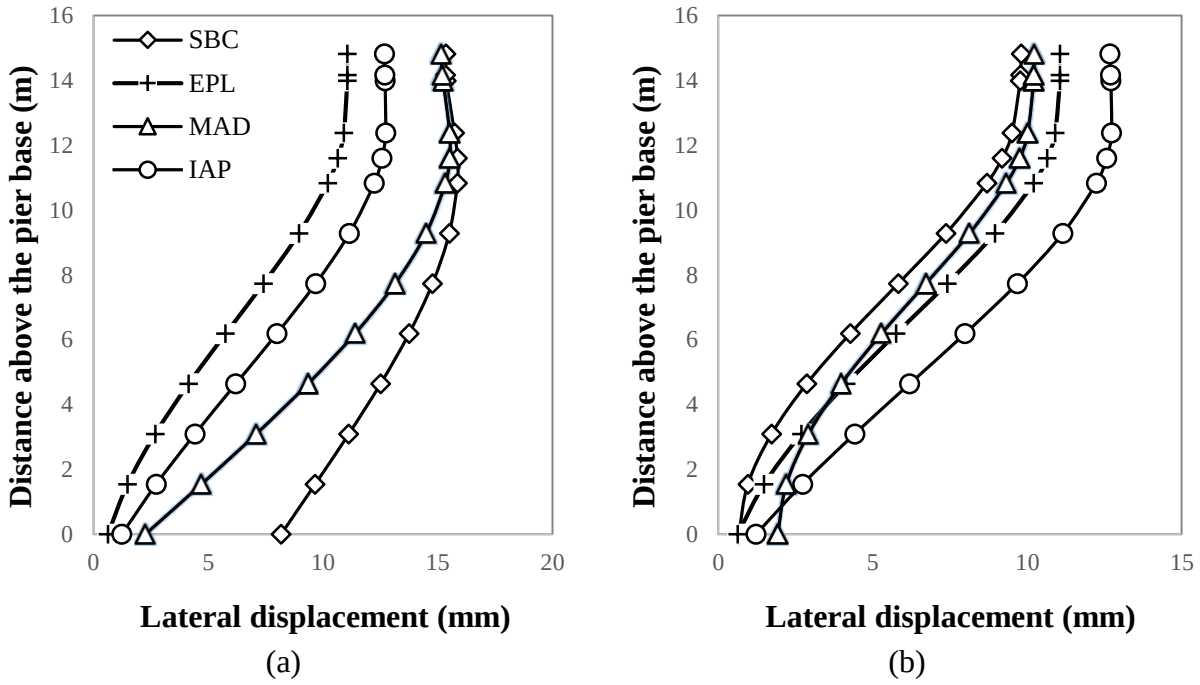

Fig A12: Lateral displacement profile along pier #2 in dense sand (a) Free pile head; (b) Fixed pile head

Appendix B

Substructure Response of SBC, MAD, and IAP in soft clay, stiff clay, multilayered soil, and dense sand.

Soft Clay

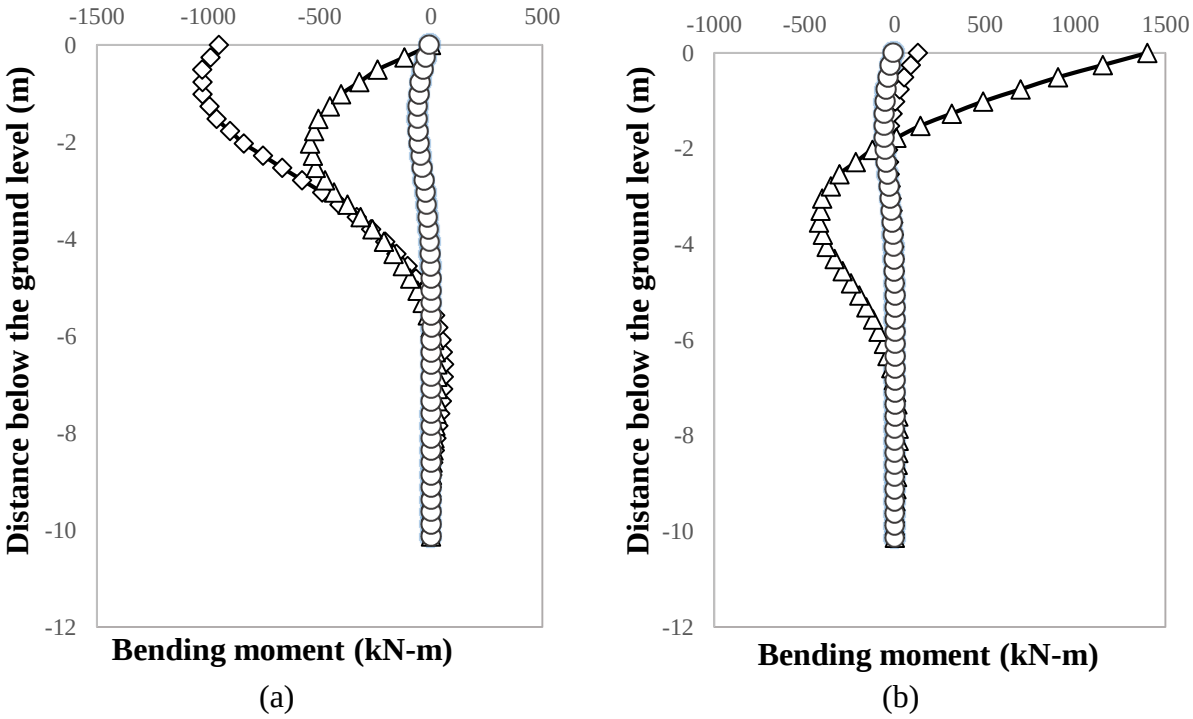

Fig B1: Bending moment along pile group #2 in soft clay (a) Free pile head; (b) Fixed pile head

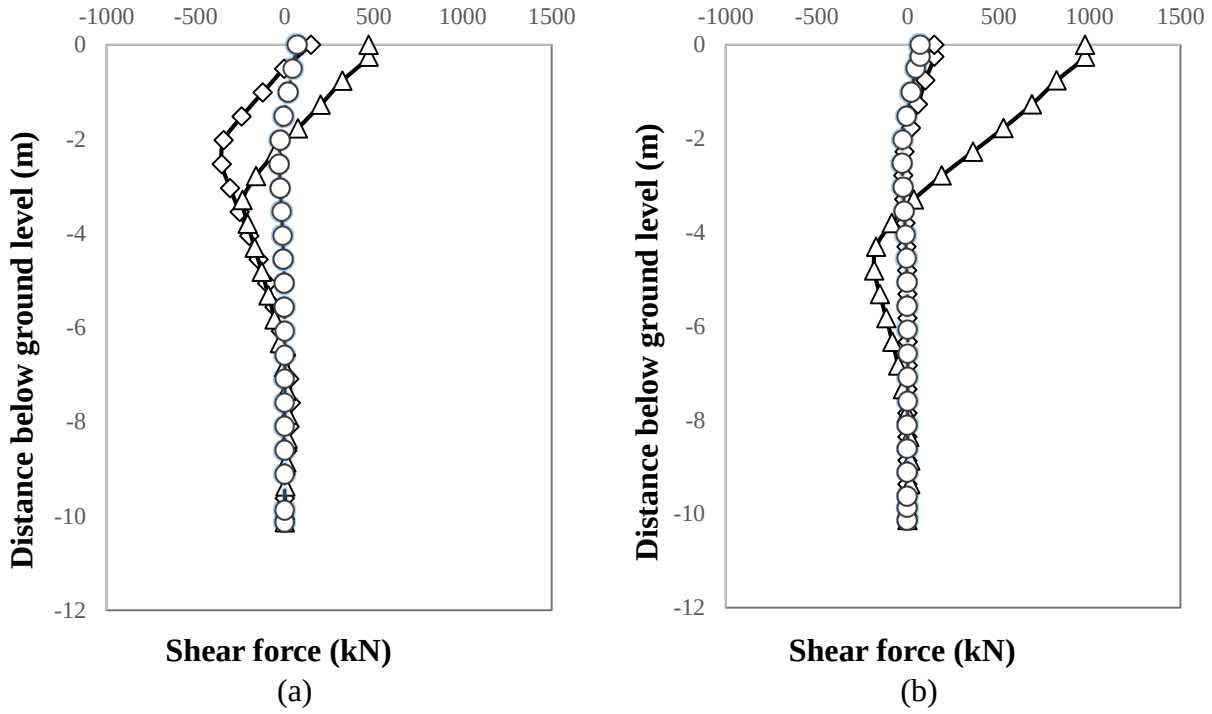

Fig B2: Shear force along pile group #2 in soft clay (a) Free head pile; (b) Fixed head pile

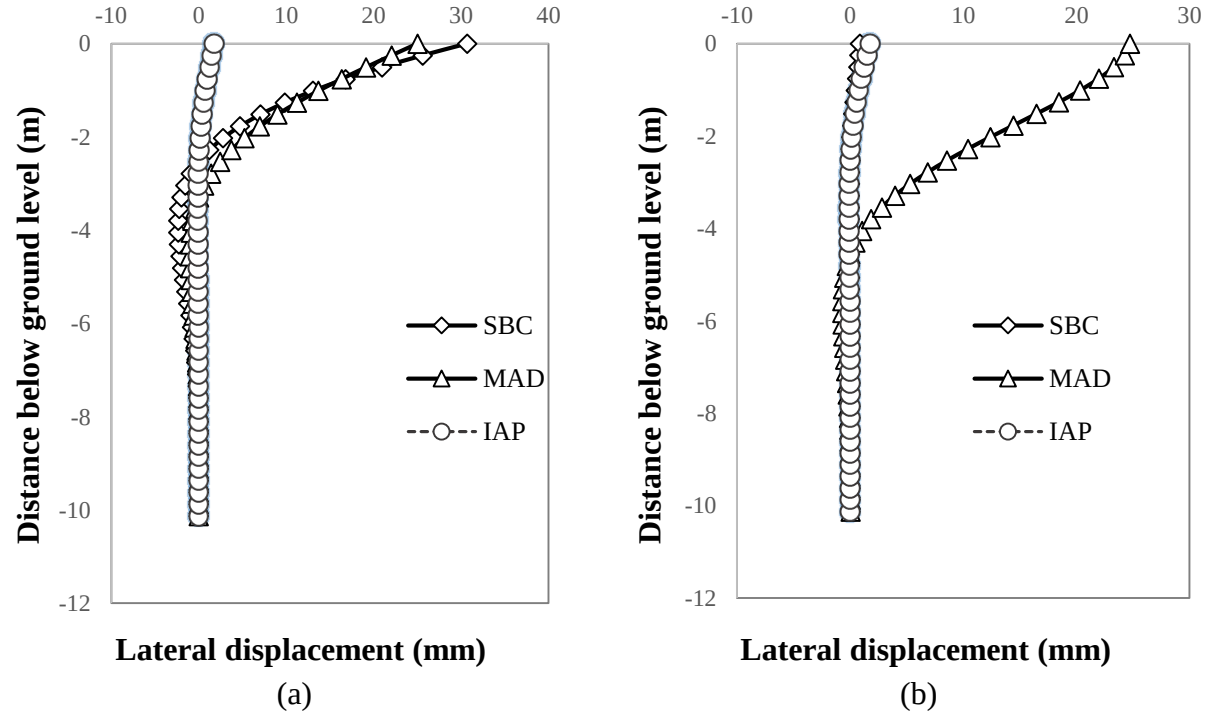

Fig B3: Lateral displacement along pier #2 in soft clay (a) Free head pile; (b) Fixed head pile

Stiff Clay

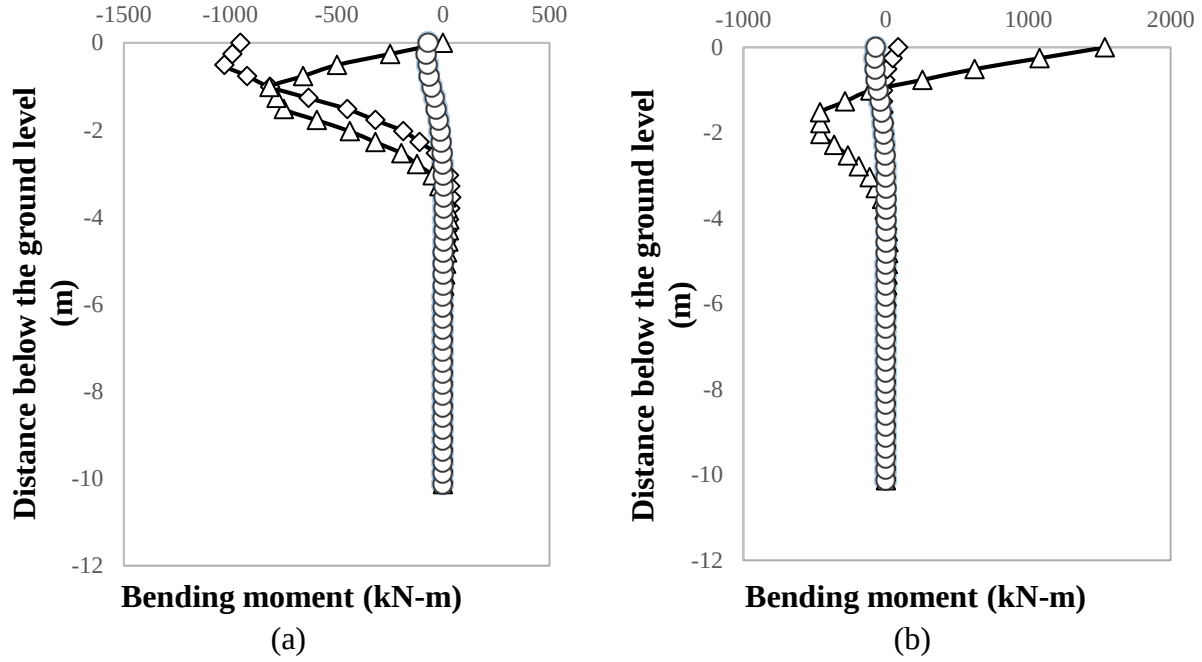

Fig B4: Bending moment along pile group #2 in stiff clay (a) Free pile head; (b) Fixed head pile

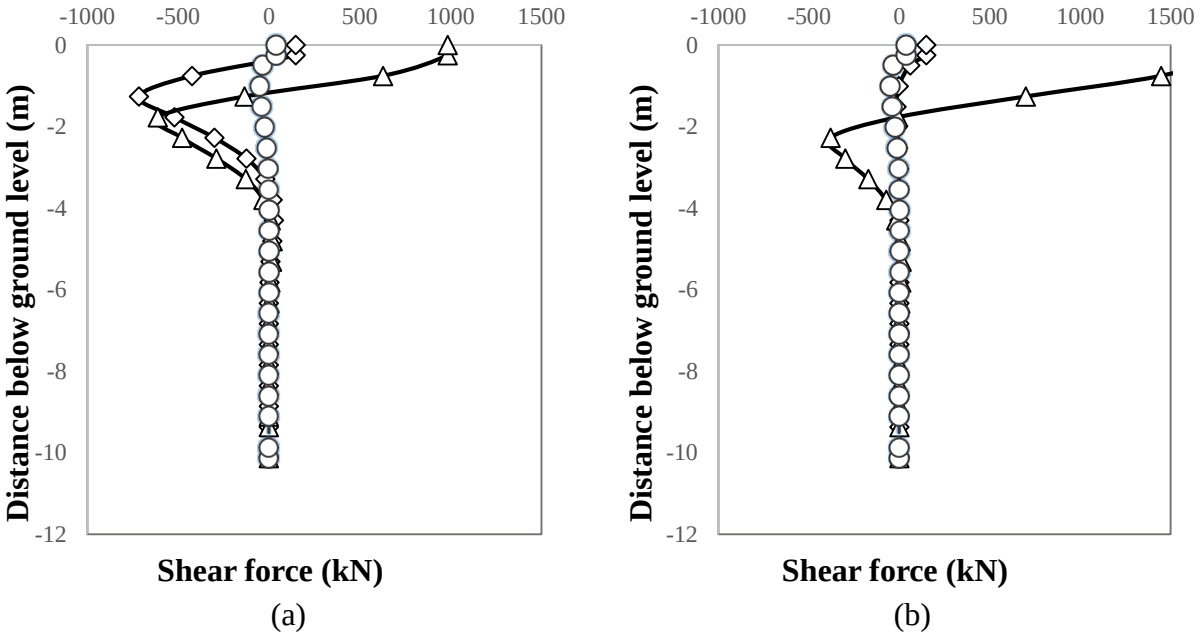

Fig B5: Shear force along pile group #2 in stiff clay (a) Free head pile; (b) Fixed head pile

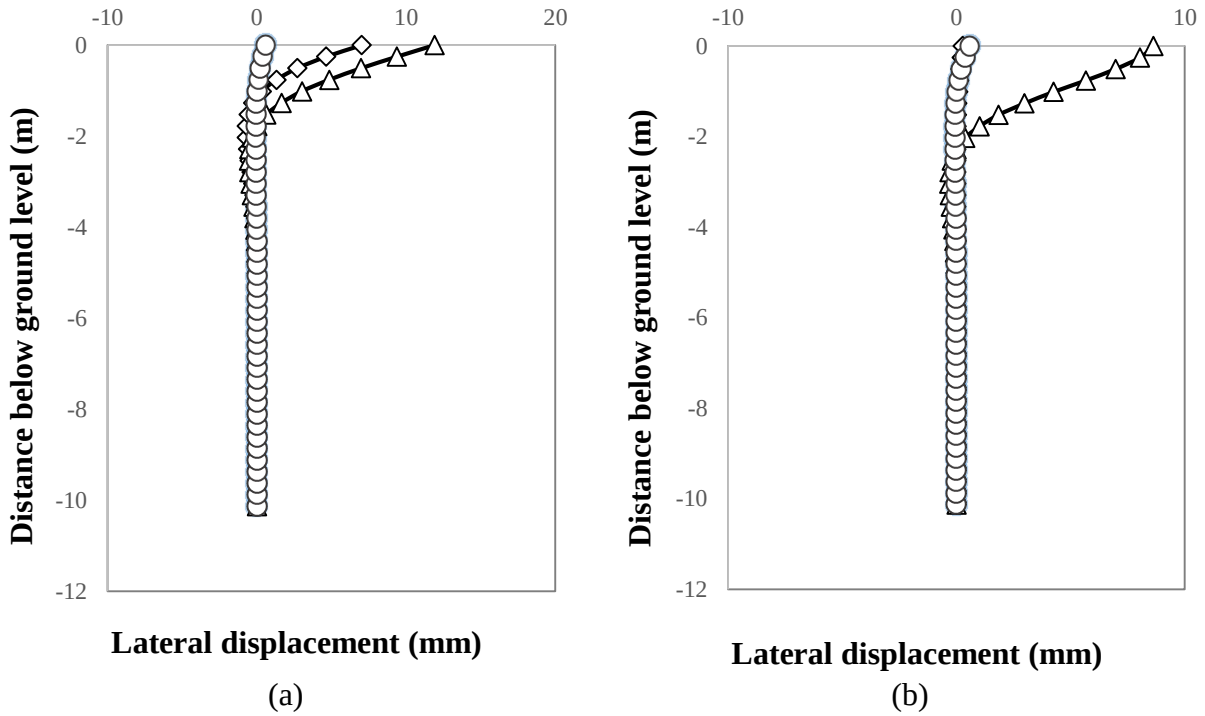

Fig B6: Lateral displacement profile along pile #2 in stiff clay (a) Free pile head; (b) Fixed pile head

Multilayered Soil

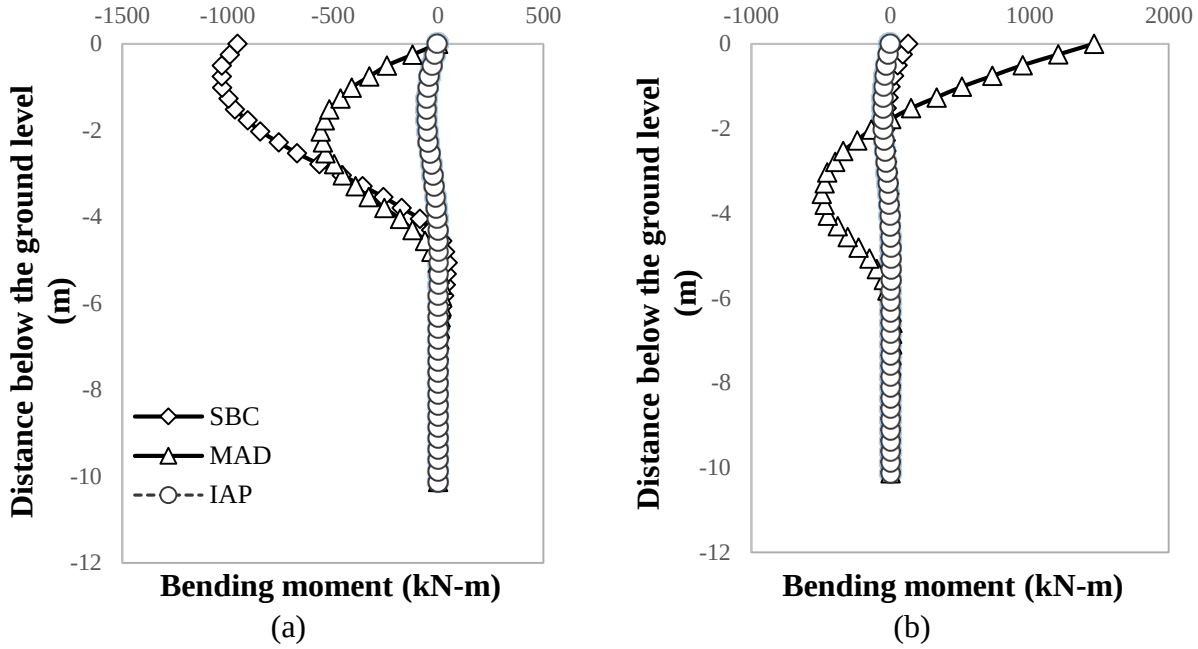

Fig B7: Bending moment along pile group #2 in multilayered soil (a) Free pile head; (b) Fixed head pile

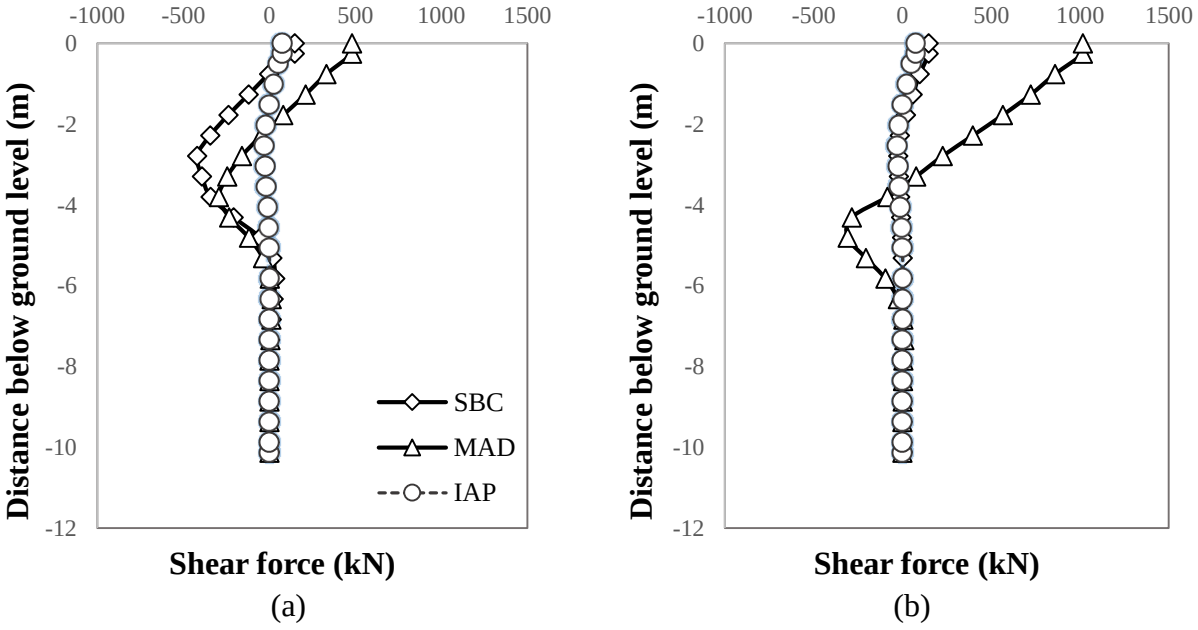

Fig B8: Shear force along pile group #2 in multilayered soil (a) Free head pile; (b) Fixed head pile

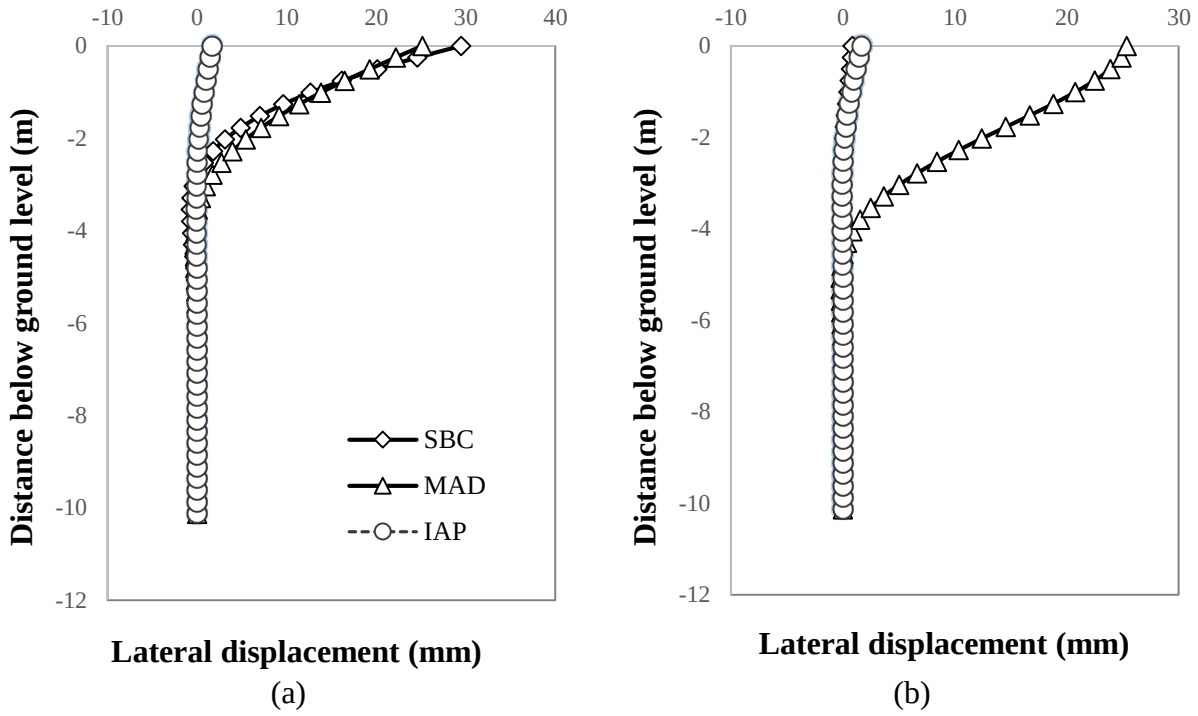

Fig B9: Lateral displacement profile along pile #2 in multilayered soil (a) Free pile head; (b) Fixed pile head

Dense sand

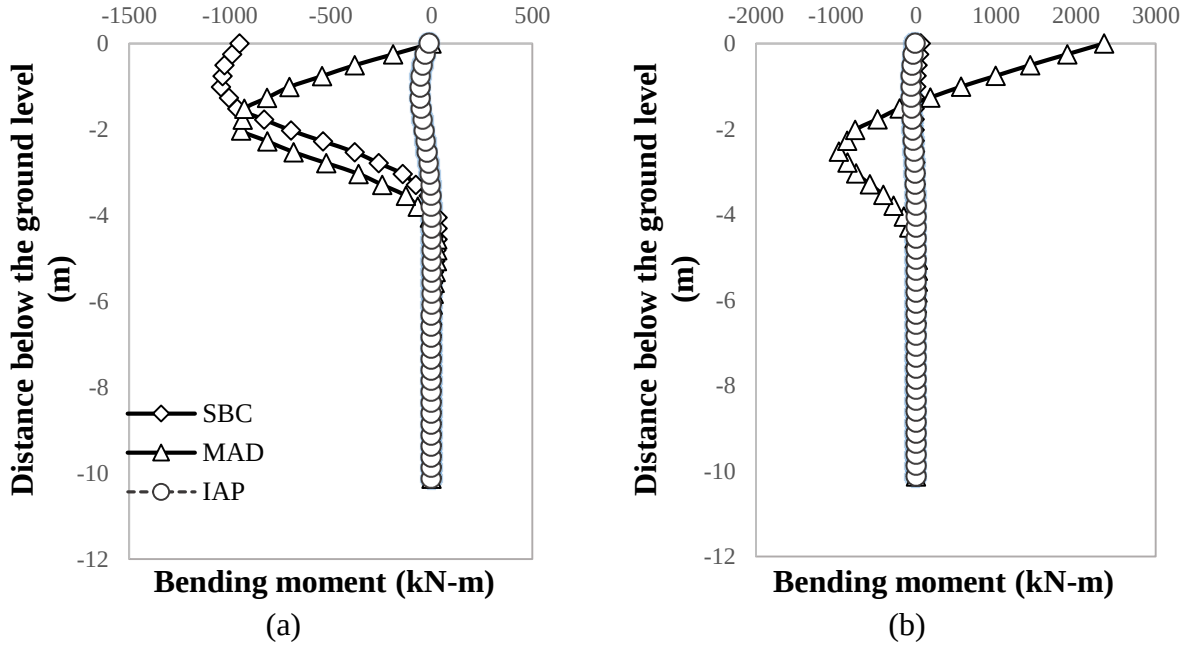

Fig B10: Bending moment along pile group #2 in dense sand (a) Free pile head; (b) Fixed head pile

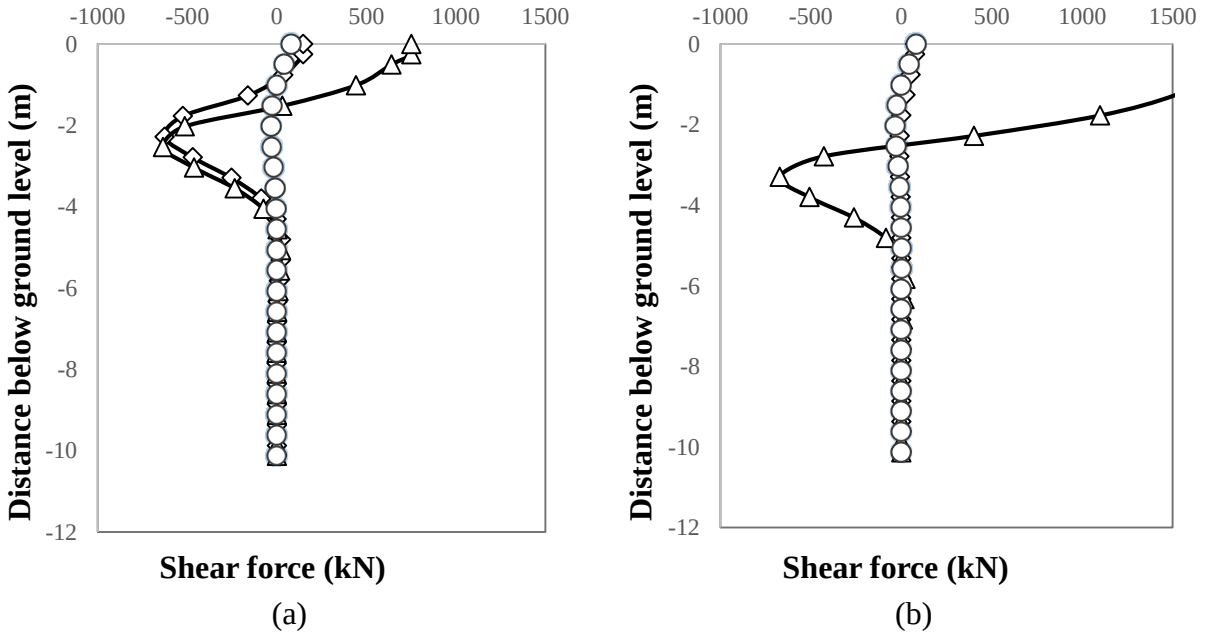

Fig B11: Shear force along pile group #2 in dense sand (a) Free head pile; (b) Fixed head pile

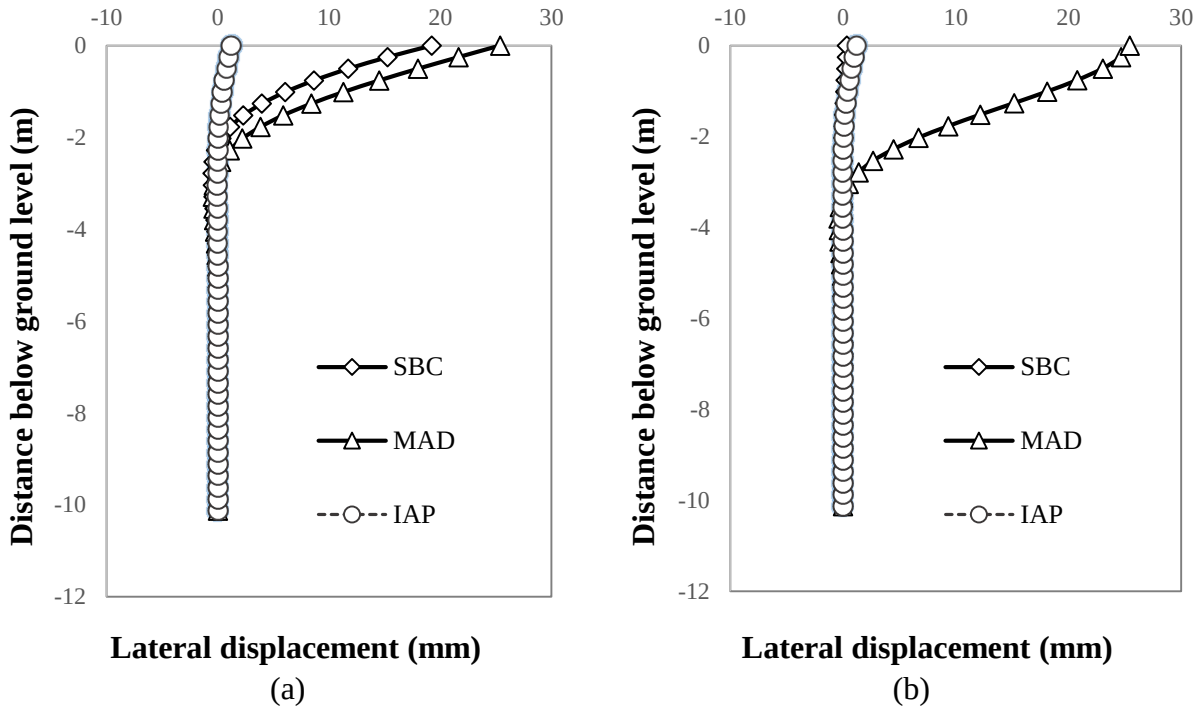

Fig B12: Lateral displacement along pile #2 in dense sand (a) Free pile head; (b) Fixed pile head